THE NCEP CLIMATE FORECAST SYSTEM REANALYSIS

THE ENVIRONMENTAL MODELING CENTER

NCEP/NWS/NOAA

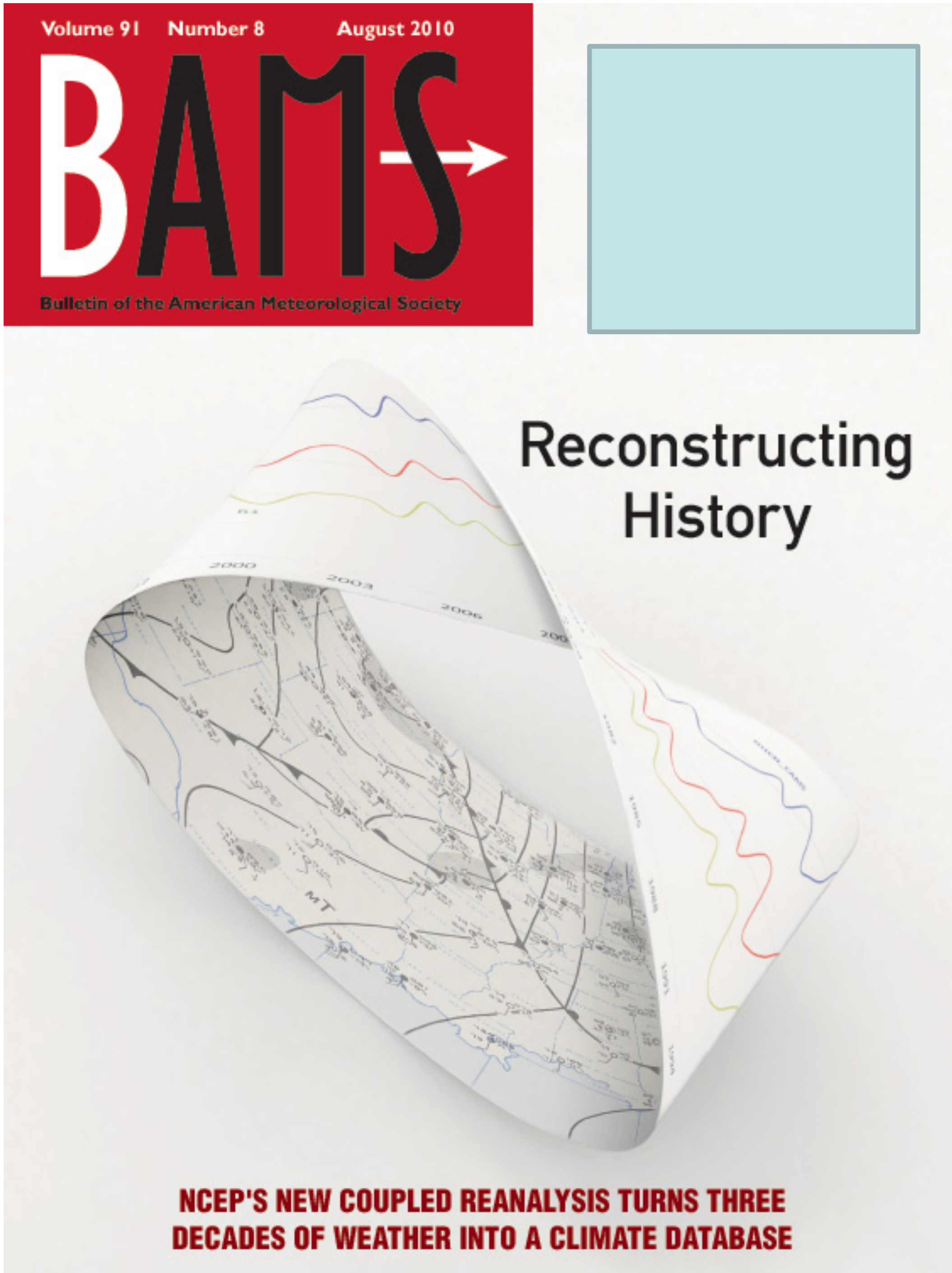

The NCEP Climate Forecast System Reanalysis

Suranjana Saha, Shrinivas Moorthi, Hua-Lu Pan, Xingren Wu, Jiande Wang, Sudhir Nadiga, Patrick Tripp, Robert Kistler, John Woollen, David Behringer, Haixia Liu, Diane Stokes, Robert Grumbine, George Gayno, Jun Wang, Yu-Tai Hou, Hui-ya Chuang, Hann-Ming H. Juang, Joe Sela, Mark Iredell, Russ Treadon, Daryl Kleist, Paul Van Delst, Dennis Keyser, John Derber, Michael Ek, Jesse Meng, Helin Wei, Rongqian Yang, Stephen Lord, Huug van den Dool, Arun Kumar, Wanqiu Wang, Craig Long, Muthuvel Chelliah, Yan Xue, Boyin Huang, Jae-Kyung Schemm, Wesley Ebisuzaki, Roger Lin, Pingping Xie, Mingyue Chen, Shuntai Zhou, Wayne Higgins, Cheng-Zhi Zou, Quanhua Liu, Yong Chen, Yong Han, Lidia Cucurull, Richard W. Reynolds, Glenn Rutledge, Mitch Goldberg

Bulletin of the American Meteorological Society
Volume 91, Issue 8, pp 1015-1057.
doi: 10.1175/2010BAMS3001.1

- WHAT IS AN ANALYSIS SYSTEM?
- WHAT IS A REANALYSIS SYSTEM ?

ONE DAY OF ANALYSIS

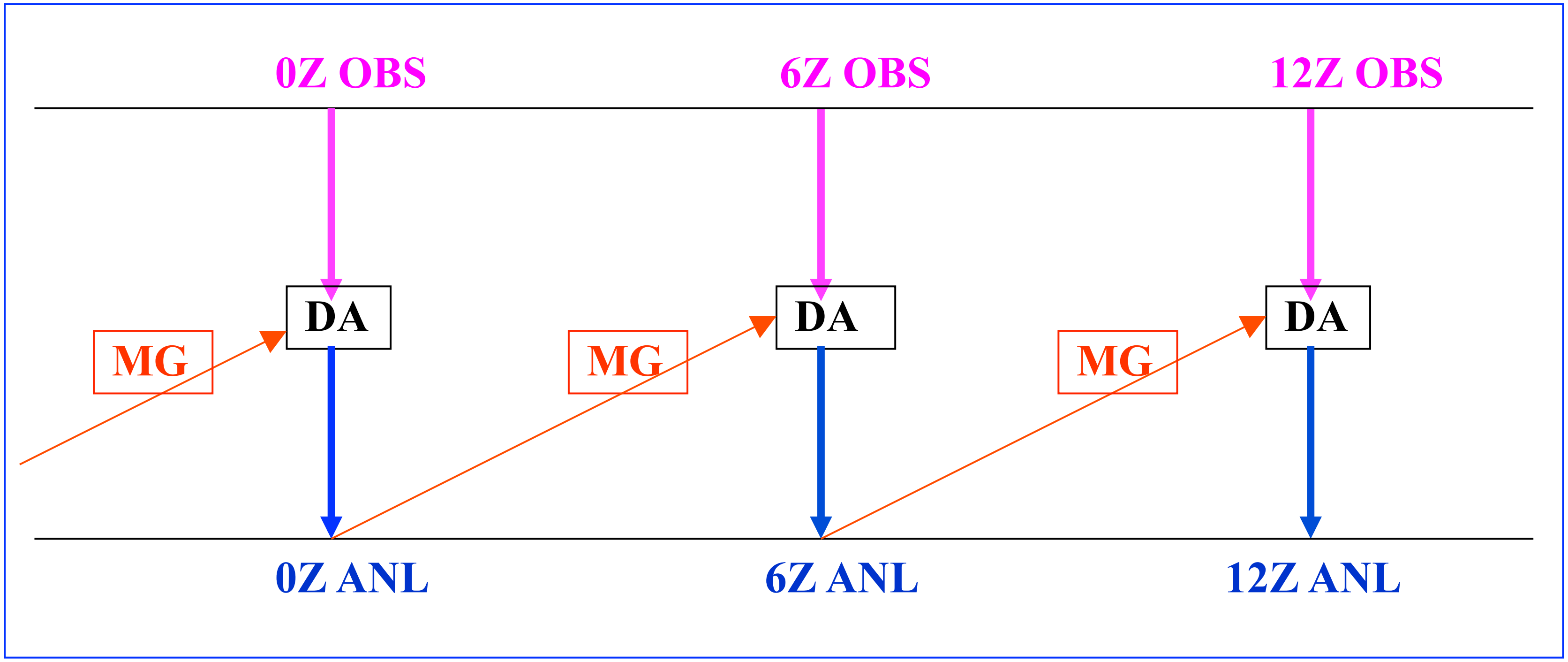

OBS: Observations

DA: Data Assimilation

MG: Model Guess

ANL: Analysis

- Analysis is always ongoing in operational ***weather*** prediction centers in real time
- Consecutive analyses over many years may constitute some sort of a ***climate*** record
- Analysis also provide initial states for model forecasts

What is a Reanalysis ?

- analysis made after the fact (not ongoing in real time)
- with an unchanging model to generate the model guess (MG)
- with an unchanging data assimilation method (DA)
- no data cut-off windows and therefore more quality controlled observations (usually after a lot of data mining)

Motivation to make a Reanalysis ?

- To create a homogeneous and consistent climate record

Examples: R1/CDAS1: NCEP/NCAR Reanalysis (1948-present) Kalnay et al., Kistler et al

R2/CDAS2 : NCEP/DOE Reanalysis (1979-present) Kanamitsu et al

ERA40, ERA-Interim, MERRA, JRA25, NARR, etc….

- To create a large set of initial states for Reforecasts (hindcasts, retrospective forecasts..) to calibrate real time extended range predictions (error bias correction).

An upgrade to the NCEP Climate Forecast System (CFS)

is being planned for 18 Jan 2011.

For a new Climate Forecast System (CFS) implementation

Two essential components:

A new Reanalysis of the atmosphere, ocean, seaice and land over the 32-year period (1979-2010) is required to provide consistent initial conditions for:

A complete Reforecast of the new CFS over the 29-year period (1982-2010), in order to provide stable calibration and skill estimates of the new system, for operational seasonal prediction at NCEP

For a new CFS implementation (contd)

1. Analysis Systems : Operational GDAS:
   Atmospheric (GADAS)-GSI
   Ocean-ice (GODAS) and
   Land (GLDAS)

2. Atmospheric Model : Operational GFS

   New Noah Land Model

3. Ocean Model : New MOM4 Ocean Model

   New Sea Ice Model

An upgrade to the coupled atmosphere-ocean-seaice-land NCEP Climate Forecast System (CFS) is being planned for 18 Jan 2011.

This upgrade involves changes to all components of the CFS, namely:

- **improvements to the data assimilation of the atmosphere with the new NCEP Gridded Statistical Interpolation Scheme (GSI) and major improvements to the physics and dynamics of operational NCEP Global Forecast System (GFS)**

- **improvements to the data assimilation of the ocean and ice with the NCEP Global Ocean Data Assimilation System, (GODAS) and a new GFDL MOM4 Ocean Model**

- **improvements to the data assimilation of the land with the NCEP Global Land Data Assimilation System, (GLDAS) and a new NCEP Noah Land model**

For a new CFS implementation (contd)

1. An atmosphere at high horizontal resolution (spectral T382, ~38 km) and high vertical resolution (64 sigma-pressure hybrid levels)
2. An interactive ocean with 40 levels in the vertical, to a depth of 4737 m, and horizontal resolution of 0.25 degree at the tropics, tapering to a global resolution of 0.5 degree northwards and southwards of 10N and 10S respectively
3. An interactive 3 layer sea-ice model
4. An interactive land model with 4 soil levels

There are three main differences with the earlier two NCEP Global Reanalysis efforts:

- Much higher horizontal and vertical resolution (T382L64) of the atmosphere (earlier efforts were made with T62L28 resolution)
- The guess forecast was generated from a coupled atmosphere – ocean – seaice - land system
- Radiance measurements from the historical satellites were assimilated in this Reanalysis

To conduct a Reanalysis with the atmosphere, ocean, seaice and land coupled to each other was a novelty, and will hopefully address important issues, such as the correlations between sea surface temperatures and precipitation in the global tropics, etc.

6 Simultaneous Streams

1 Dec 1978 to 31 Dec 1986
1 Nov 1985 to 31 Dec 1989
1 Jan 1989 to 31 Dec 1994
1 Jan 1994 to 31 Mar 1999
1 Apr 1998 to 31 Mar 2005
1 Apr 2004 to 31 Dec 2009

Full 1-year overlap between streams to account for ocean, stratospheric and land spin up issues

Reanalysis covers 31 years (1979-2009) + 5 overlap years
And will continue into the future in real time.

ONE DAY OF REANALYSIS

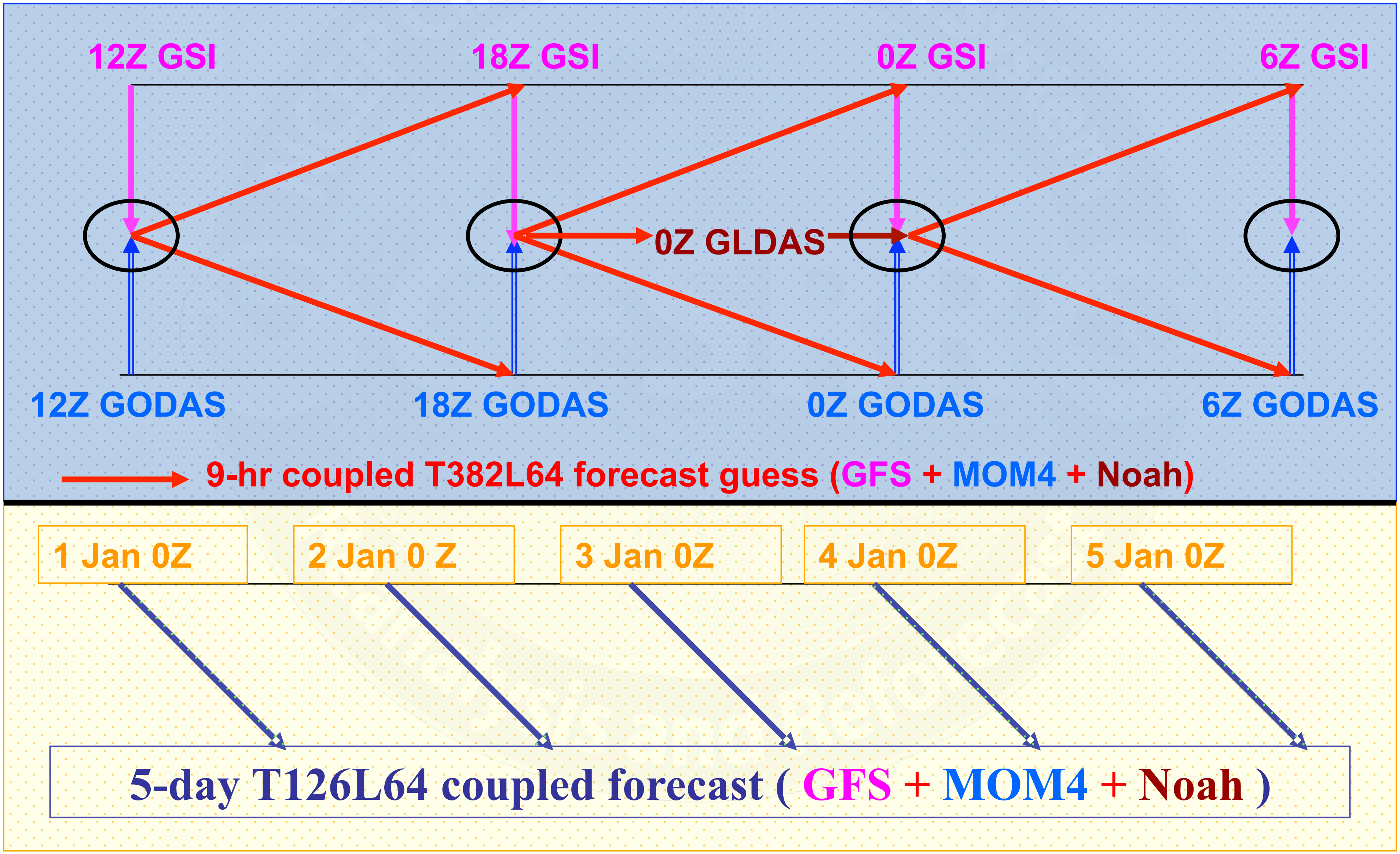

ONE DAY OF REANALYSIS

- Atmospheric T382L64 (GSI) Analysis at 0,6,12 and 18Z, using radiance data from satellites, as well as all conventional data
- Ocean and Sea Ice Analysis (GODAS) at 0,6,12 and 18Z
- From each of the 4 cycles, a 9-hour coupled guess forecast (GFS at T382L64) is made with 30-minute coupling to the ocean (MOM4 at 1/4^{o} equatorial, 1/2^{o} global)
- Land (GLDAS) Analysis using observed precipitation with Noah Land Model at 0Z
- Coupled 5-day forecast from every 0Z initial condition was made with the T126L64 GFS for sanity check.

R1	CFSR
T62 horizontal resolution (~200 Km)	T382 horizontal resolution (~38 Km)
Sigma vertical coordinate with 28 levels with top pressure ~3 hPa	Sigma-pressure hybrid vertical coordinate with 64 levels with top pressure ~0.266 hPa
Simplified Arakawa-Schubert convection	Simplified Arakawa-Schubert convection with momentum mixing
Tiedtke (1983) shallow convection	Tiedtke (1983) shallow convection modified to have zero diffusion above the low level inversions
Seasonal and zonal mean climatological ozone for radiation	Prognostic ozone with climatological production and destruction terms computed from 2D chemistry models
Diagnostic clouds parameterized based on relative humidity	Prognostic cloud condensate from which cloud cover is diagnosed
Orographic gravity wave drag based on GLAS/GFDL approach Courtesy: Shrinivas Moorthi	Orographic gravity wave drag based on Kim and Arakawa(1995) approach and sub-grid scale mountain blocking following Lott and Miller (1997)

R1 (contd)	**CFSR (contd)**
GFDL IR radiation with random cloud overlap and fixed CO2 of 330 ppmv	AER RRTM IR radiation with maximum/ random cloud overlap and observed global mean CO2
GFDL SW based on Lacis-Hansen (1974) scheme with random cloud overlap and fixed CO2 of 330 ppmv. No aerosols or rare gases	AER RRTM SW radiation with maximum/ random overlap and observed global mean CO2, aerosols including volcanic origin plus rare gases.
Local-*K* vertical diffusion both in PBL and free atmosphere with a uniform background diffusion coefficient	Non-local vertical diffusion in the PBL with local-K in the free atmosphere with exponentially decaying background diffusion coefficient
Second order horizontal diffusion	Eighth order horizontal diffusion
Virtual temperature as prognostic variable	Specific enthalpy as a prognostic variable. More accurate thermodynamic equation.
OSU 2 layer land surface model	Noah 4 layer land surface model
Prescribed SST and sea-ice as lower boundary condition	Coupled to GFDL MOM4 and a 3 layer sea-ice model

Courtesy: Shrinivas Moorthi

The vertical structure of model levels as a meridional cross section at 90E

R1 Troposphere

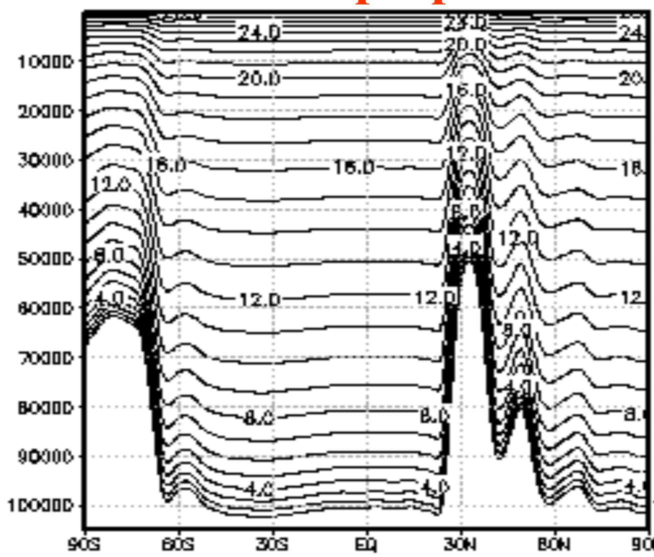

CFSR Troposphere

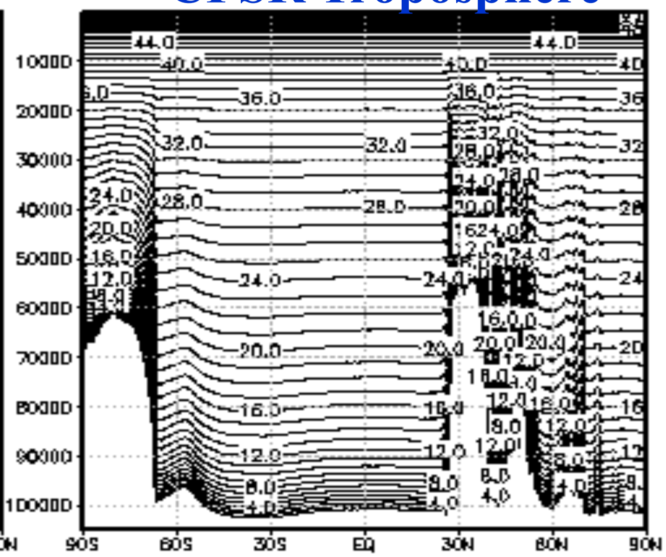

28 levels

64 levels

R1 Stratosphere

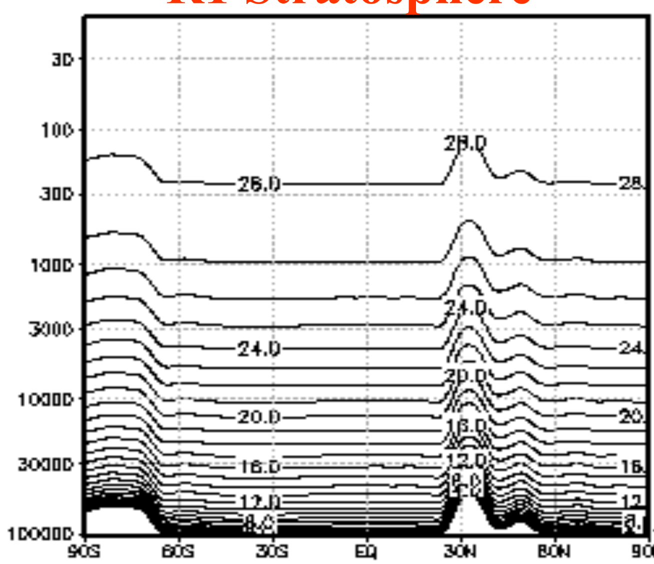

CFSR Stratosphere

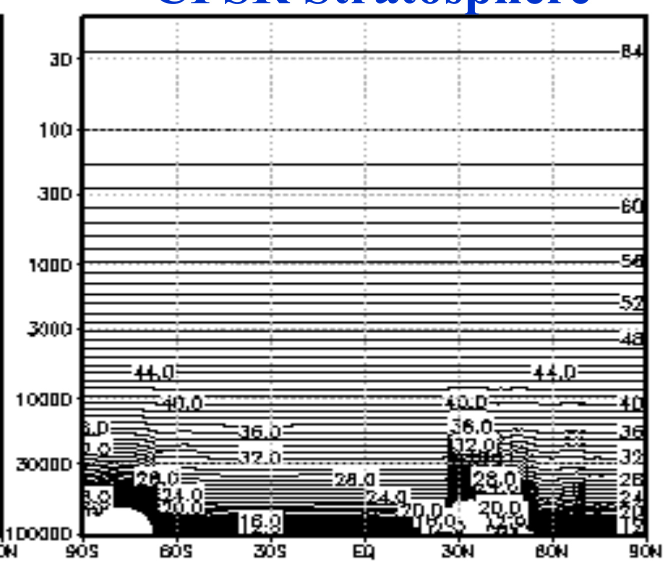

Courtesy: Shrinivas Moorthi

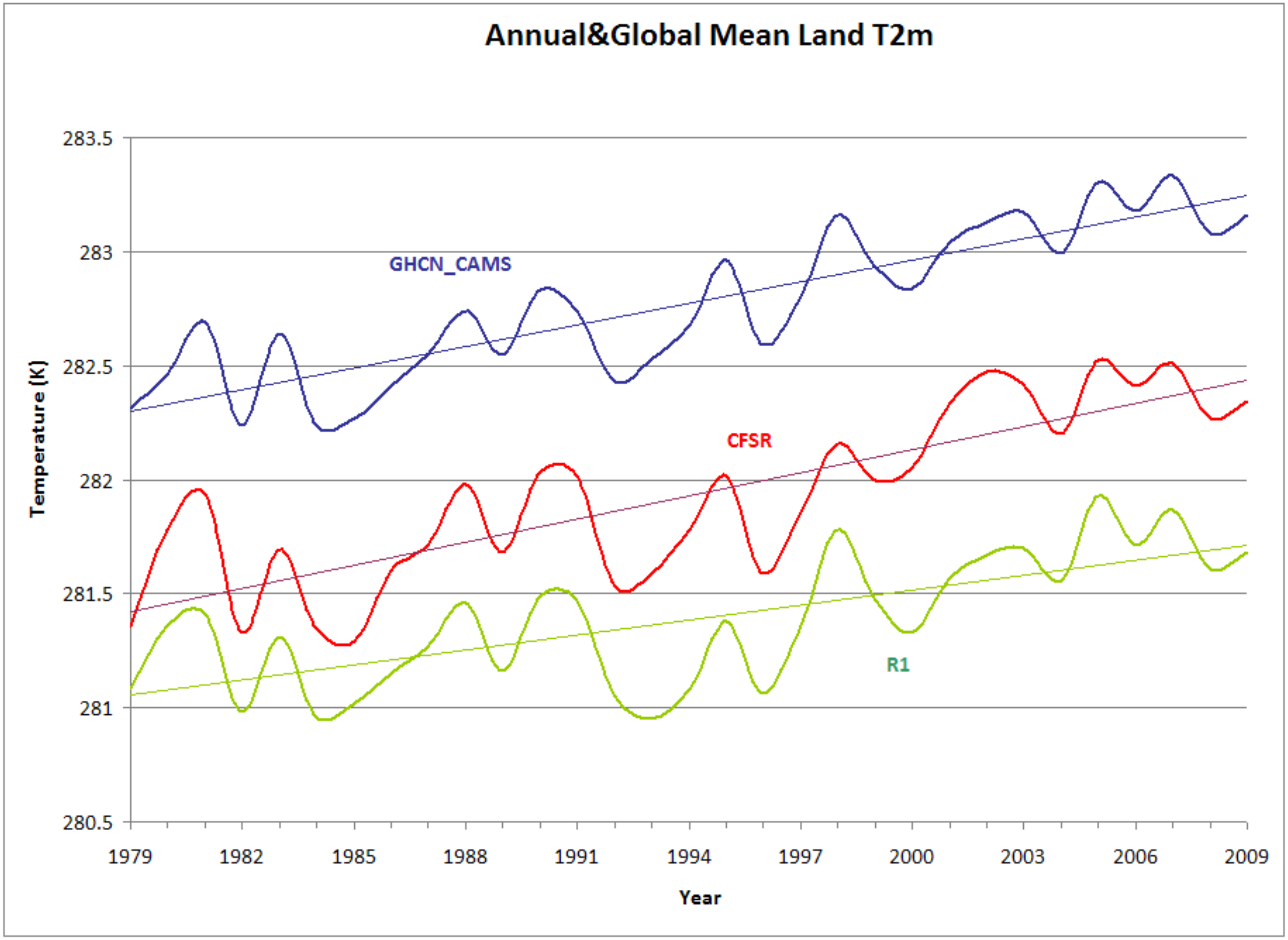

The linear trends are 0.66, 1.02 and 0.94K per 31 years for R1, CFSR and GHCN_CAMS respectively. (Keep in mind that straight lines may not be perfectly portraying climate change trends).

Courtesy: Huug van den Dool

5-day T126L64 forecast anomaly correlations

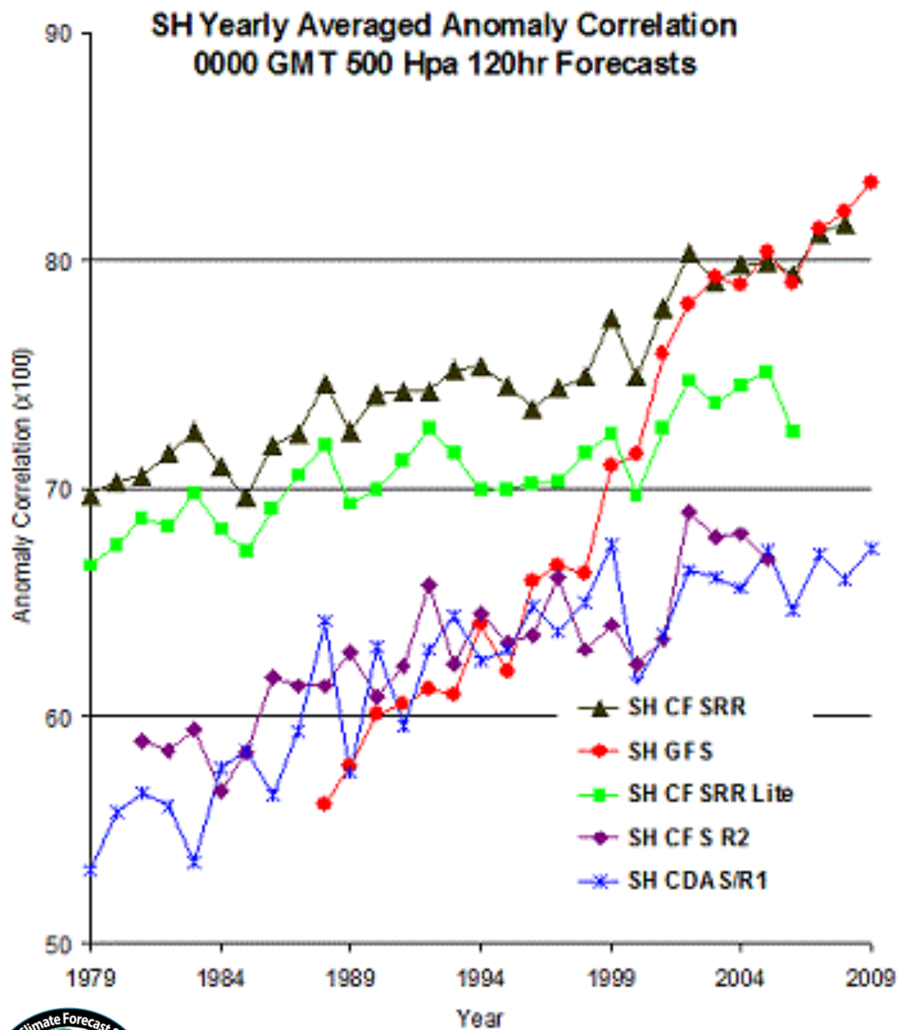

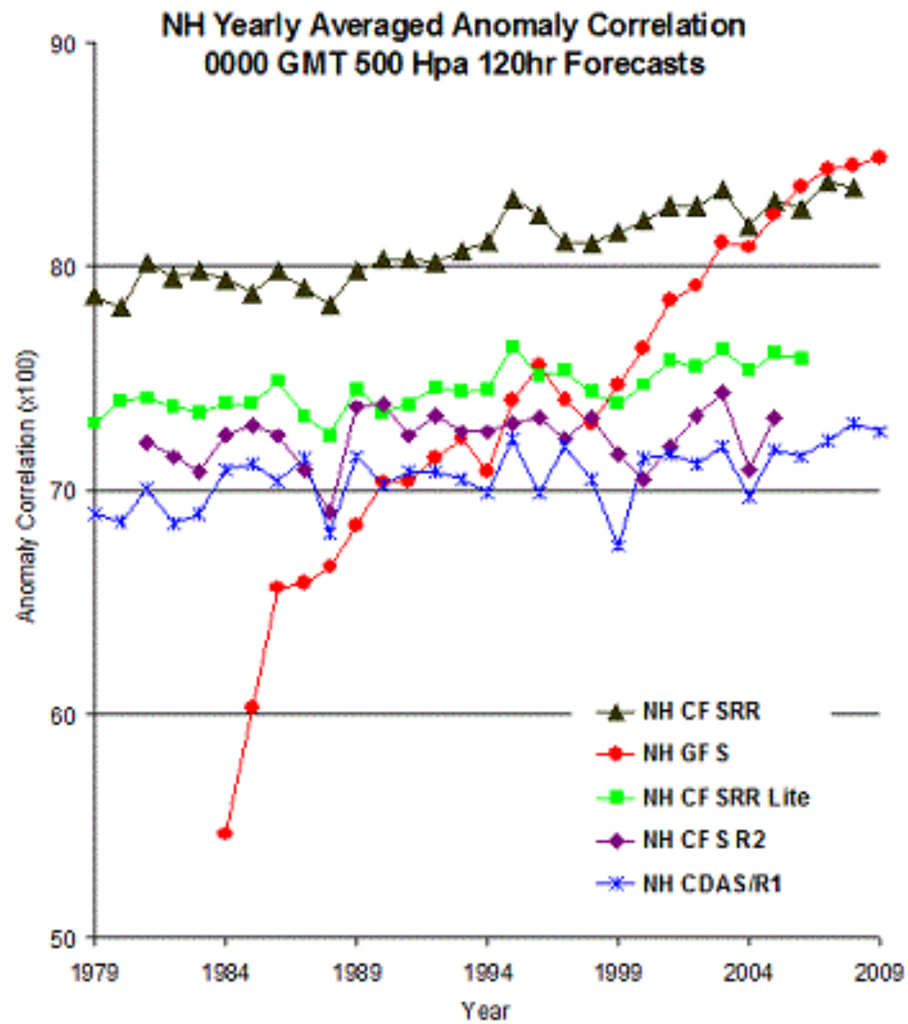

Courtesy: Bob Kistler

SST-Precipitation Relationship in CFSR

Precipitation-SST lag correlation in tropical Western Pacific

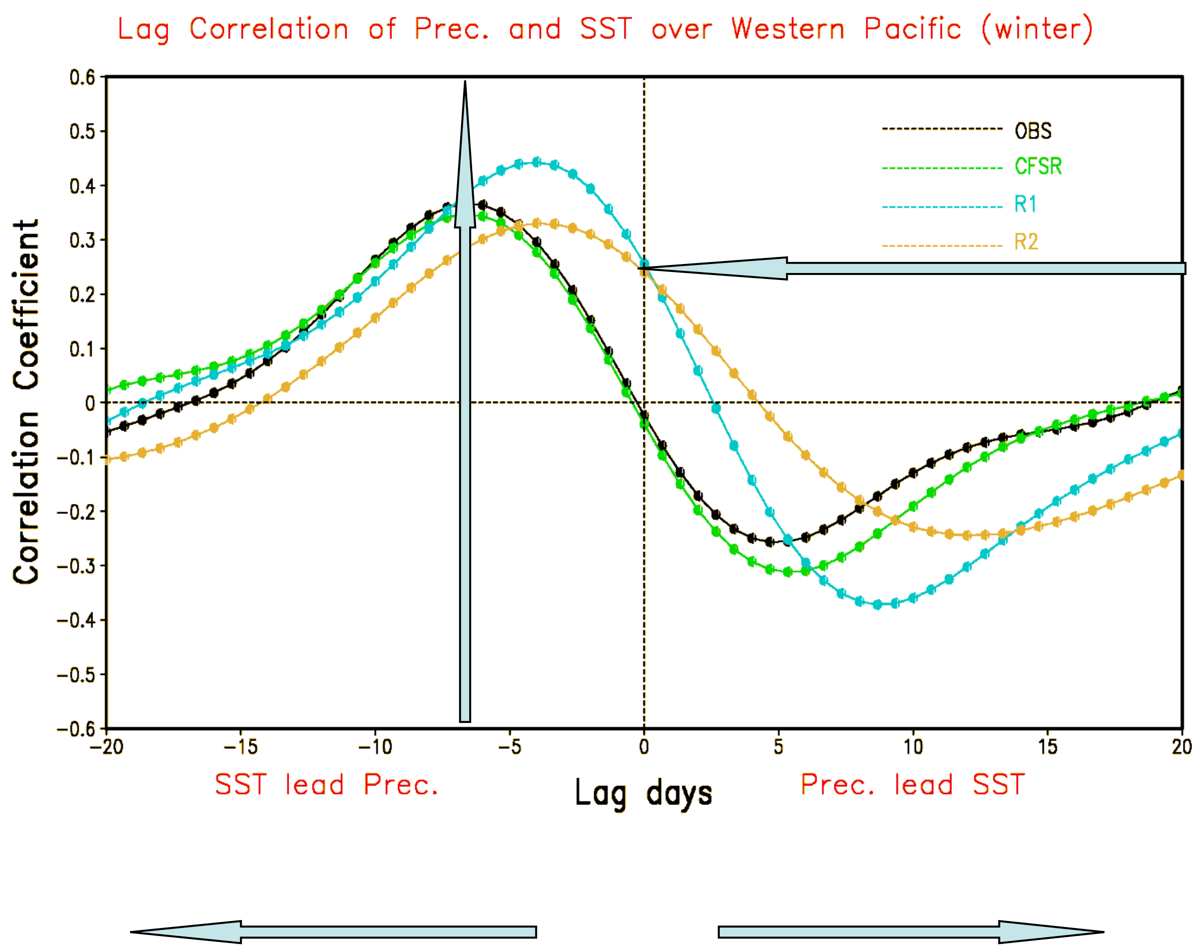

Response of Prec. To SST increase : warming too quick in R1 and R2

simultaneous positive correlation in R1 and R2

Courtesy: Jiande Wang

CFSR data dump volumes, 1978-2009, in GB/month

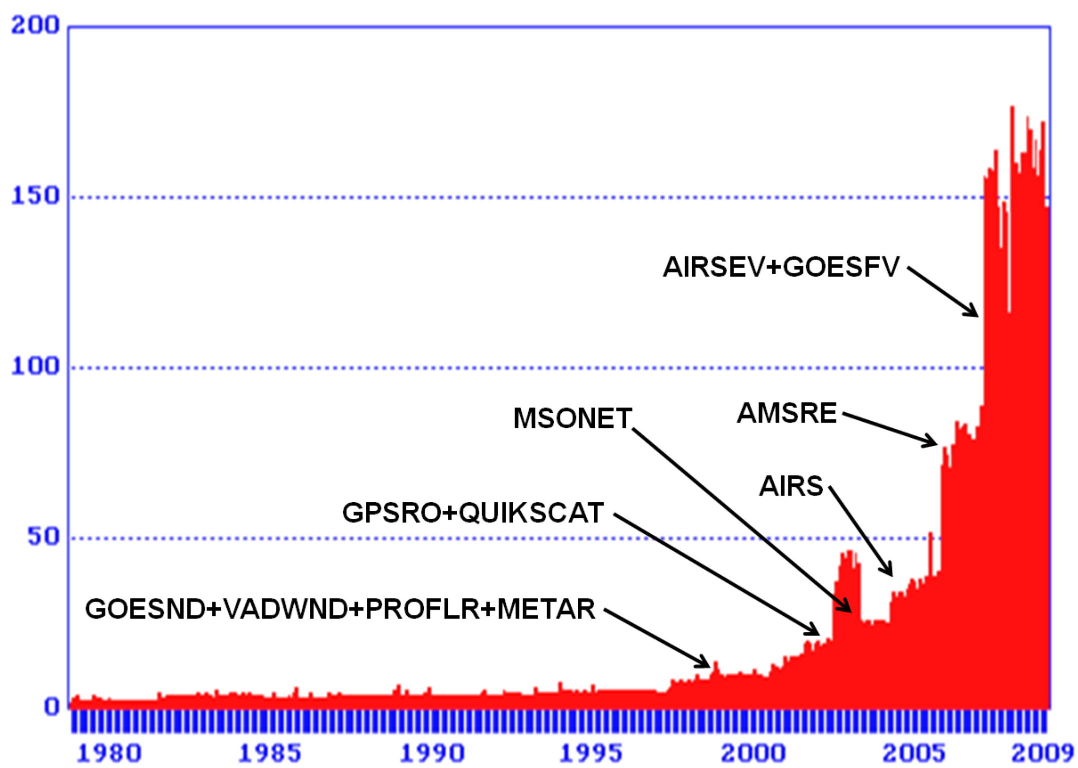

Courtesy: Jack Woollen

Performance of 500mb radiosonde temperature observations

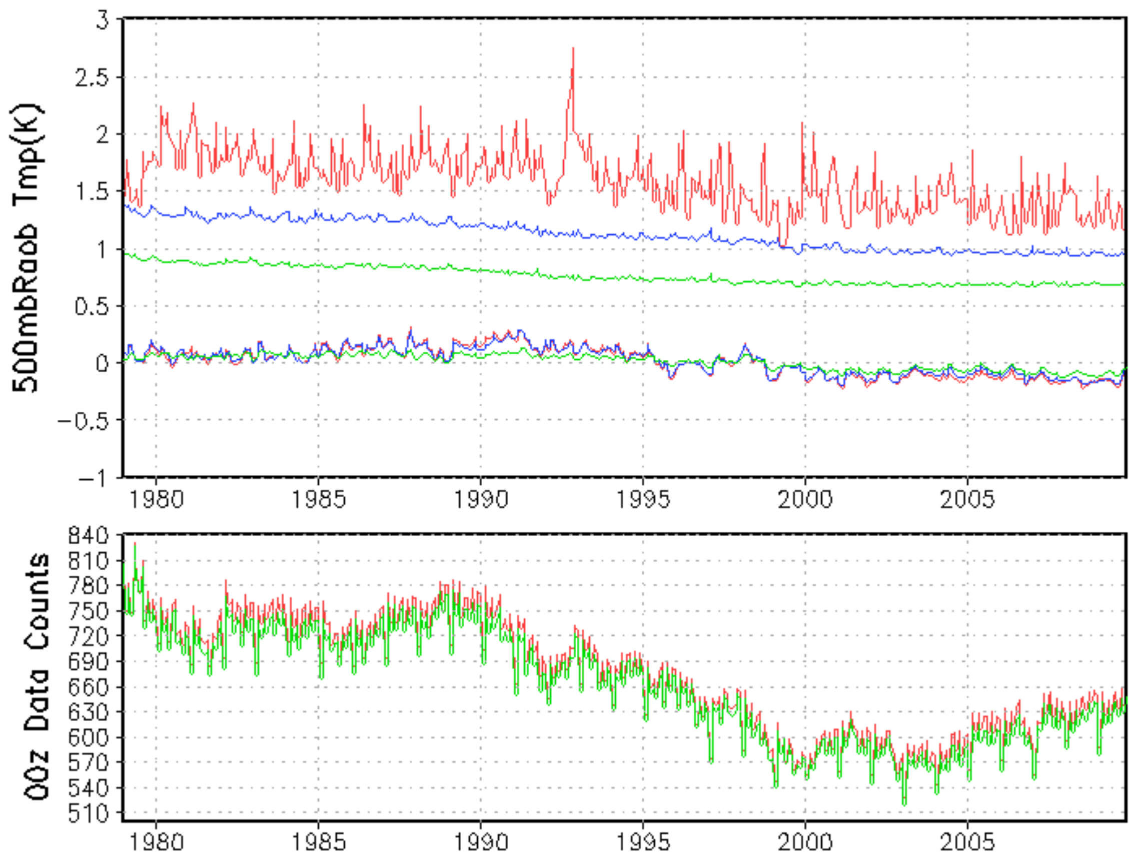

The top panel shows monthly RMS and mean fits of quality controlled observations to the first guess (blue) and the analysis (green). The fits of all observations, including those rejected by the QC, are shown in red.

The bottom panel shows the 00z data counts of all observations (in red) and those which passed QC and were assimilated in green.

Courtesy: Jack Woollen

Several innovative features were built into the CFSR version of the GSI

- The first of these was to apply flow dependence to the background error variances, in an effort to improve upon the climatological estimates previously in use.

- The static variances undergo a simple rescaling based on the 6-hr tendency in the model forecast, where the variances are increased (decreased) where the model tendencies are relatively large (small).

- The rescaling is performed level by level for each variable independently, and done in such a way as to approximately preserve the global mean variance as specified by the static estimate (i.e. it is not designed to increase or decrease the global mean error variance on a cycle to cycle basis).

- This procedure transforms the simple latitude and height dependent fixed variances into a fully three-dimensional, time-varying estimate.

Courtesy: Daryl Kliest

Application of flow dependence to the background error variances

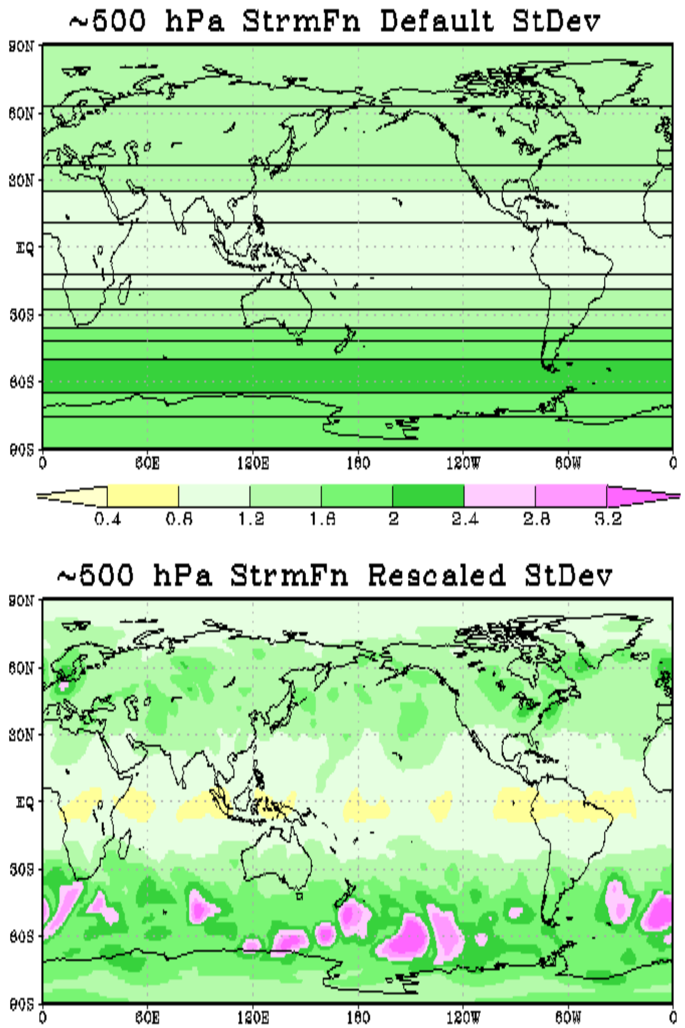

Upper panel is the static, zonal invariant, 500 hPa stream function (1e6) background error valid 2007110600.

Lower panel is the flow dependent adjusted background standard deviation.

Courtesy: Daryl Kleist

FOTO
First-Order Time-extrapolation to Observations

- Many observation types are available throughout 6 hour assimilation window
  - 3D-VAR does not account for time aspect
  - FOTO is a step in this direction
- Generalize operators in minimization to use time tendencies of state variables
  - Improves fit to observations
  - Some slowing of convergence
    - compensated by adding additional iterations

Courtesy: Miodrag Rancic, John Derber, Dave Parrish, Daryl Kleist

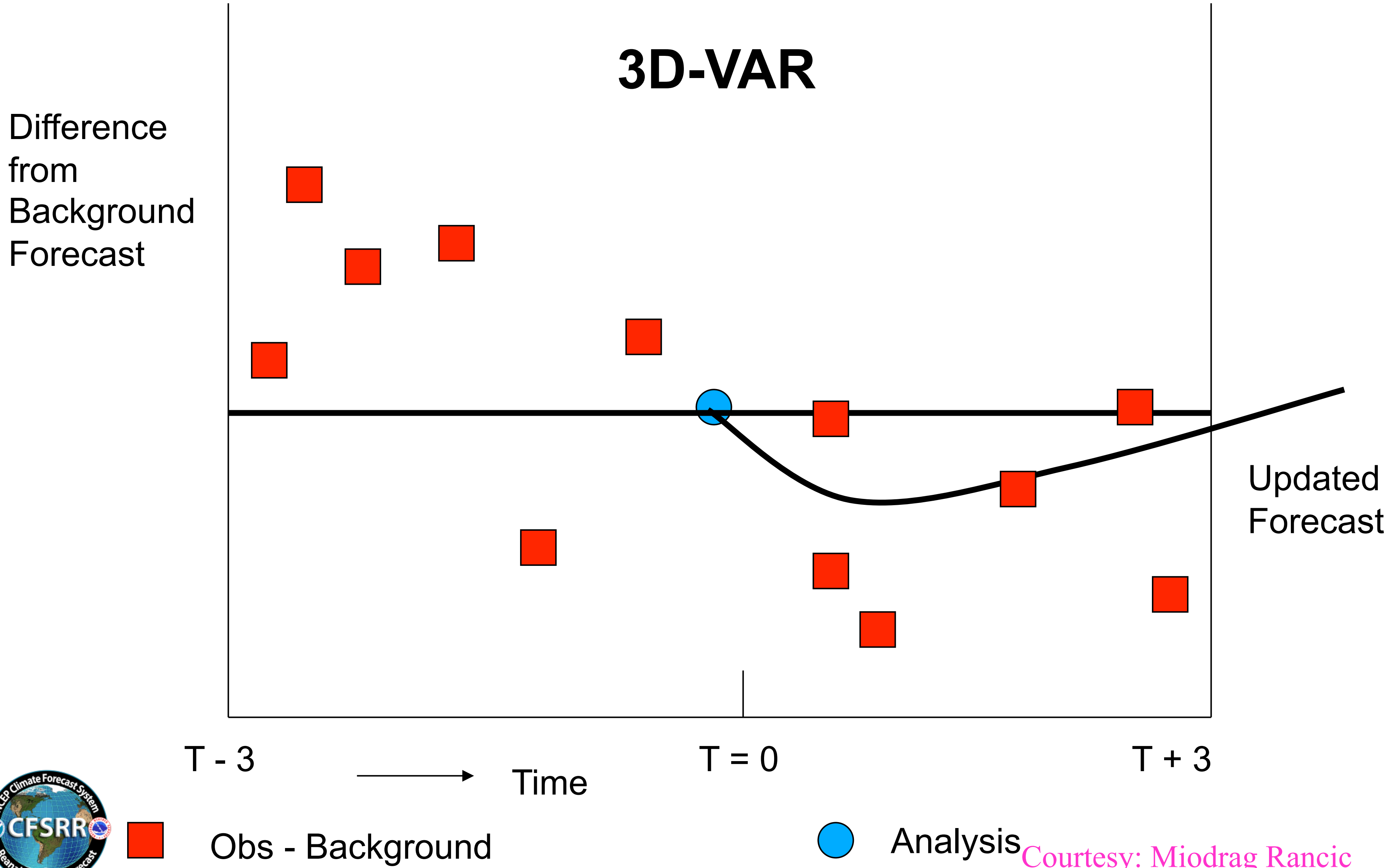

Courtesy: Miodrag Rancic

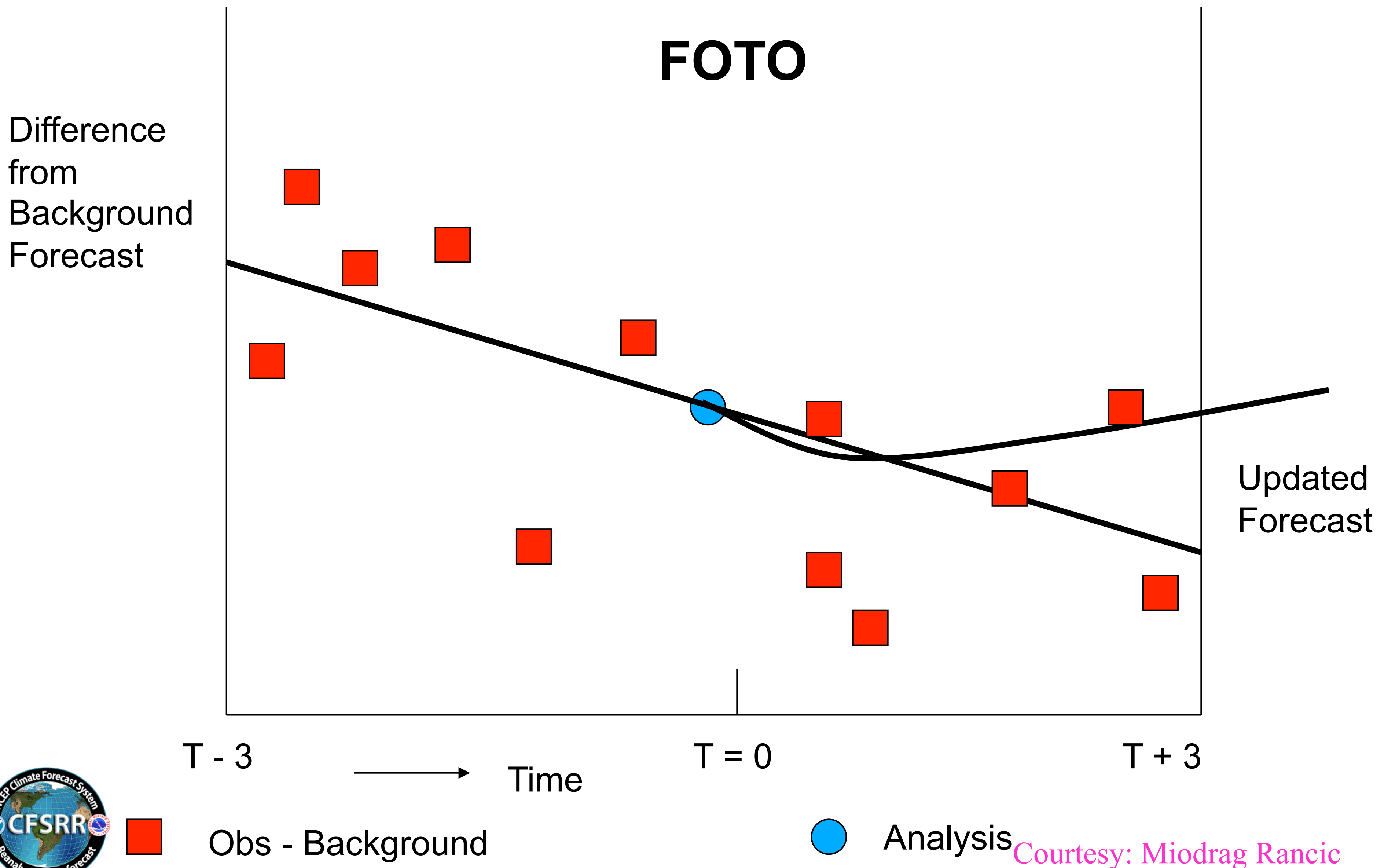

Courtesy: Miodrag Rancic

Variational QC

- Most conventional data quality control is currently performed outside GSI
  - Optimal interpolation quality control (OIQC)
    - Based on OI analysis along with very complicated decision making structure
- Variational QC (VarQC) pulls decision making process into GSI
  - NCEP development based on Andersson and Järvinen (*QJRMS*,1999)
  - Iteratively adjust influence of observations on analysis as part of the variational solution → consistency

Courtesy: Xiujuan Su/Jack Woollen

Variational QC implementation

- Only applied to conventional data
- Slowly turned on in first outer loop to prevent shocks to the system
- Some slowing of convergence
  - compensated by adding additional iterations
- In principle, VarQC allows removal of OIQC step
    - This, however, has not been done (yet).
    - When VarQC on, GSI ignores OIQC flags
    - In the VarQC procedure, conventional GSI observation innovations must first pass gross error checks. Then an innovation weight is computed based on its consistency with the solution of the variational minimization based on all available observations, including radiances, with additional input coming from the probabilities of error for the various observations.
    - Any observation with a weight of .25 or greater is used in the minimization, in contrast to a typical pass/fail QC procedure where observations with a comparable weight of less than approximately .7, would be rejected from the process completely.

Courtesy: Xiujuan Su/Jack Woollen

Another innovative feature of the CFSR GSI is the use of the historical concentrations of carbon dioxide when the historical TOVS instruments were retrofit into the CRTM.

Satellite Platform	Mission Mean (ppmv)b
TIROS-N	337.10
NOAA-6	340.02
NOAA-7	342.96
NOAA-8	343.67
NOAA-9	355.01
NOAA-10	351.99
NOAA-11	363.03
NOAA-12	365.15
GEOS-8	367.54
GEOS-0	362.90
GEOS-10	370.27
NOAA-14 to NOAA-18	380.00
IASI METOP-A	389.00
NOAA-19	391.00

Courtesy: http://gaw.kishou.go.jp

Use of the SSU in CFSR

- The SSU (Stratospheric Sounding Unit) instruments, onboard the majority of TOVS satellites, provide unique 29-year observations for studying stratospheric temperatures.

- The SSU is a step-scanned infrared spectrometer with three modulated cell pressures for the original 15 micron carbon dioxide (CO_2) absorption band to be shifted up and split into three weighting functions, approximately located at 15, 5, and 1.5 hPa, for SSU channels 1, 2, and 3 respectively.

- However, historical use of the SSU radiances posed a challenge due to this complicated sensor response and a leaking problem in the instrument's CO_2 cell pressure modulator that caused the radiances from each satellite to exhibit a unique drift in time (Kobiashi, et. al, 2009).

- The CRTM (Community Radiative Transfer Model), with its advanced surface emissivity model and radiative solver (Liu and Weng, 2006) was used to quantitatively correct the leaking effect.

Use of the SSU in CFSR (contd)

- By comparison to the detailed line-by-line calculation, the root mean square error due to the fitting and interpolation of the CO2 cell pressure in the fast transmittance model is less than 0.1 K (Liu and Weng, 2009).

- The SSU radiative transfer calculations were then compared to the SSU radiances from NOAA-14. The input temperature profiles are taken from the Earth Observing System (EOS) Aura microwave limb sounding (MLS) product for November 2004, a completely independent data source.

- The MLS temperature product precision throughout the stratosphere is generally less than 1 K. More than 7000 match-up data points are found, and all the data points are analyzed. The SSU and the MLS measurements are very consistent.

Comparisons of the SSU brightness temperature between calculations and MLS measurements for Nov 2004

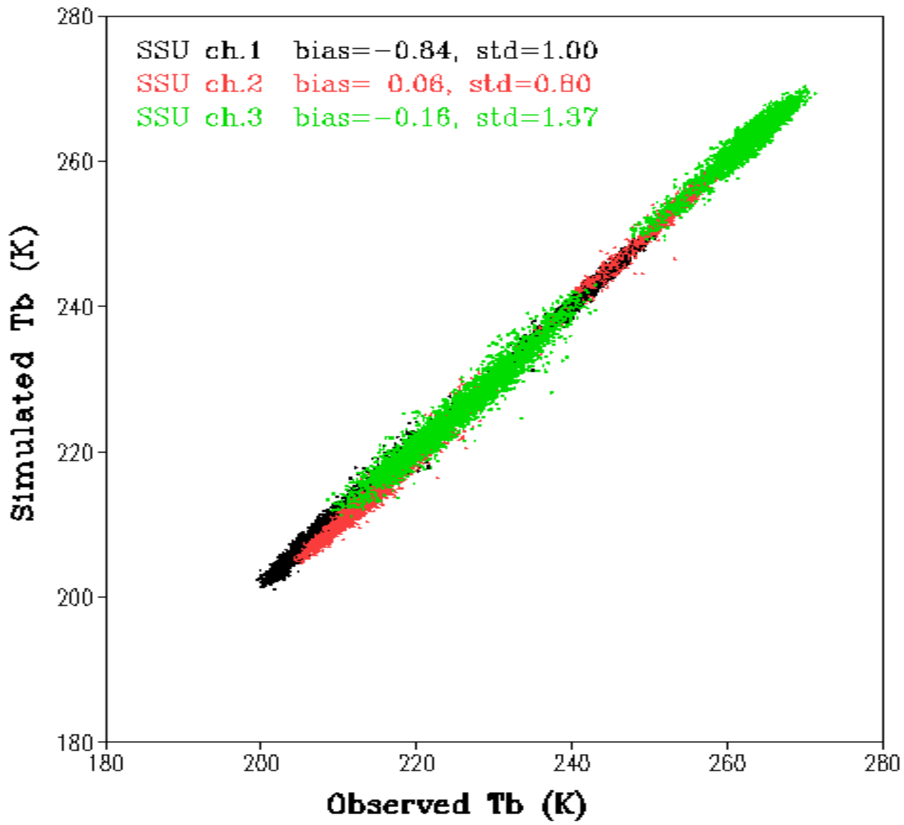

Courtesy: Quanhua (Mark) Liu

Satellite bias correction spin up for CFSR

- The direct assimilation of radiances represents one of the major improvements of the CFSR over R2. However, substantial biases exist when observed radiances are compared to those simulated by the CRTM depiction of the guess.

- These biases are complicated and relate to instrument calibration, data processing and deficiencies in the radiative transfer model.

- A variational satellite bias correction scheme was introduced by Derber and Wu (1998) to address this issue when direct assimilation of radiances began at NCEP. This scheme has been continually developed and is used in the GSI system adapted for the CFSR.

- Before the radiances of a new instrument can be assimilated, its unique set of starting bias corrections must be determined by a separate spin-up assimilation.

Satellite bias correction spin up for CFSR (contd)

.

- In the case of CFSR, each set of historical instruments required an individual spin-up. Since the TOVS instruments had never been assimilated by a GSI based GDAS, a preliminary set of tests were run (not shown) which determined that a 3 month spin-up was required prior to the introduction of those historical instruments in the CFSR.

- Examples of the bias correction values actually applied to the CFSR over the TOVS period of the CFSR, 1979-1998, may be seen in global averaged, 4 times daily averaged time series for MSU channels 1-4 and SSU channels 1-3 in the next Figure. (The spin-up of the SSU channels was done at the same time).

- The one measure of the successful spin-up procedures is the lack of discontinuities in the transitions between successive instruments. The breaks in the MSU time series are a result of the recalibration that was applied beginning in 1986.

TOVS period, 1979-1998, 4xdaily averaged, globally averaged, total bias correction

Courtesy: Kistler/Woollen

MSU

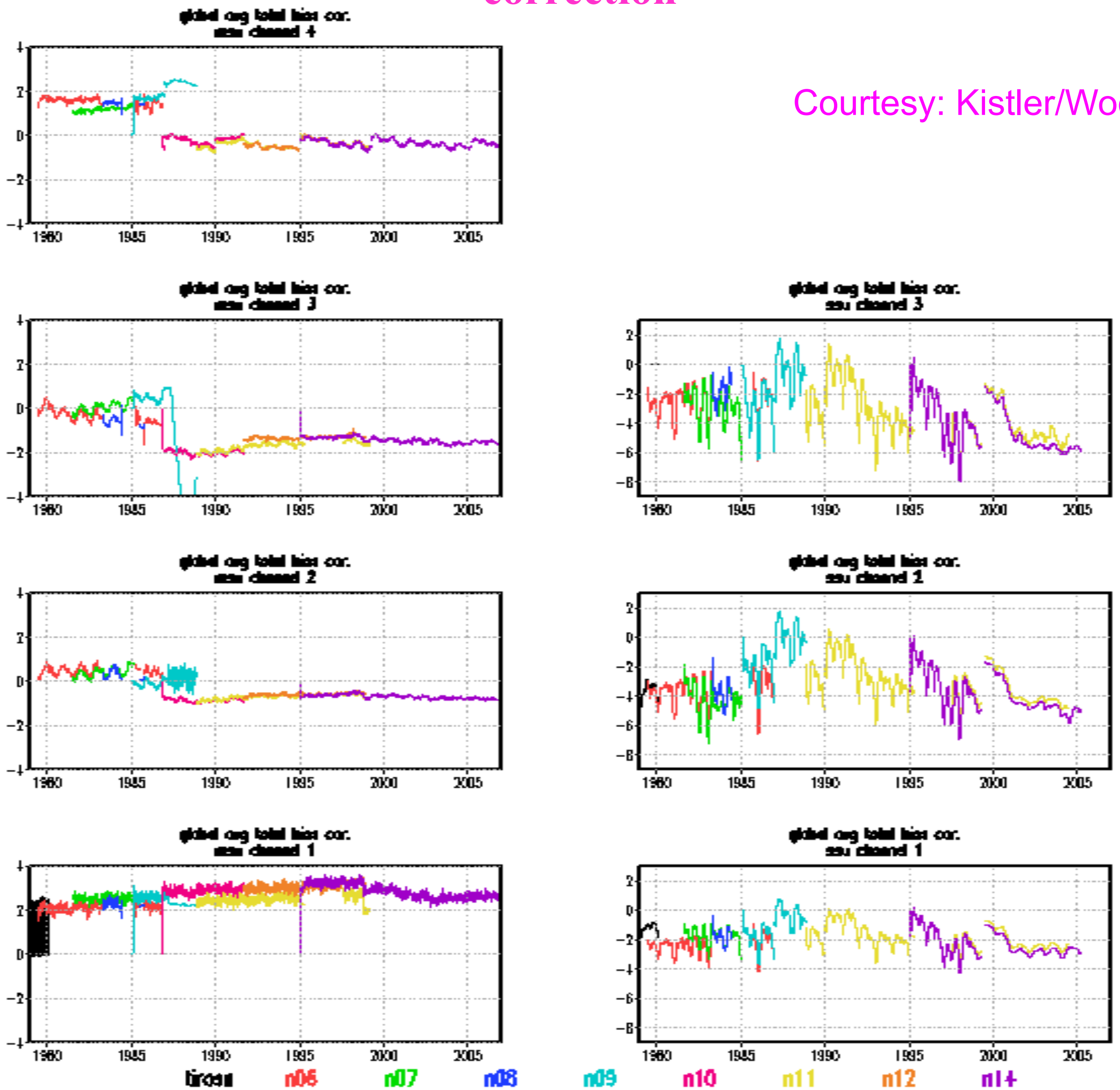

SSU

QBO problem in the GSI

- The quasi-biennial oscillation (**QBO**) is a quasi-periodic oscillation of the equatorial zonal wind between easterlies and westerlies in the tropical stratosphere with a mean period of 28 to 29 months.
- The QBO can only be fully depicted in assimilation systems by sufficient direct wind observations, since the underlying physical mechanism is based on the dissipation of upwardly propagating gravity waves (Lindzen and Holton, 1968) which are filtered out by the hydrostatic assumption.
- Soon after CFSR production began, it was noticed that streams 2 and 3, completely missed the QBO wind transition. This was unexpected based on the ability of R1, R2 and CFSR streams 1 and 4 (starting in 1979 and 2004 respectively) to capture the QBO wind patterns.
- While searching for a comprehensive solution, it was noted that the ERA-40 tropical stratospheric wind profiles were readily available for the streams in question, included the stratospheric layers needed, and, qualitatively, adequately depicted both the QBO and semi-annual oscillation.
- In order that the streams could proceed with a reasonable QBO signature it was decided to use the ERA-40 stratospheric wind profiles as bogus observations for the period from Jul 1, 1981 to Dec 31, 1998.

QBO problem in the GSI (contd)

- Stream 1 benefited from the enhanced FGGE observation system, and stream 4 from the automation of modern radiosonde data collection which results in more reports reaching the GTS, and more stratospheric levels in the individual reports.

- The solution to this problem became apparent from consultations with several GMAO MERRA team members, after determining that the MERRA reanalysis, which uses the same GSI assimilation component, depicted the QBO very well.

- Prior to starting the MERRA project, GMAO had experienced a similar problem analyzing the QBO in an earlier grid point analysis system. The problem was resolved by **enlarging the horizontal length scale of the zonal wind correlation function in the tropical stratosphere (Gaspari, et.al, 2006).** When the GMAO assimilation system was switched to the GSI, the tropical stratospheric stream function variances of the background error reflected the changes made to fix the problem in the earlier system.

- When comparable background error variances were tested in the GSI for a case where the CFSR had failed to capture the QBO, the wind transition was successfully analyzed (not shown).

Tropical Cyclone Processing

- The first global reanalysis to assimilate historical tropical storm information was the JRA-25 reanalysis (Onogi, et.al. 2007). It assimilated synthetic wind profiles (Fiorino, 2002) surrounding the historical storm locations of Newman, 1999.

- A unique feature of the CFSR is its approach to the analysis of historical tropical storm locations. The CFSR applied the NCEP tropical storm relocation package (Liu et. al., 1999), a key component of the operational GFS analysis and prediction of tropical storms.

- By relocating a tropical storm vortex to its observed location prior to the assimilation of storm circulation observations, distortion of the circulation by the mismatch of guess and observed locations is avoided.

- Fiorino (personal communication) provided the CFSR with the historical set of storm reports (provided to NCEP by the National Hurricane Center and the US Navy Joint Typhoon Warning Center) converted into the operational format.

- A measure of the ability of the assimilation system to depict observed tropical storms is to quantify whether or not a reported storm is detected in the guess forecast. A noticeable improvement starts in 2000 coincident with the full utilization of the ATOVS satellite instruments, such that between 90-95% of reported tropical storms are detected.

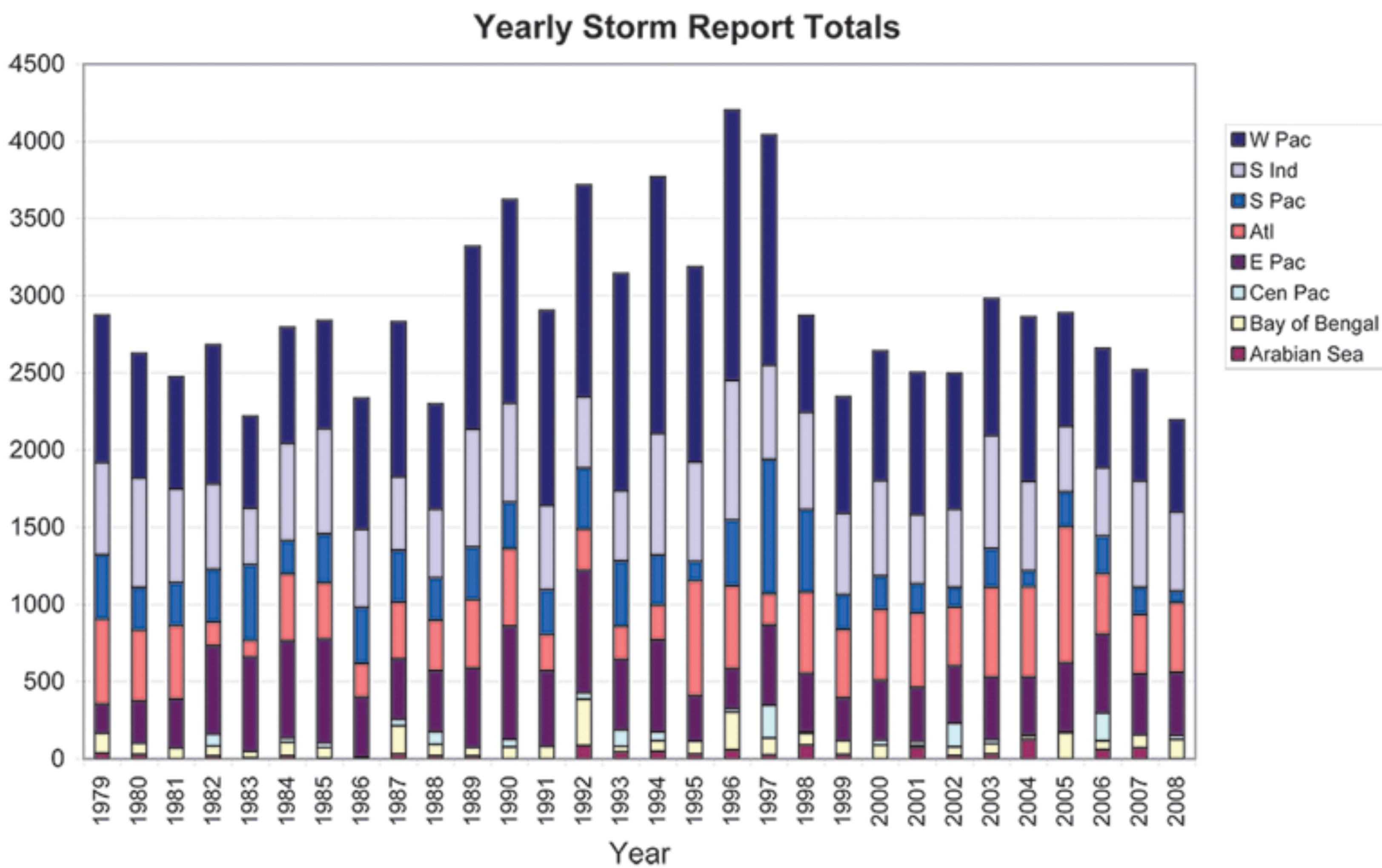

Courtesy: Bob Kistler

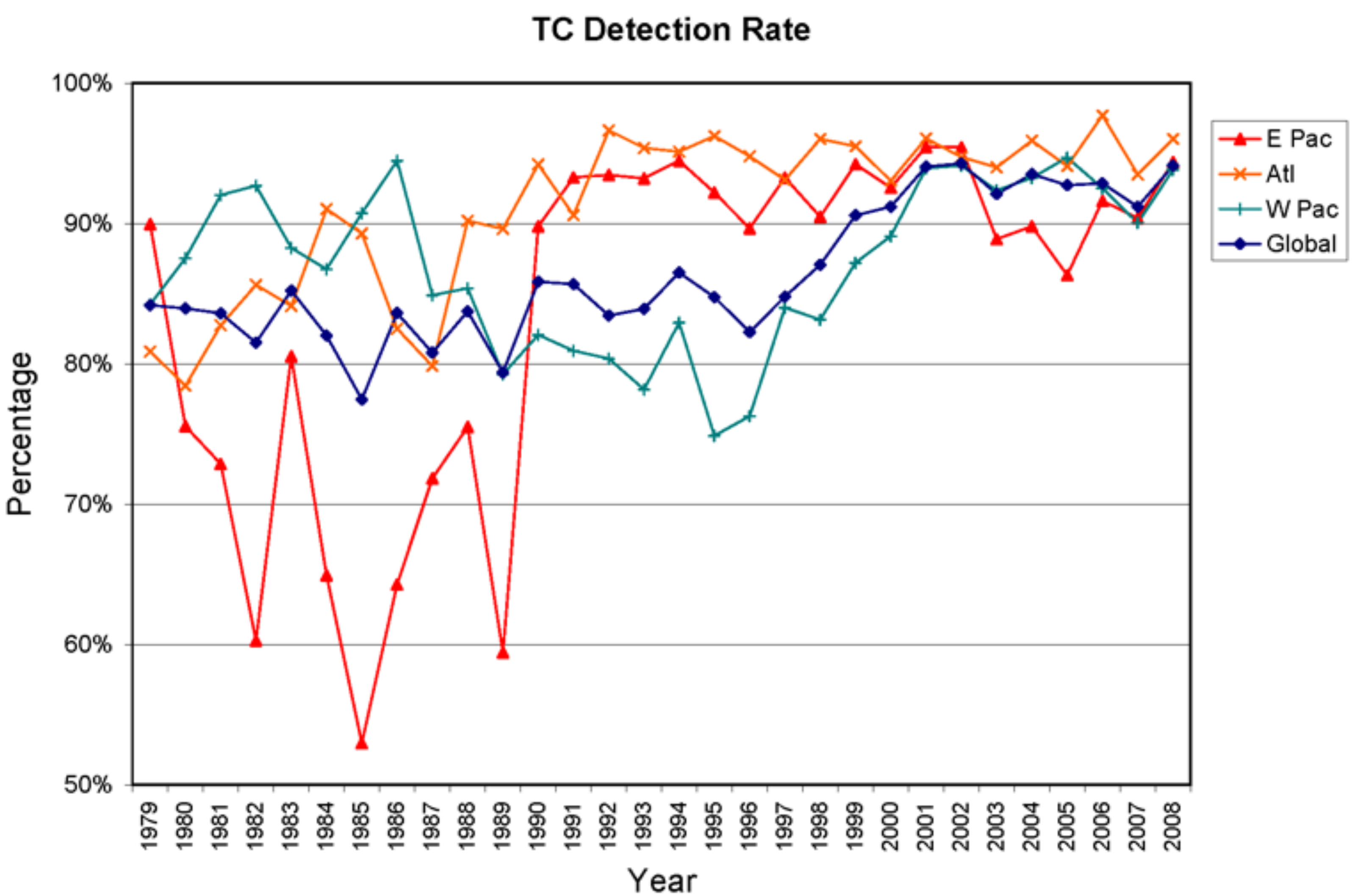

Courtesy: Bob Kistler

Transition to Real Time CFSR

- The operational GSI had gone through several upgrades during the CFSR execution. In March 2009 a major addition was made to the CRTM to simulate the hyper-spectral channels of the IASI instrument, onboard the new ESA METOP satellite and NOAA-19 was added in Dec 2009.

- In order to continue to meet the goal of providing the best available initial conditions to the CFS, in the absence of staff and resources to maintain the CFSR GSI into the future, it was decided to make the transition to the CDAS mode of CFSR in April 2008.

- The operational GSI, present and future implementations, will replace the CFSR GSI, and the coupled prediction model will be "frozen" to that of the CFS v2.

- Historical observational datasets would be replaced with the operational data dumps.

THE OCEAN, SEA ICE AND COUPLER

The global number of temperature observations assimilated per month by the ocean component of the CFSR as a function of depth for the years 1980-2009.

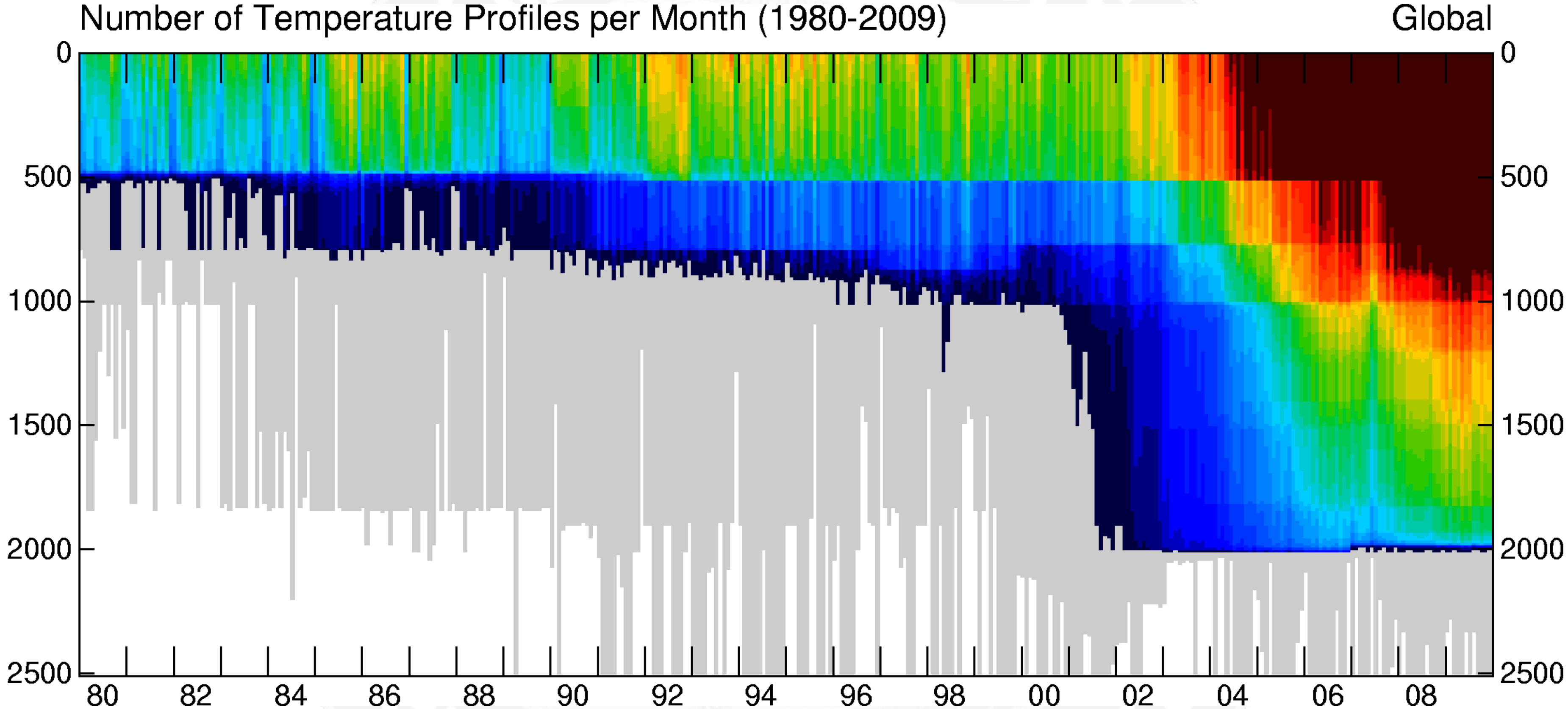

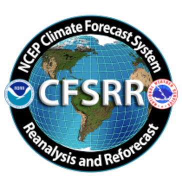

Courtesy: Dave Behringer

The global distribution of all temperature profiles assimilated by the ocean component of the CFSR for the year 1985. The distribution is dominated by XBT profiles collected along shipping routes.

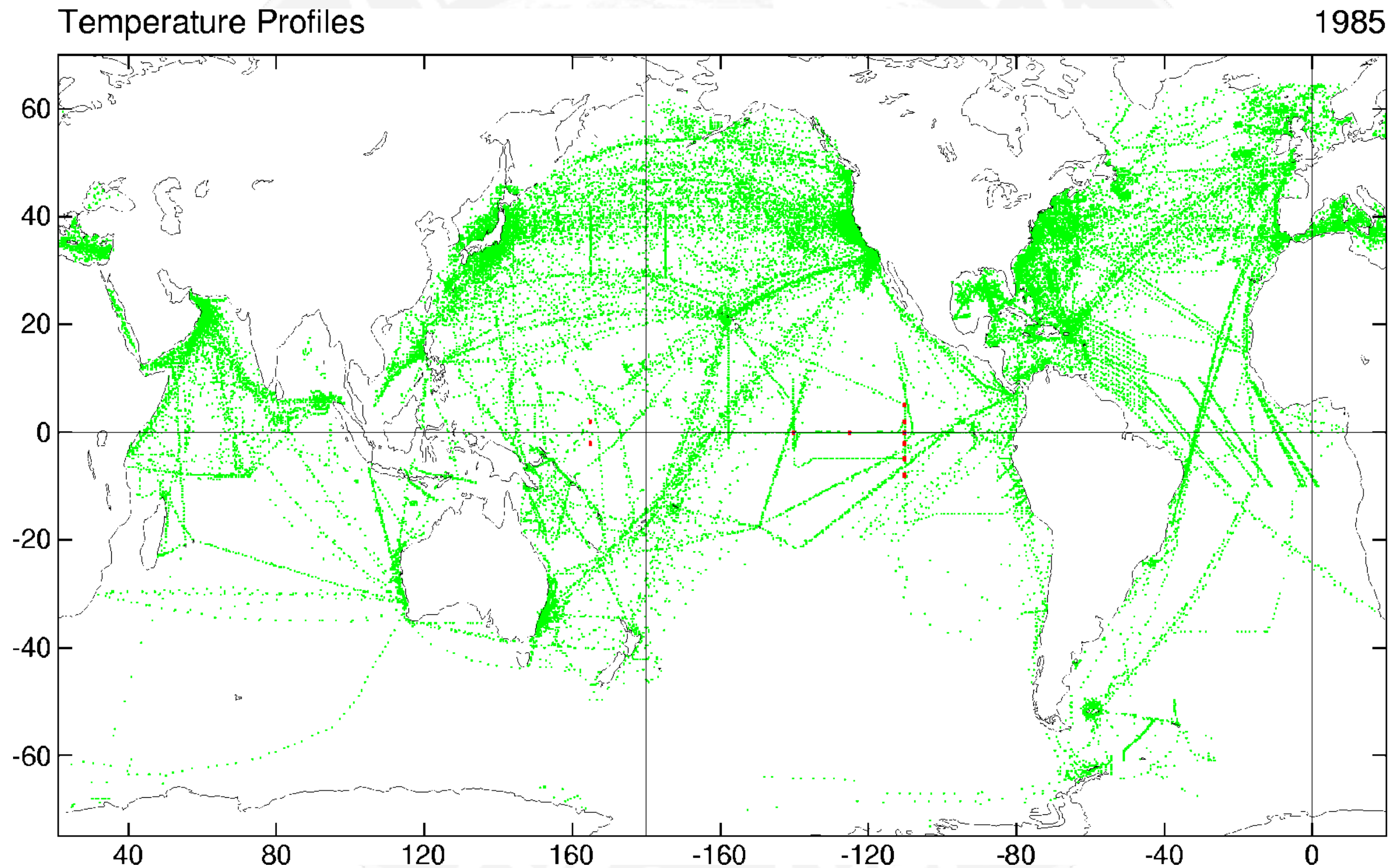

Courtesy: Dave Behringer

The global distribution of all temperature profiles assimilated by the ocean component of the CFSR for the year 2008. The Argo array (blue) provides a nearly uniform global distribution of temperature profiles

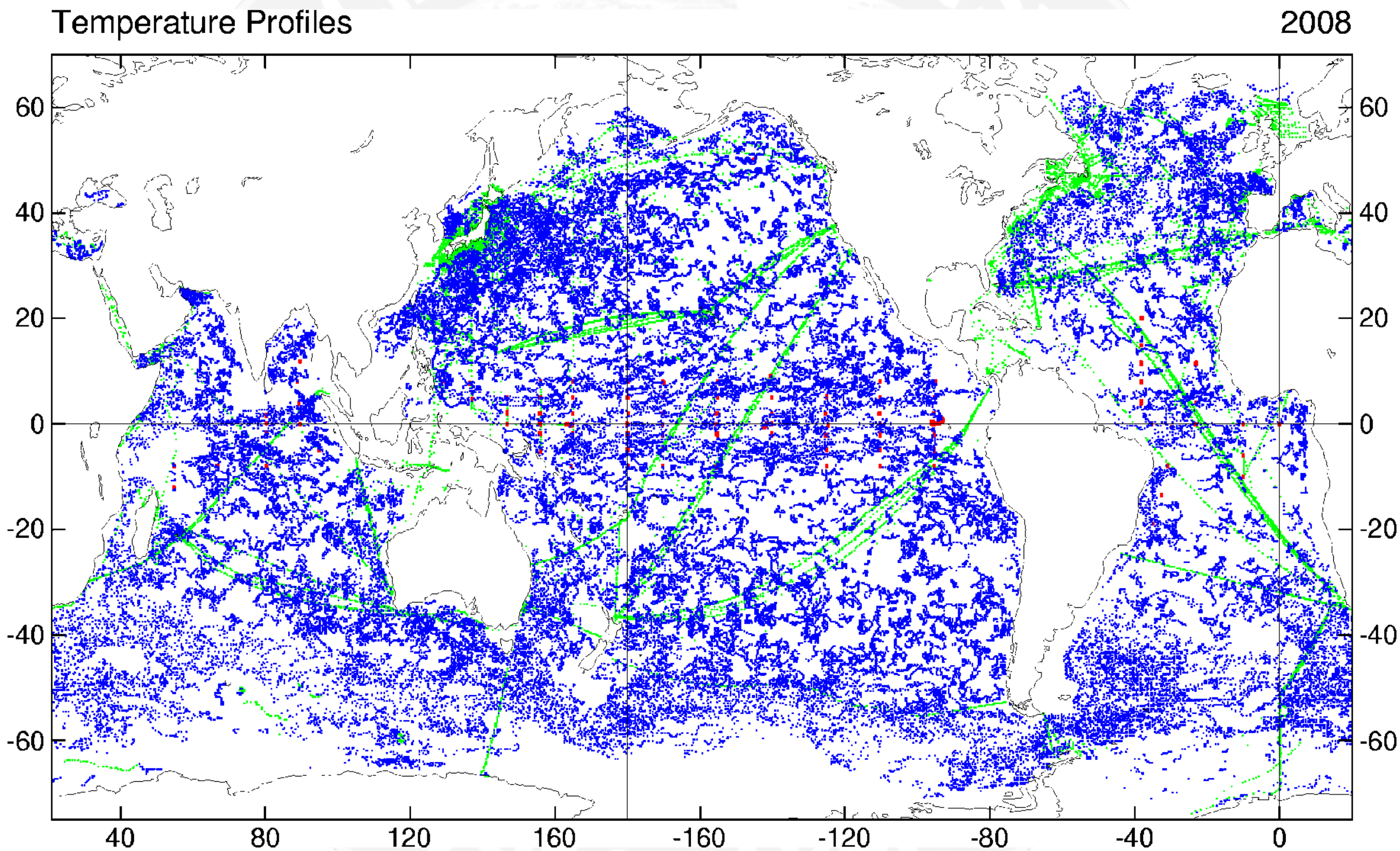

Courtesy: Dave Behringer

The subsurface temperature mean for an equatorial cross-section

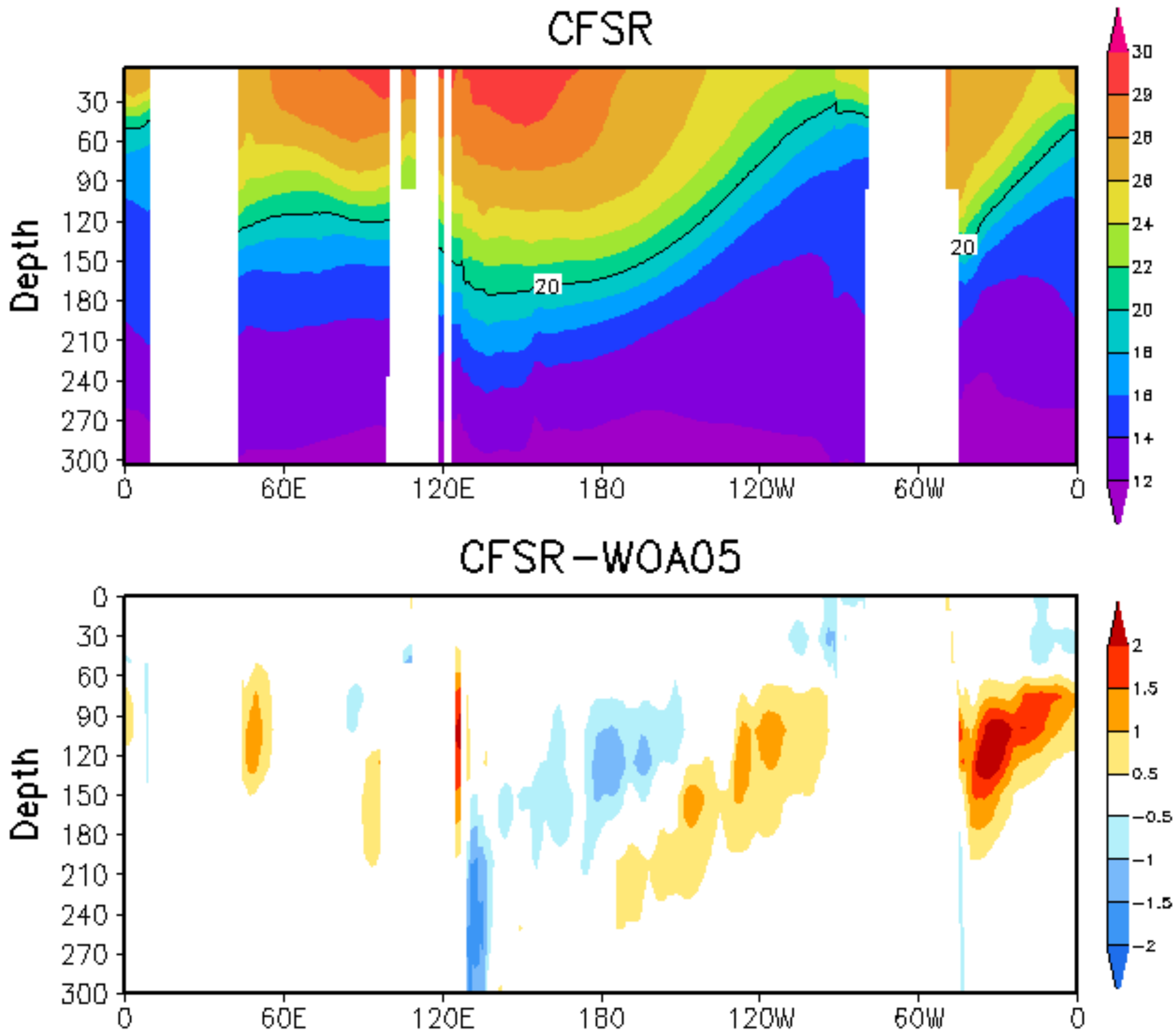

Courtesy: Sudhir Nadiga

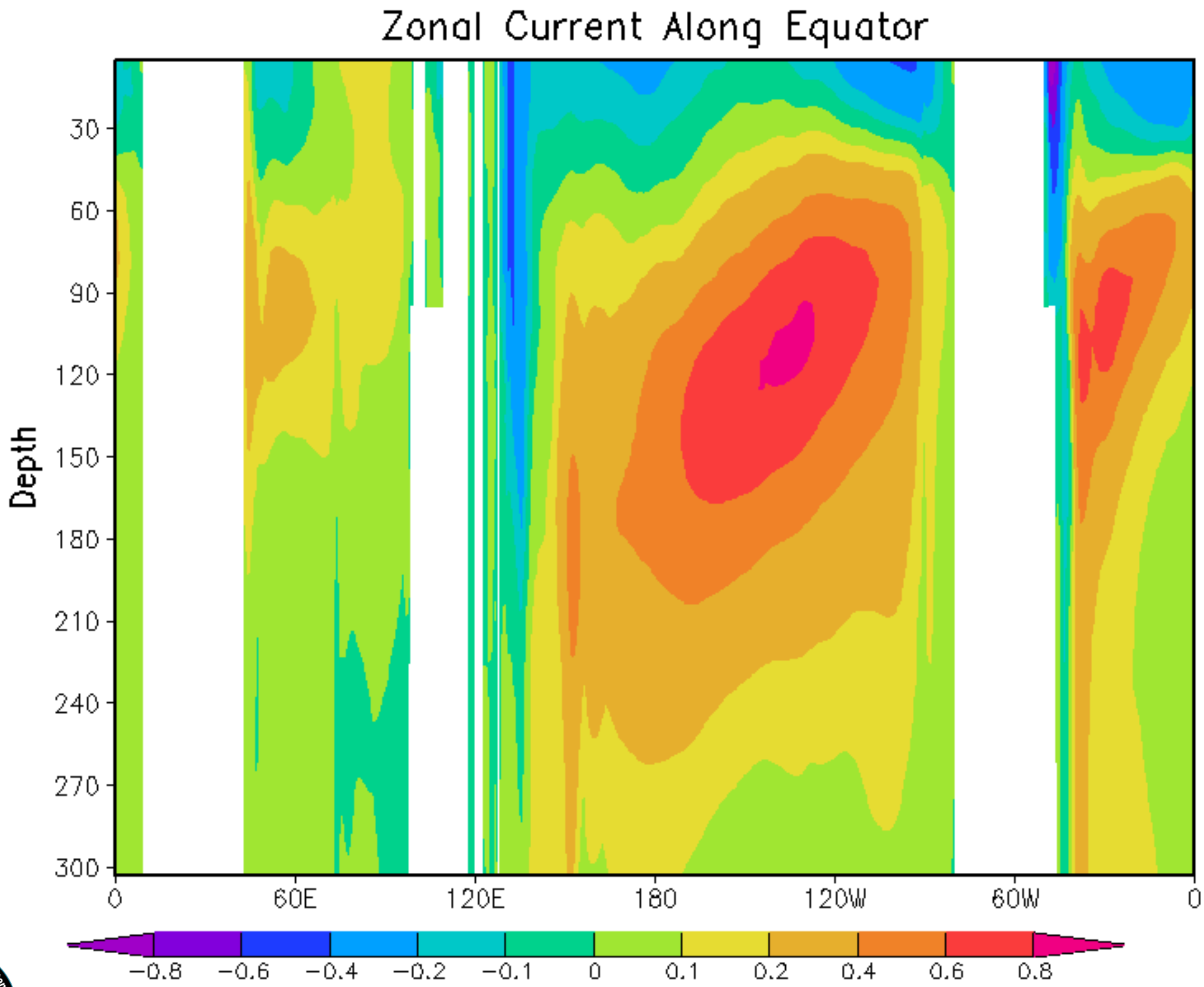

Courtesy: Sudhir Nadiga

The Diurnal Cycle of SST in CFSR

The diurnal cycle of SST in the TAO data (black line) and CFSR (blue line) in the Equatorial Pacific for DJF (top three panels) and JJA (bottom three panels).

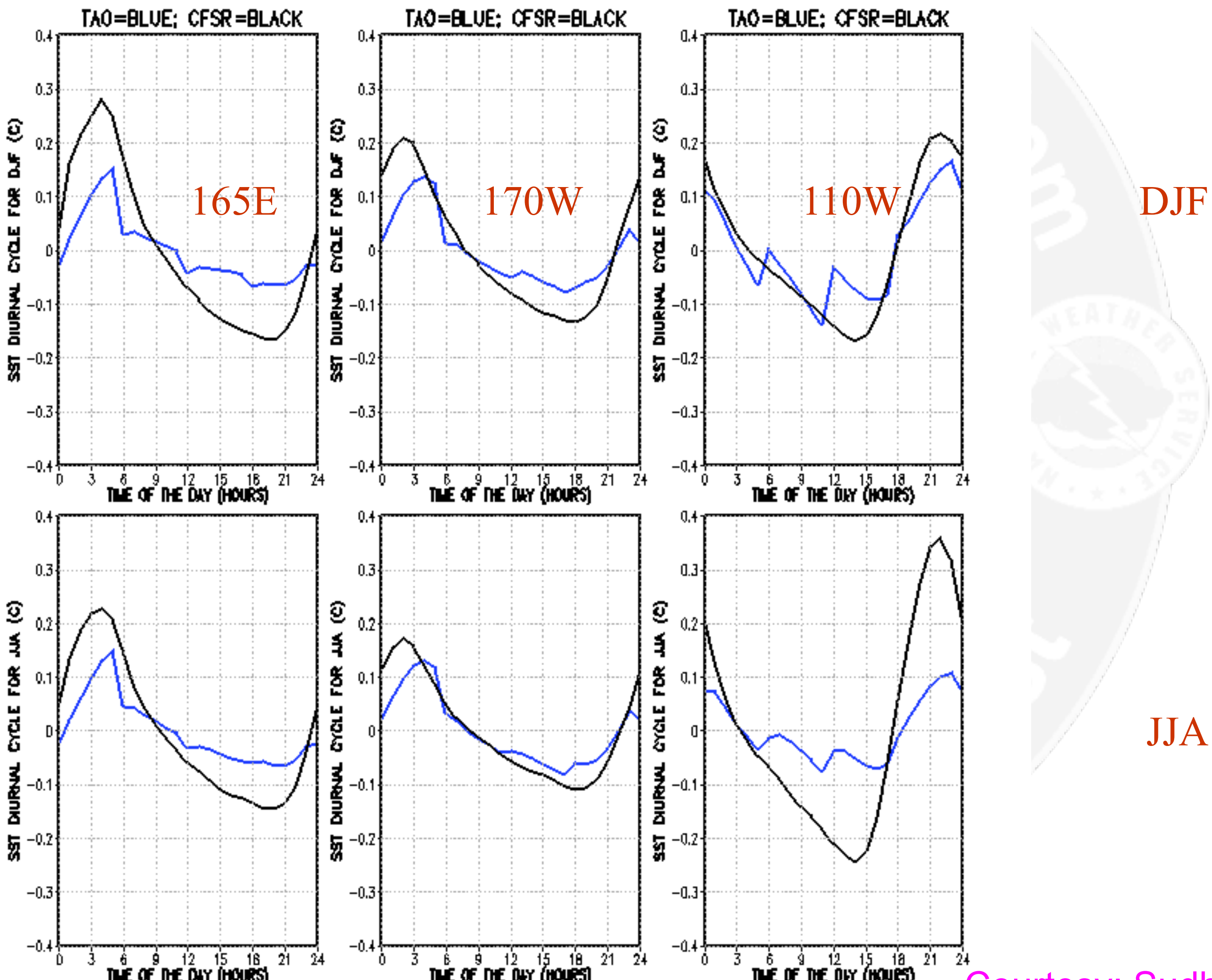

Courtesy: Sudhir Nadiga

The vertically averaged temperature (surface to 300 m depth) for CFSR for 1979-2008, and its difference with observations from World Ocean Atlas

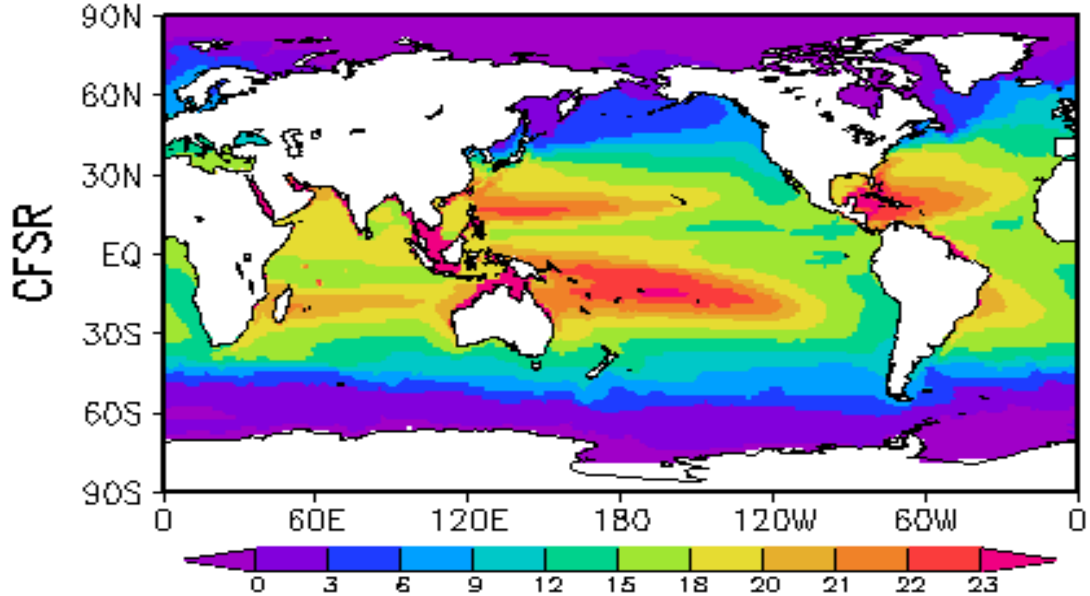

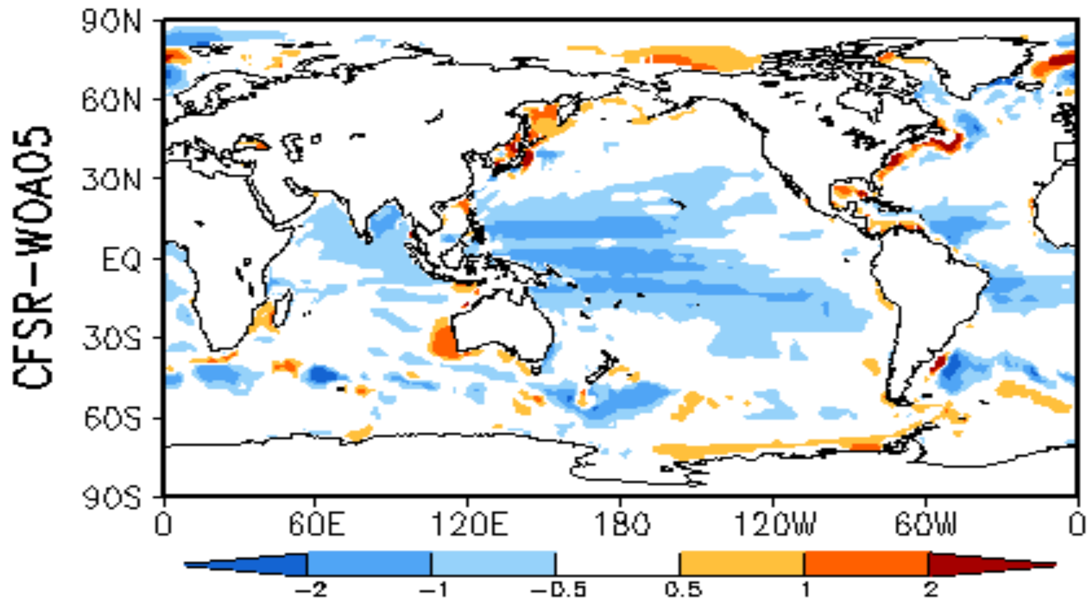

Courtesy: Sudhir Nadiga

Zonal and meridional surface velocities for CFSR (top left and top right) and differences between CFSR and drifters from the Surface Velocity Program of TOGA (bottom panels).

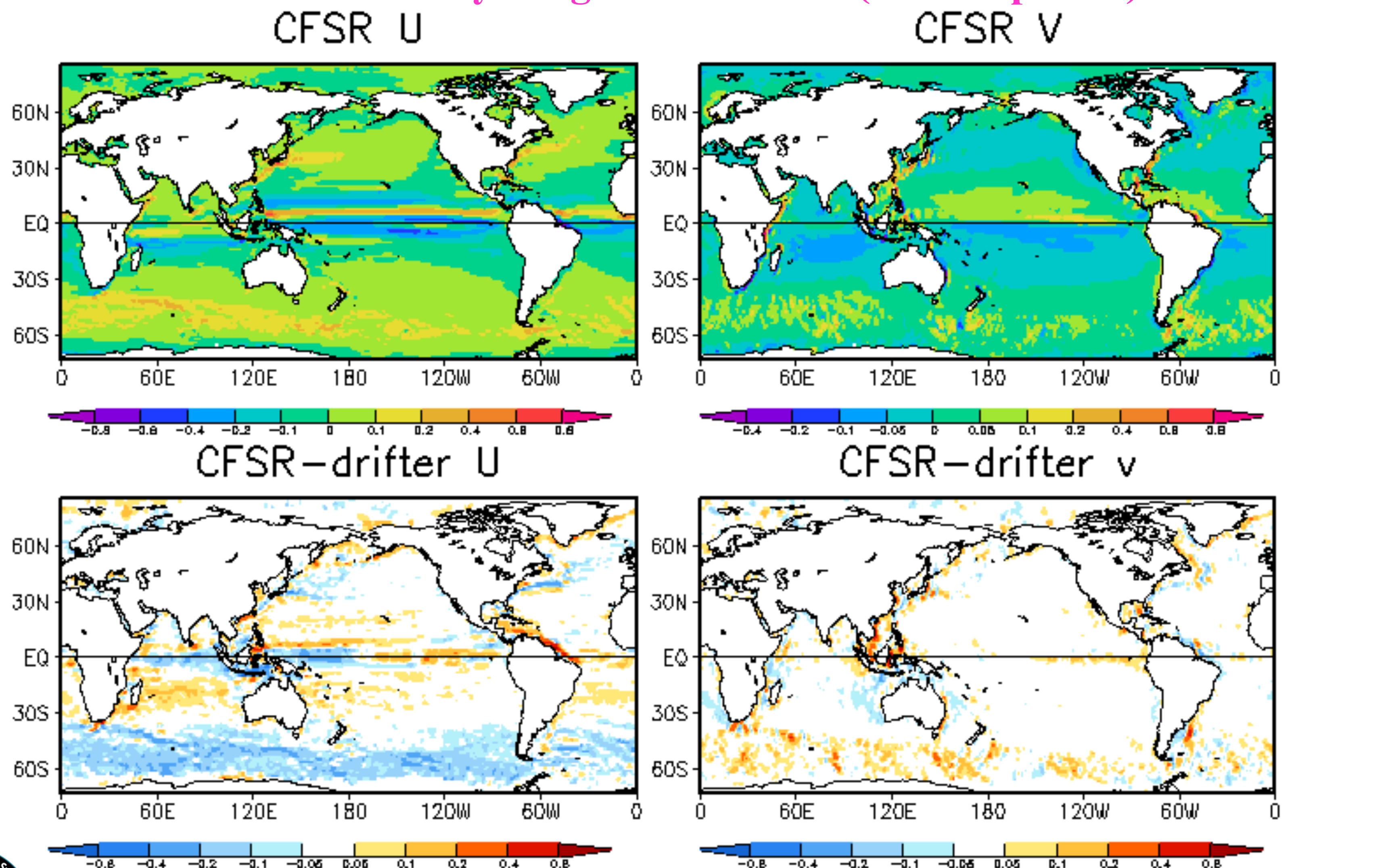

Courtesy: Sudhir Nadiga

The first two EOFs of the SSH variability for the CFSR (left) and for TOPEX satellite altimeter data (right) for the period: 1993-2008.
The time series amplitude factors are plotted in the bottom panel.

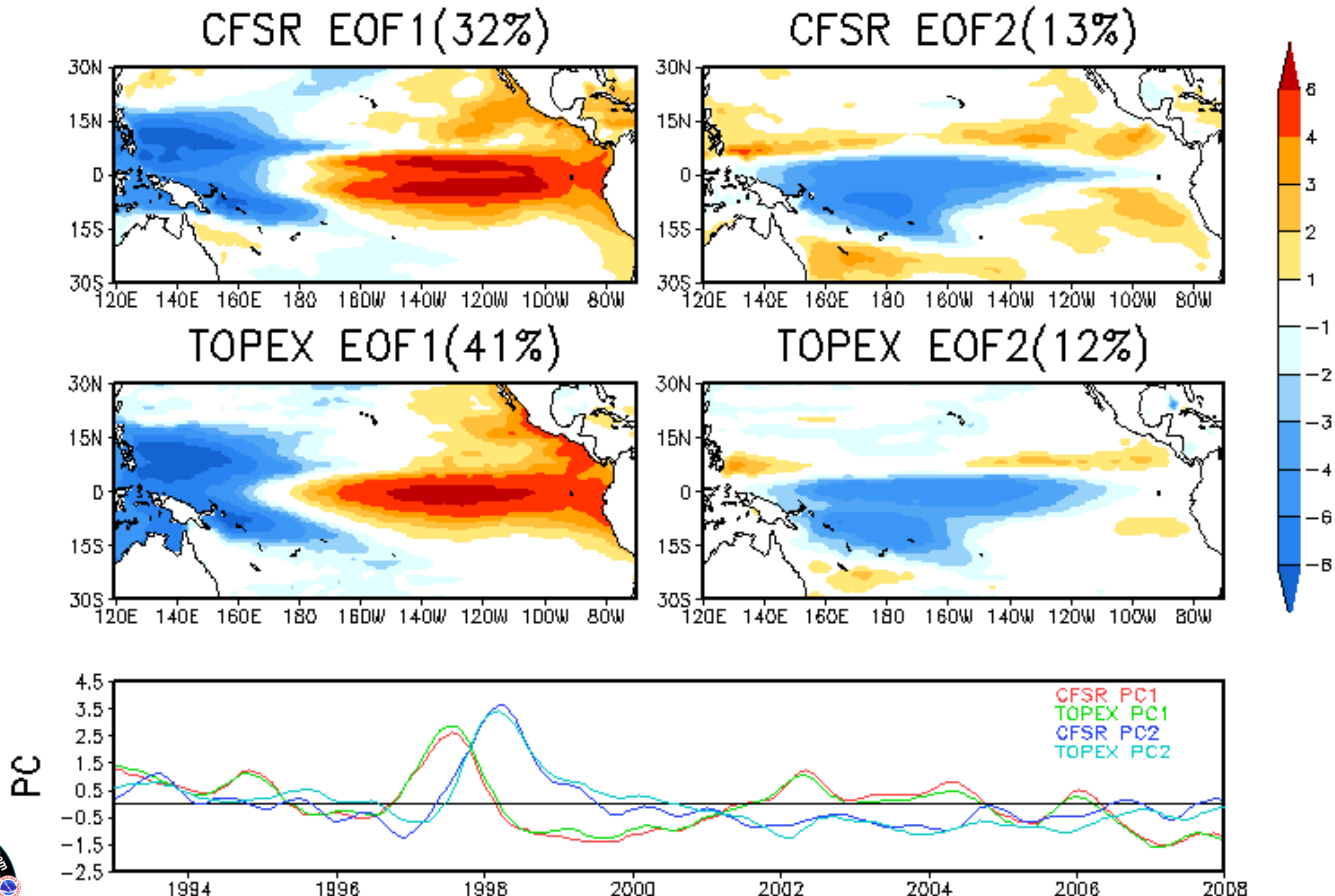

Courtesy: Sudhir Nadiga

Monthly mean sea ice concentration for the Arctic from CFSR (6-hr forecasts)

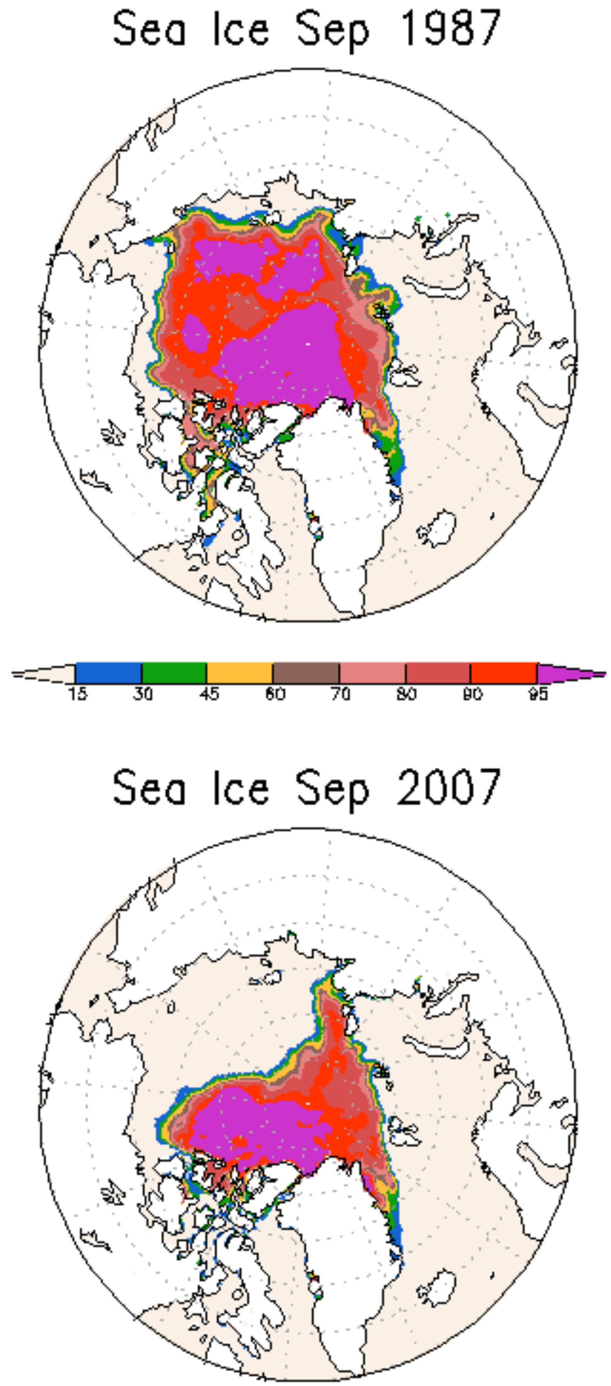

Courtesy: Xingren Wu

Monthly mean Sea ice extent (10^6 km^2) for the Arctic (top) and Antarctic (bottom) from CFSR (6-hr forecasts). 5-year running mean is added to detect long term trends.

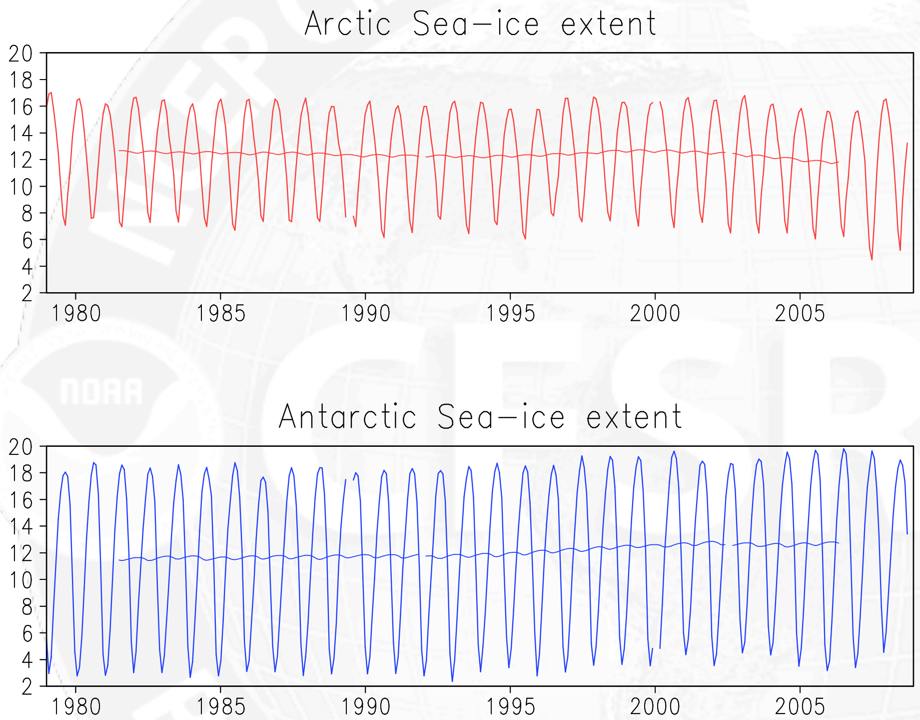

Courtesy: Xingren Wu

Problem for Sea-Ice Concentration in CFSRR for 2009:

Due to the degradation of one of the DMSP F15 sensor channels in February, and a problem from F13 in early May 2009

Extent of Sea-Ice for 2009 (from R. Grumbine)

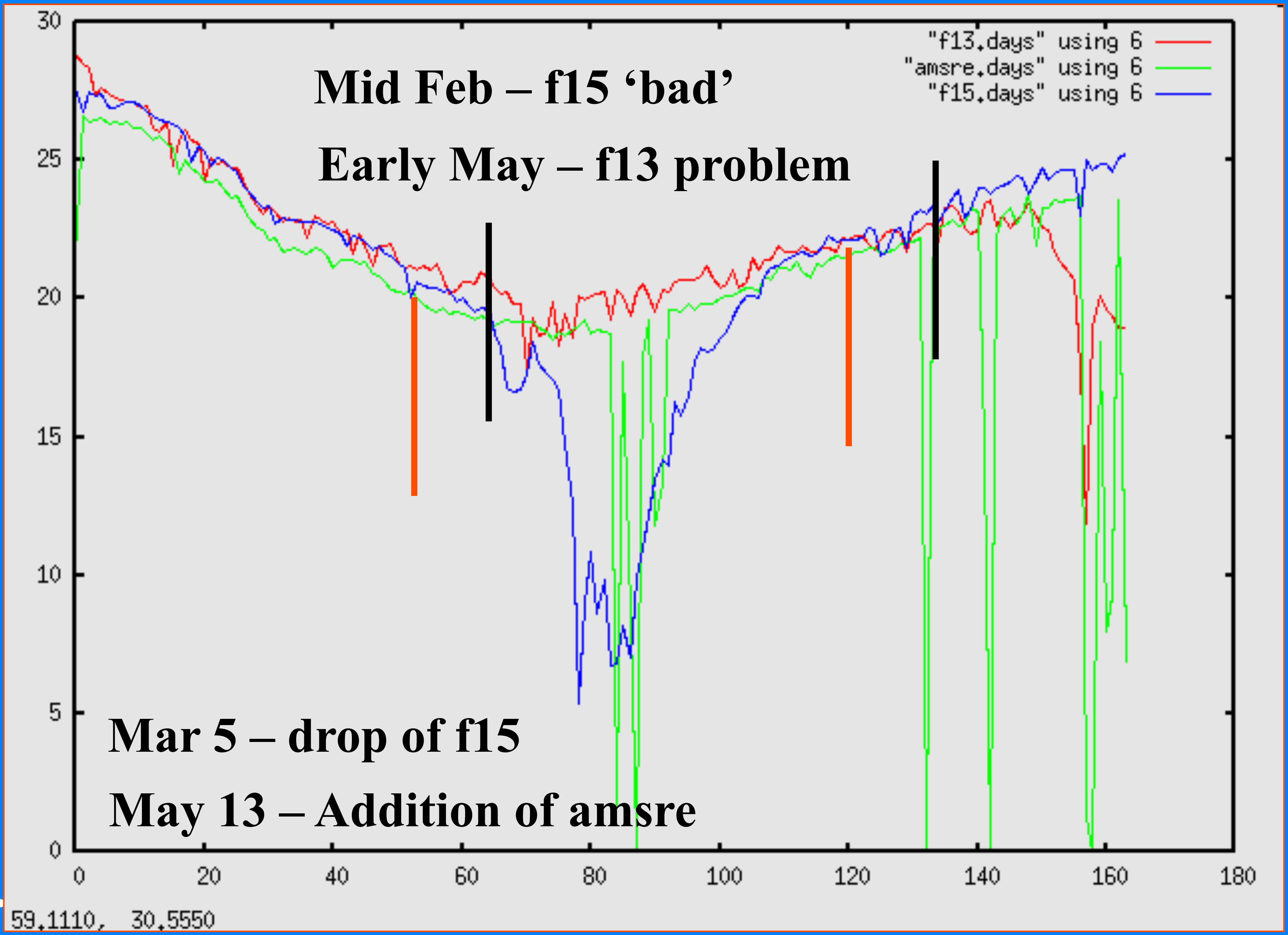

CFSRR ICE FRACTION for 00Z30APR

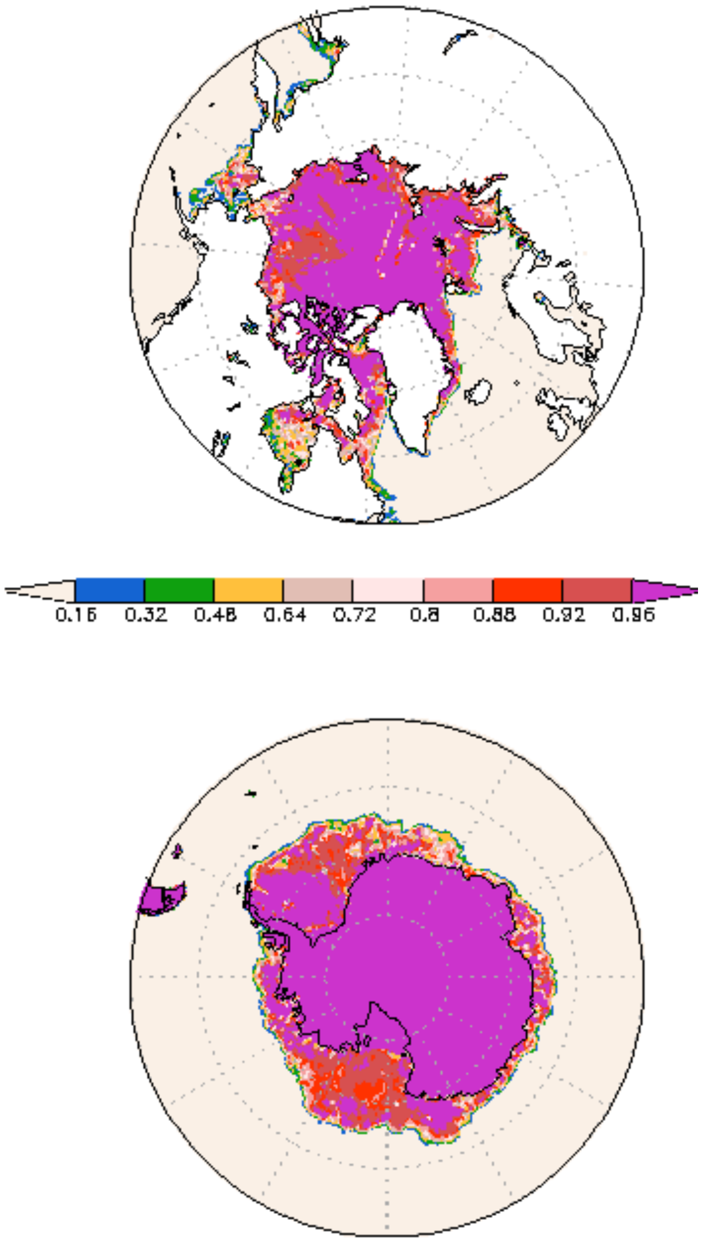

Min, Max = 0 1.57

ROBERT GRUMBINE. MMAB/EMC/NCEP/NWS/NOAA

CFSRR ICE FRACTION for 00Z01MAY2009

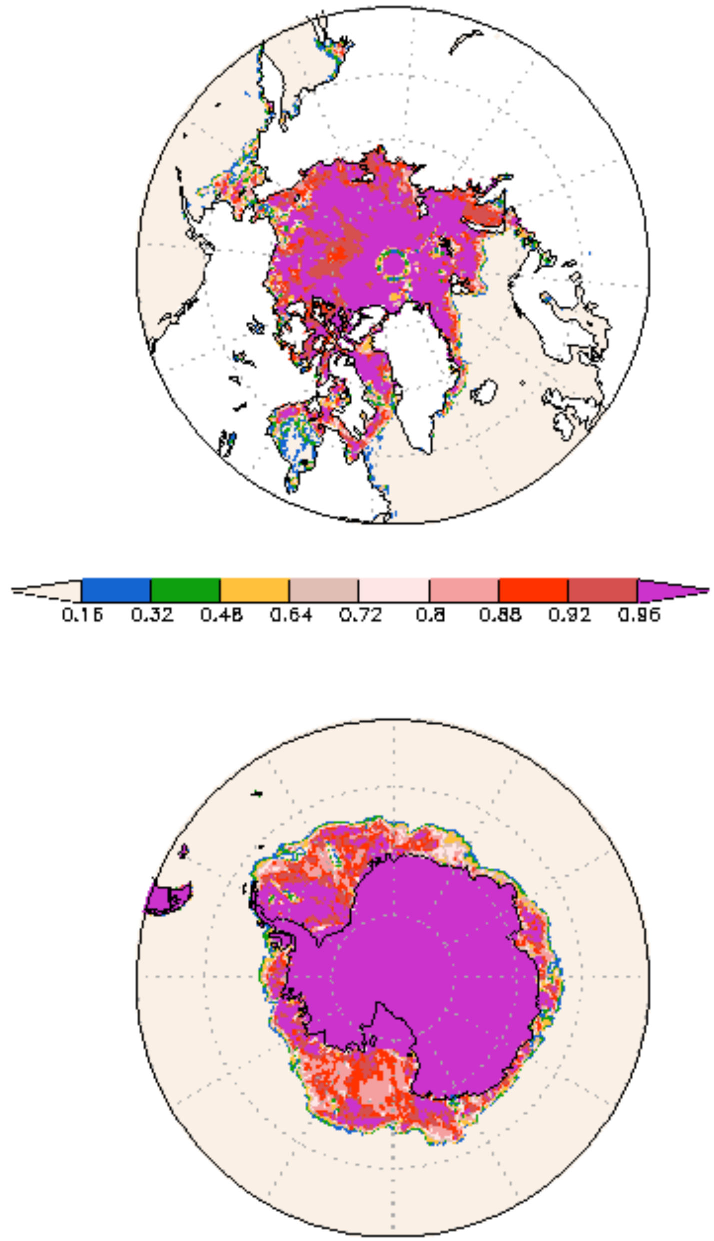

Min, Max = 0 1.57

ROBERT GRUMBINE. MMAB/EMC/NCEP/NWS/NOAA

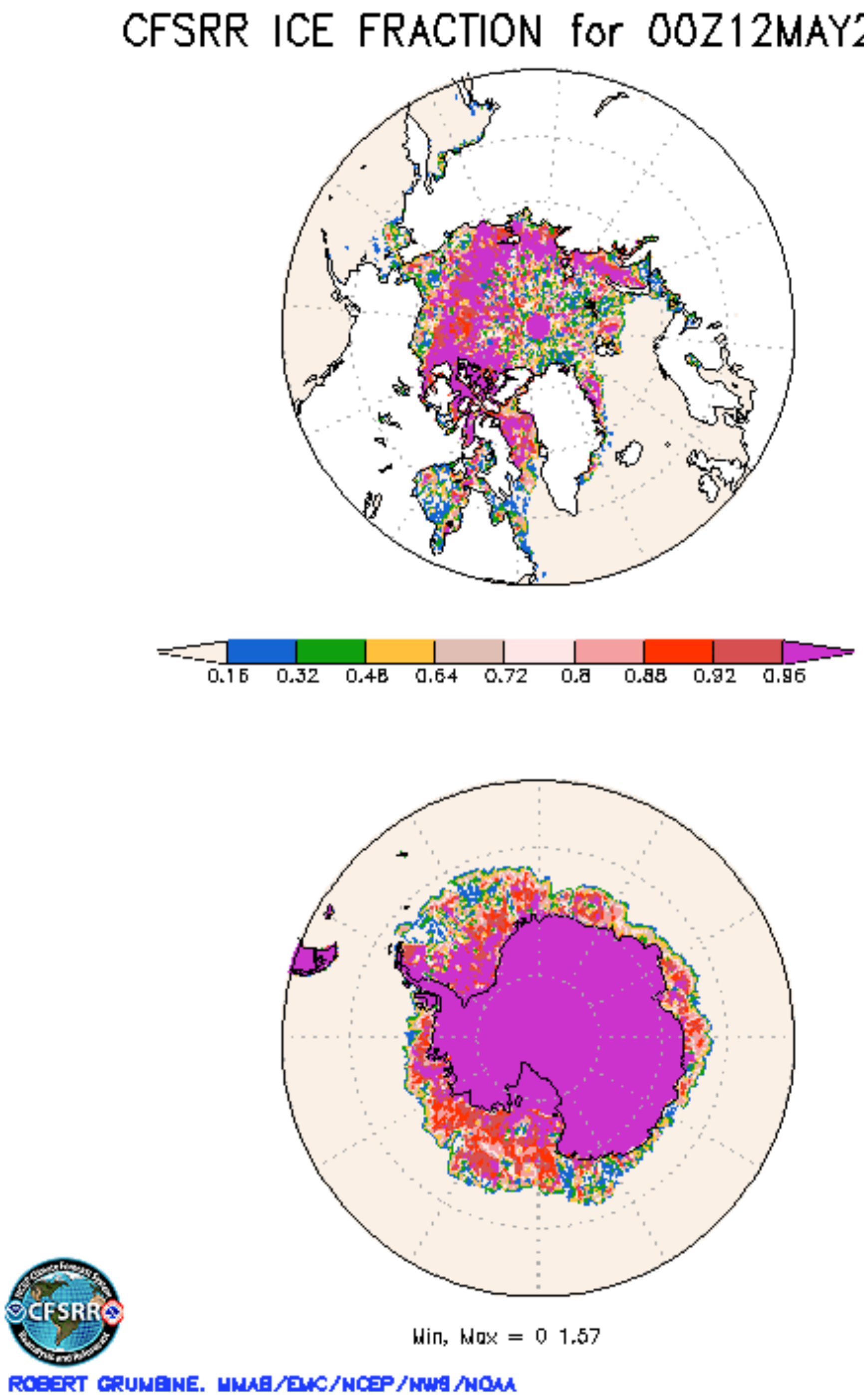
CFSRR ICE FRACTION for 00Z12MAY2
0.15 0.32 0.48 0.64 0.72 0.8 0.88 0.92 0.96
Min, Max = 0 1.57
CFSRR
ROBERT GRUMBINE, MMAB/EMC/NCEP/NWS/NOAA

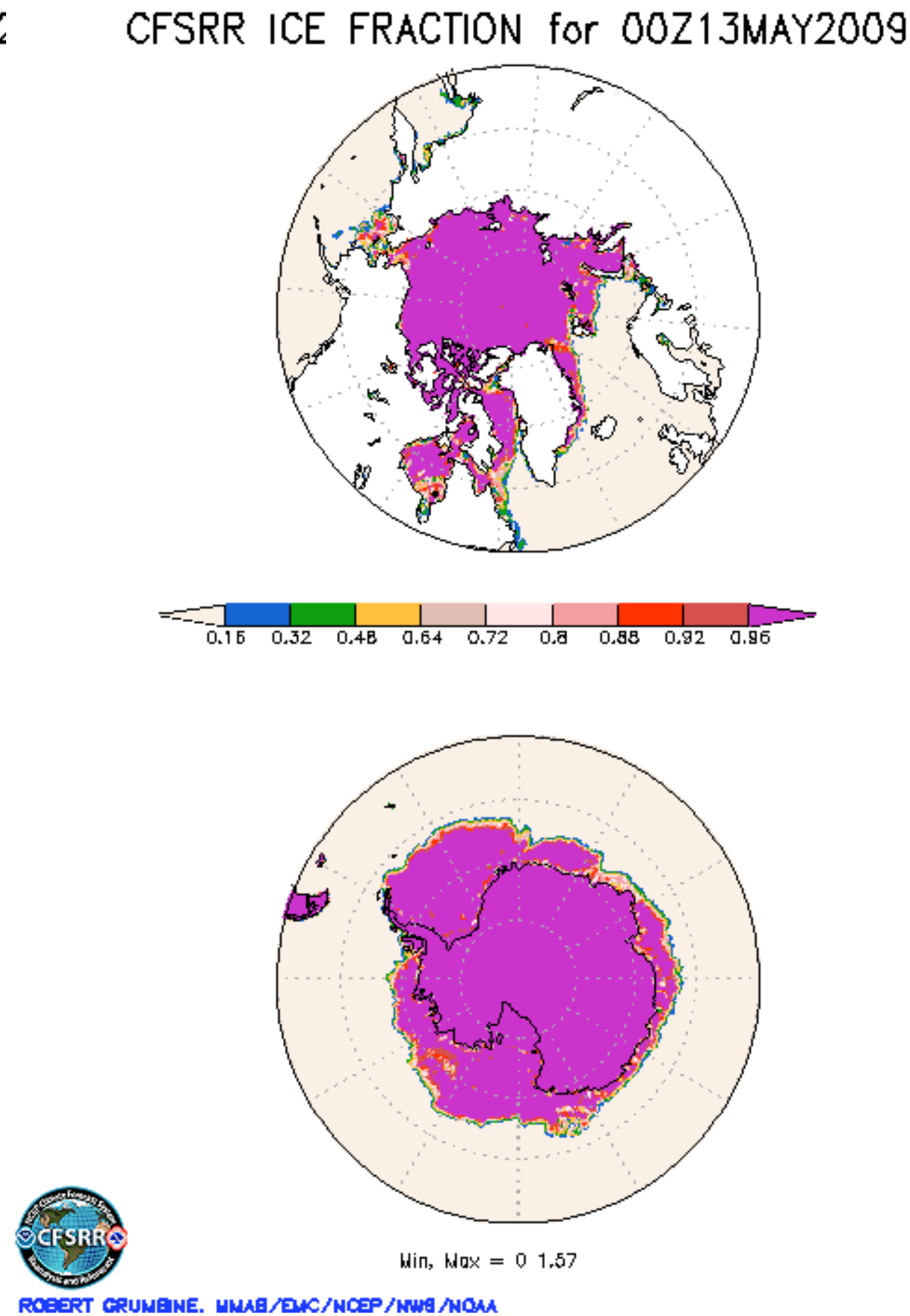
CFSRR ICE FRACTION for 00Z13MAY2009
0.15 0.32 0.48 0.64 0.72 0.8 0.88 0.92 0.96
Min, Max = 0 1.57
CFSRR
ROBERT GRUMBINE, MMAB/EMC/NCEP/NWS/NOAA

Possible Solution:

(1) Model guess

(2) **Persistence**

(3) …

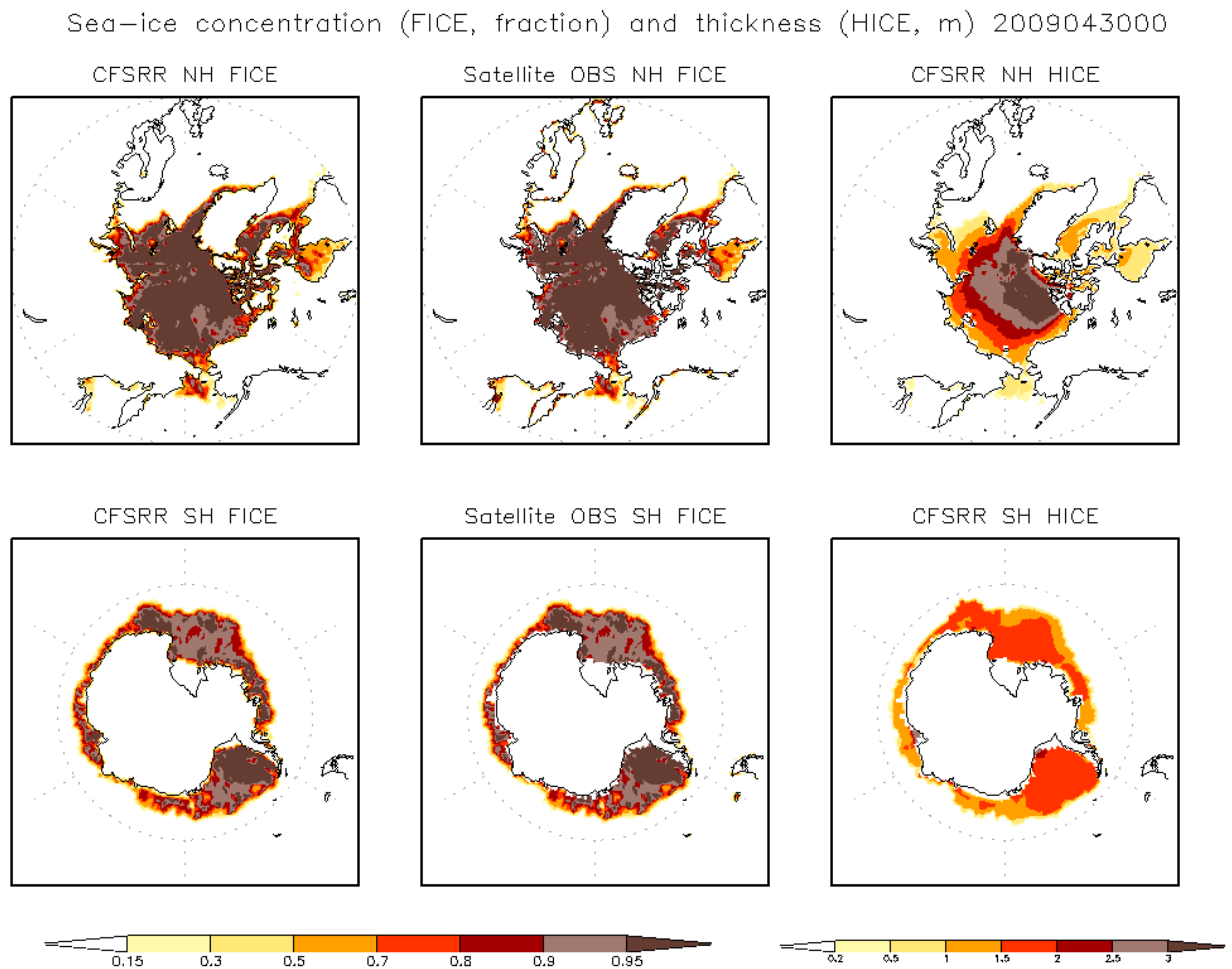

Sea–ice concentration (FICE, fraction) and thickness (HICE, m) 2009043000
CFSRR NH FICE
Satellite OBS NH FICE
CFSRR NH HICE
CFSRR SH FICE
Satellite OBS SH FICE
CFSRR SH HICE
0.15
0.3
0.5
0.7
0.8
0.9
0.95
0.2
0.5
1
1.5
2
2.5
3

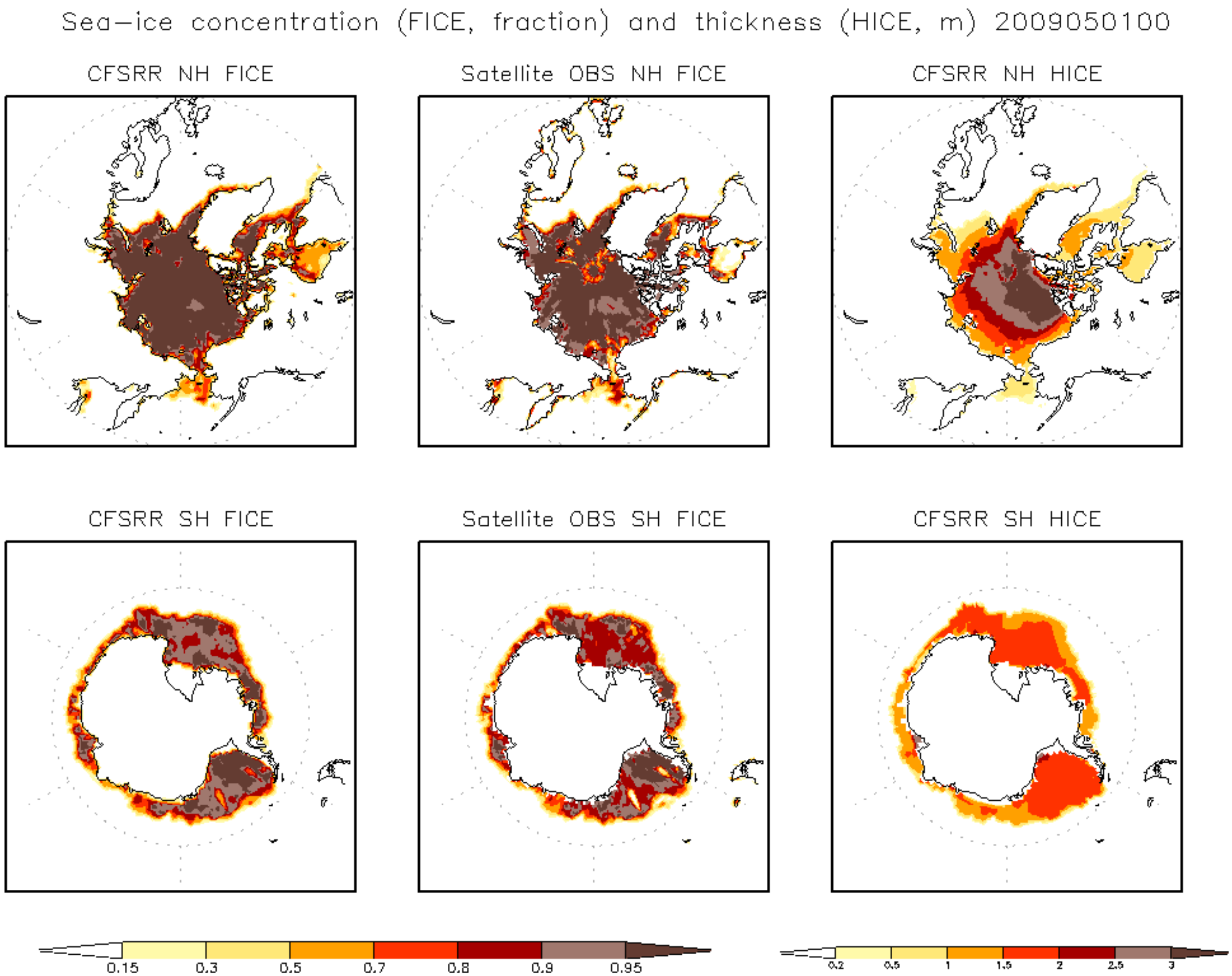
Sea–ice concentration (FICE, fraction) and thickness (HICE, m) 2009050100
CFSRR NH FICE
Satellite OBS NH FICE
CFSRR NH HICE
CFSRR SH FICE
Satellite OBS SH FICE
CFSRR SH HICE
0.15 0.3 0.5 0.7 0.8 0.9 0.95
0.2 0.5 1 1.5 2 2.5 3

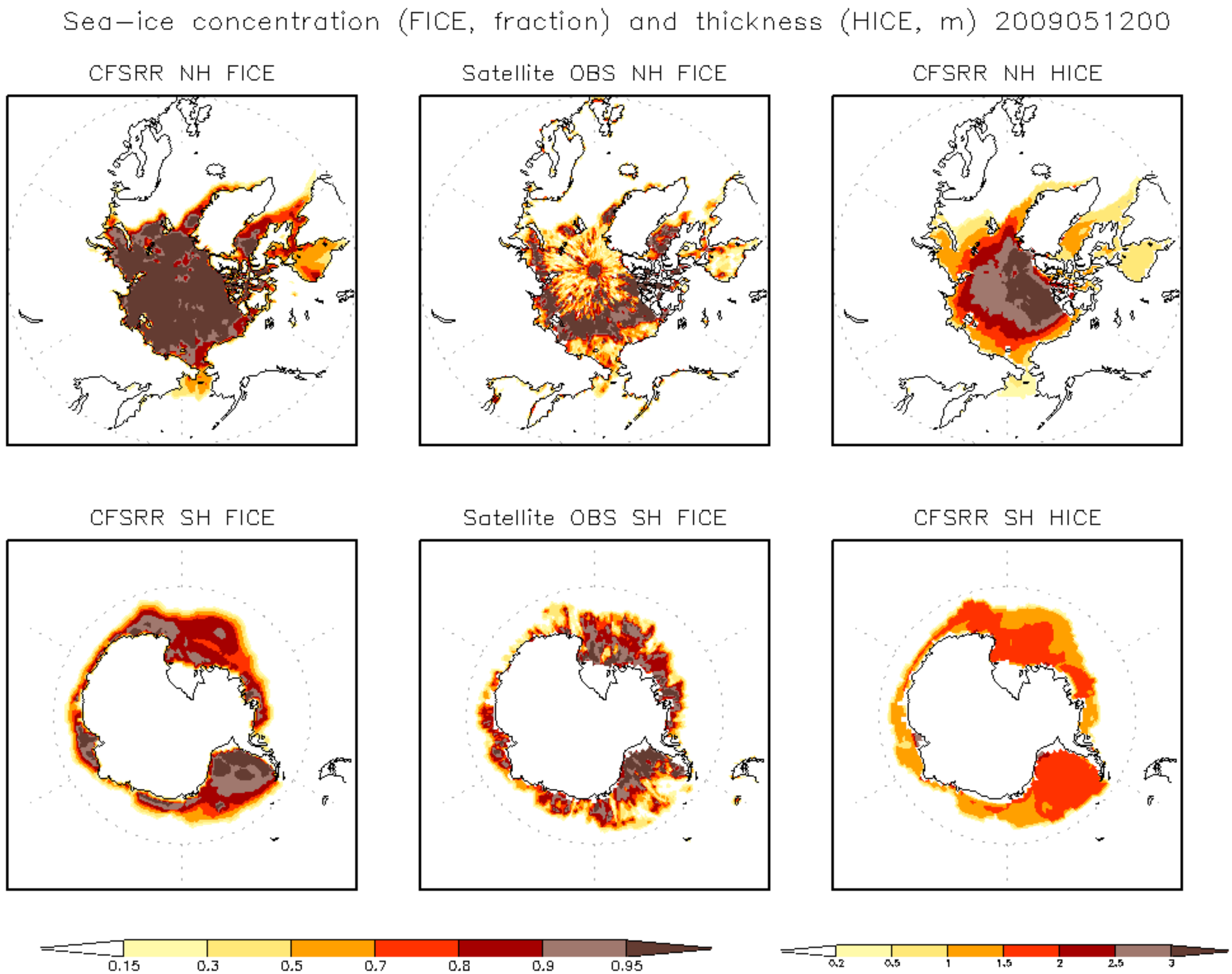
Sea–ice concentration (FICE, fraction) and thickness (HICE, m) 2009051200
CFSRR NH FICE
Satellite OBS NH FICE
CFSRR NH HICE
CFSRR SH FICE
Satellite OBS SH FICE
CFSRR SH HICE
0.15 0.3 0.5 0.7 0.8 0.9 0.95
0.2 0.5 1 1.5 2 2.5 3

Sea–ice concentration (FICE, fraction) and thickness (HICE, m) 2009051300

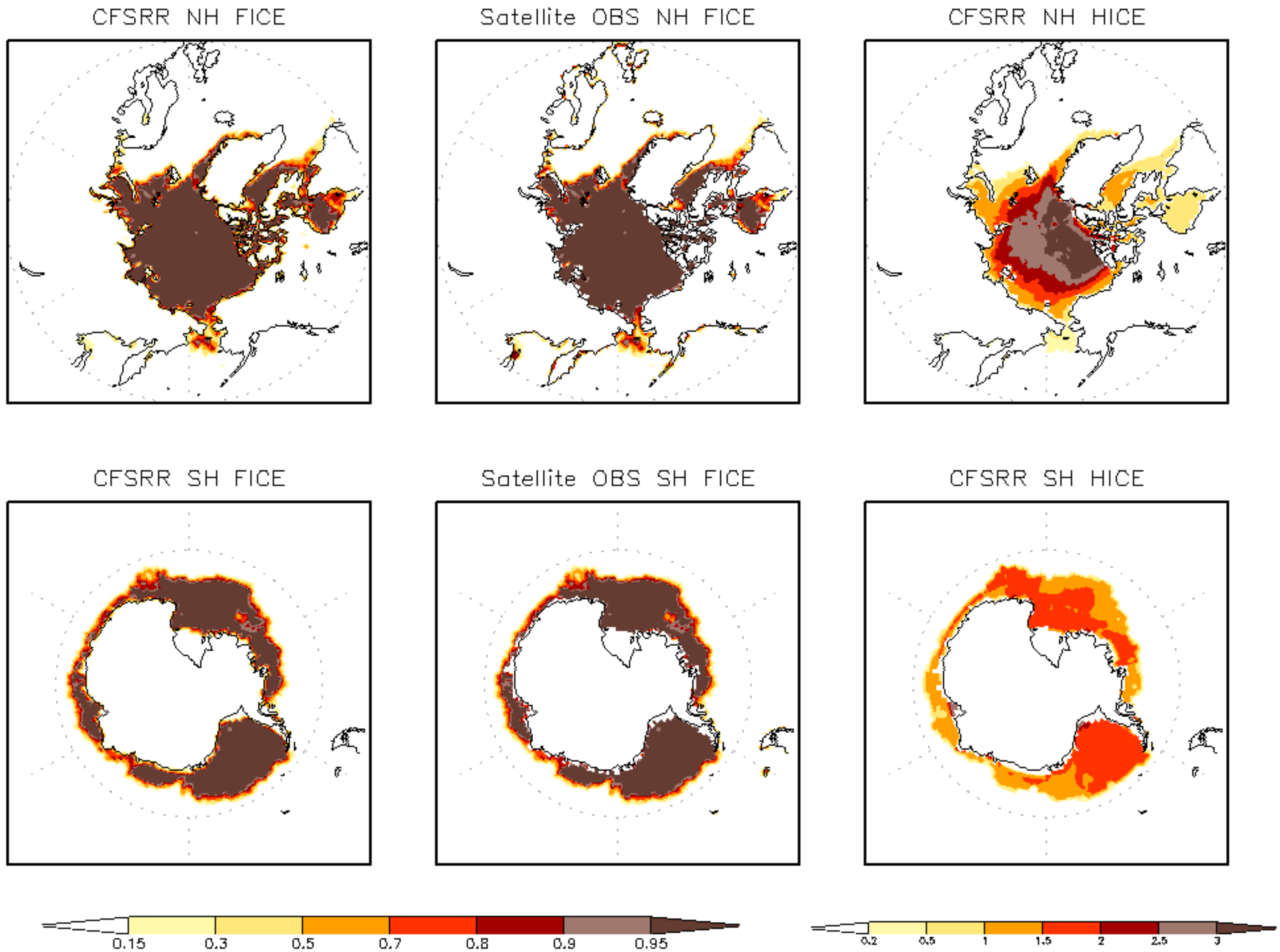

Sea–ice concentration (FICE, fraction) and thickness (HICE, m) 2009042500

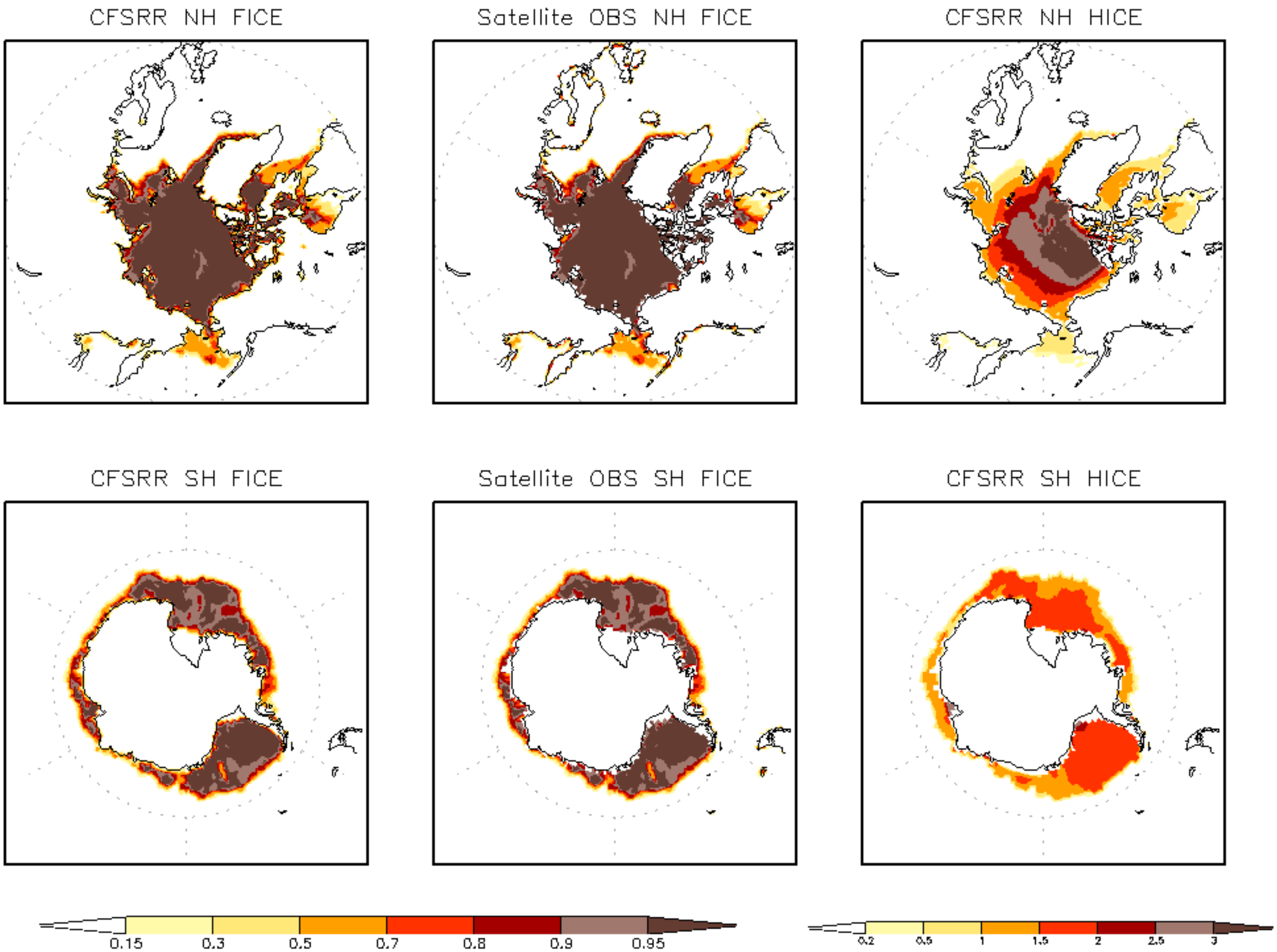

Summary

- Using model guess for sea-ice for early May 2009 produces reasonable sea-ice distribution.

- The outcome appear to be much better than using the sea-ice from analysis due to the problem caused by satellite.

CFS grid architecture in the coupler. ATM is MOM4 atmospheric model (dummy for CFS), SBL is the surface boundary layer where the exchange grid is located, LAND is MOM4 land model (dummy for CFS), ICE is MOM4 sea ice model and OCN is MOM4 ocean model.

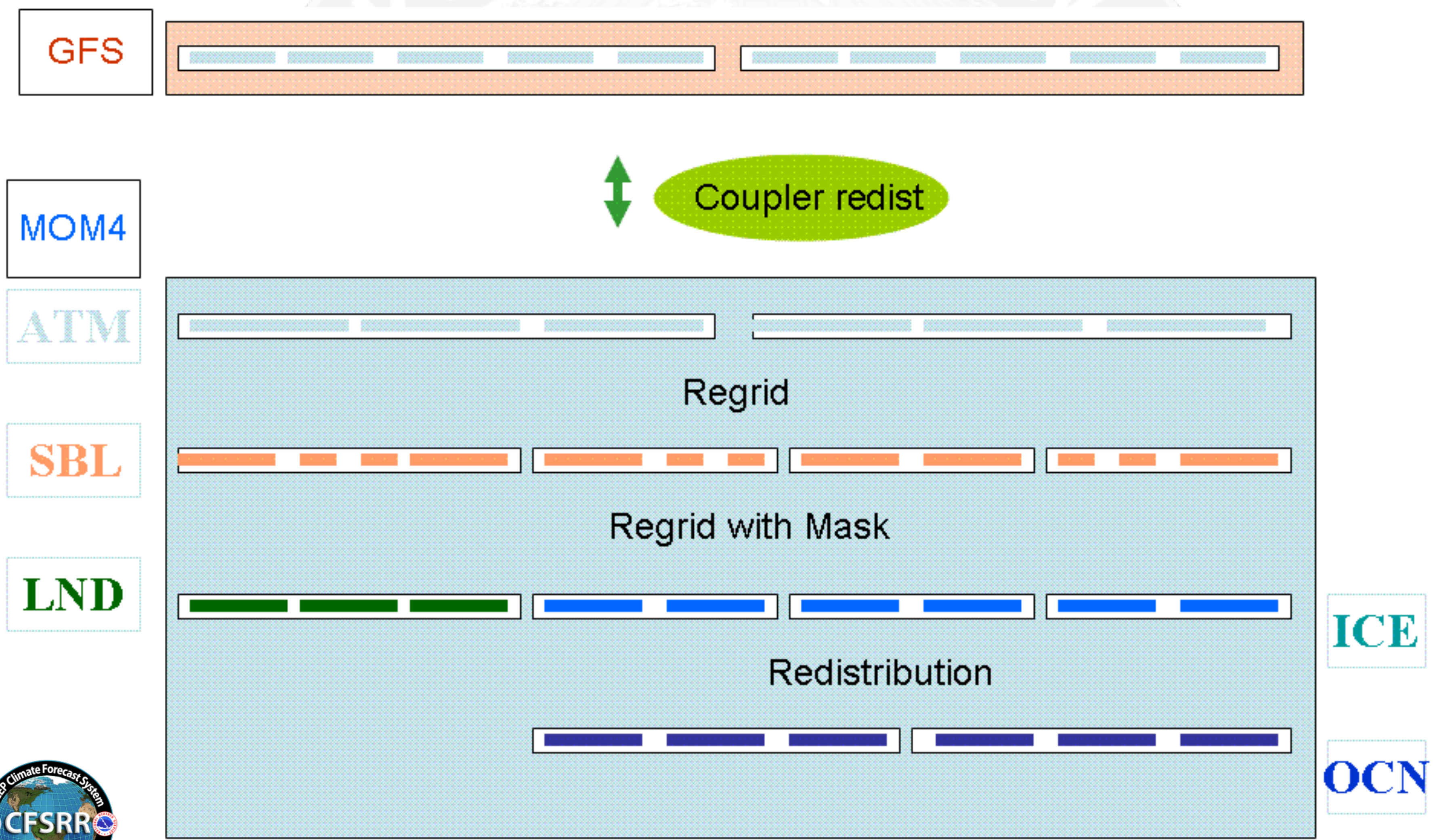

Courtesy: Jun Wang

Data Flow

Fast loop: if Δa= Δc= Δi, coupled at every time step

Slow loop: Δo

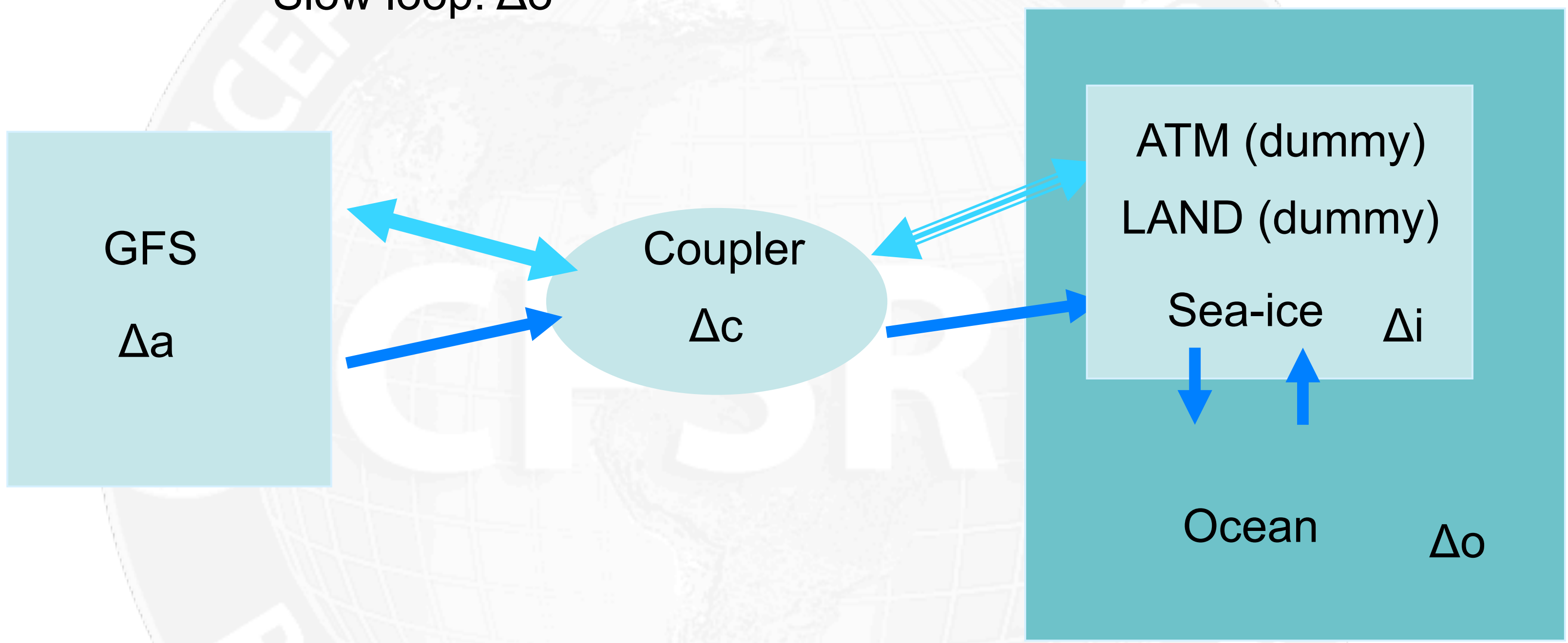

- Fast loop: can be coupled at every time step
- Slow loop:
- a. passing variables accumulated in fast loop
- b. can be coupled at each ocean time step

Courtesy: Jun Wang

Passing variables

- Atmosphere to sea-ice:
- - downward short- and long-wave radiations,
- - tbot, qbot, ubot, vbot, pbot, zbot,
- - snowfall, psurf, coszen
- Atmosphere to ocean:
- - net downward short- and long-radiations,
- - sensible and latent heat fluxes,
- - wind stresses and precipitation
- Sea-ice/ocean to atmosphere
  - surface temperature,
  - sea-ice fraction and thickness, and snow depth

Courtesy: Jun Wang

THE SURFACE

2-meter volumetric soil moisture climatology of CFSR for May averaged over 1980-2008.

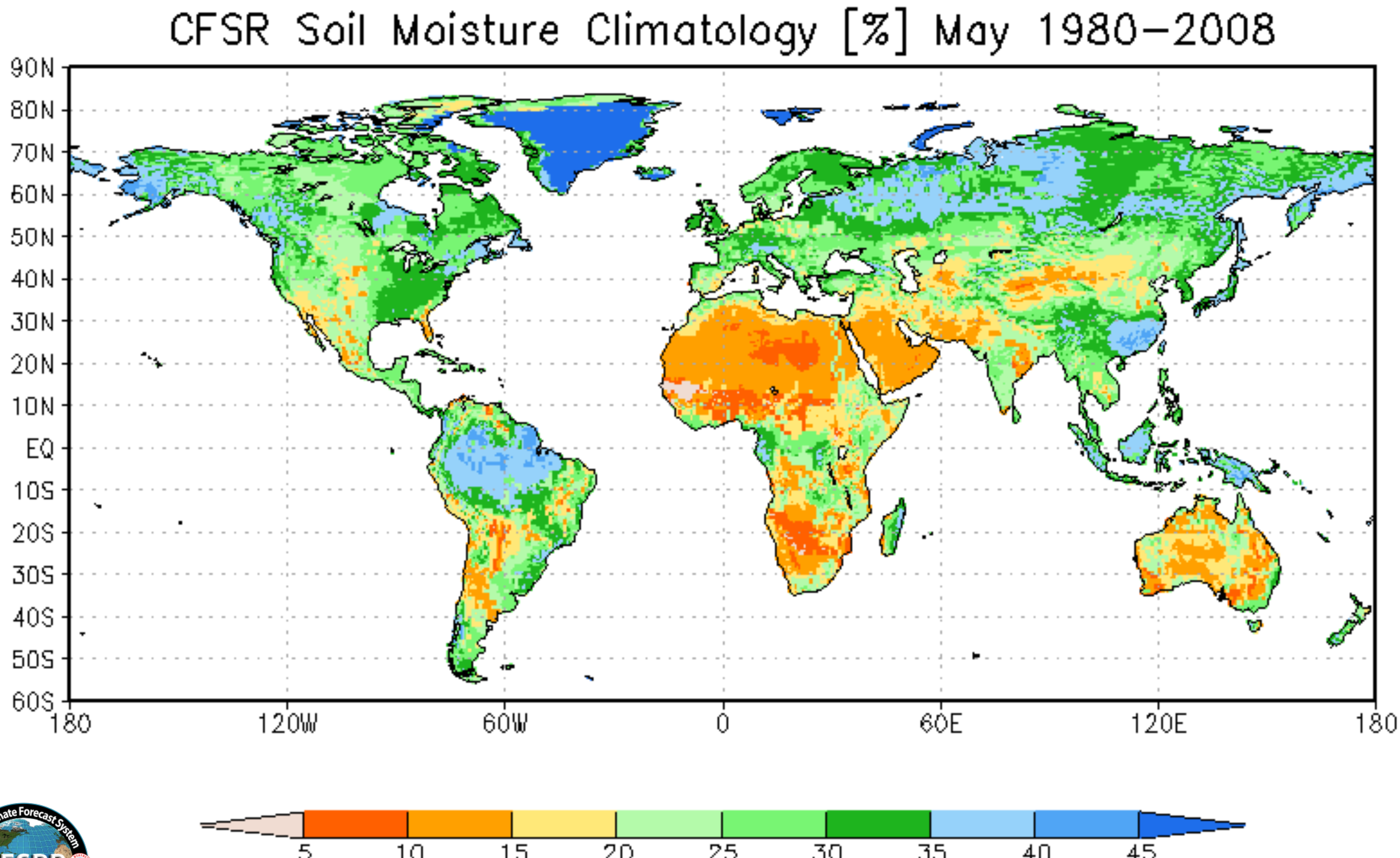

Courtesy: Jesse Meng

2-meter volumetric soil moisture climatology of CFSR for Nov averaged over 1980-2008.

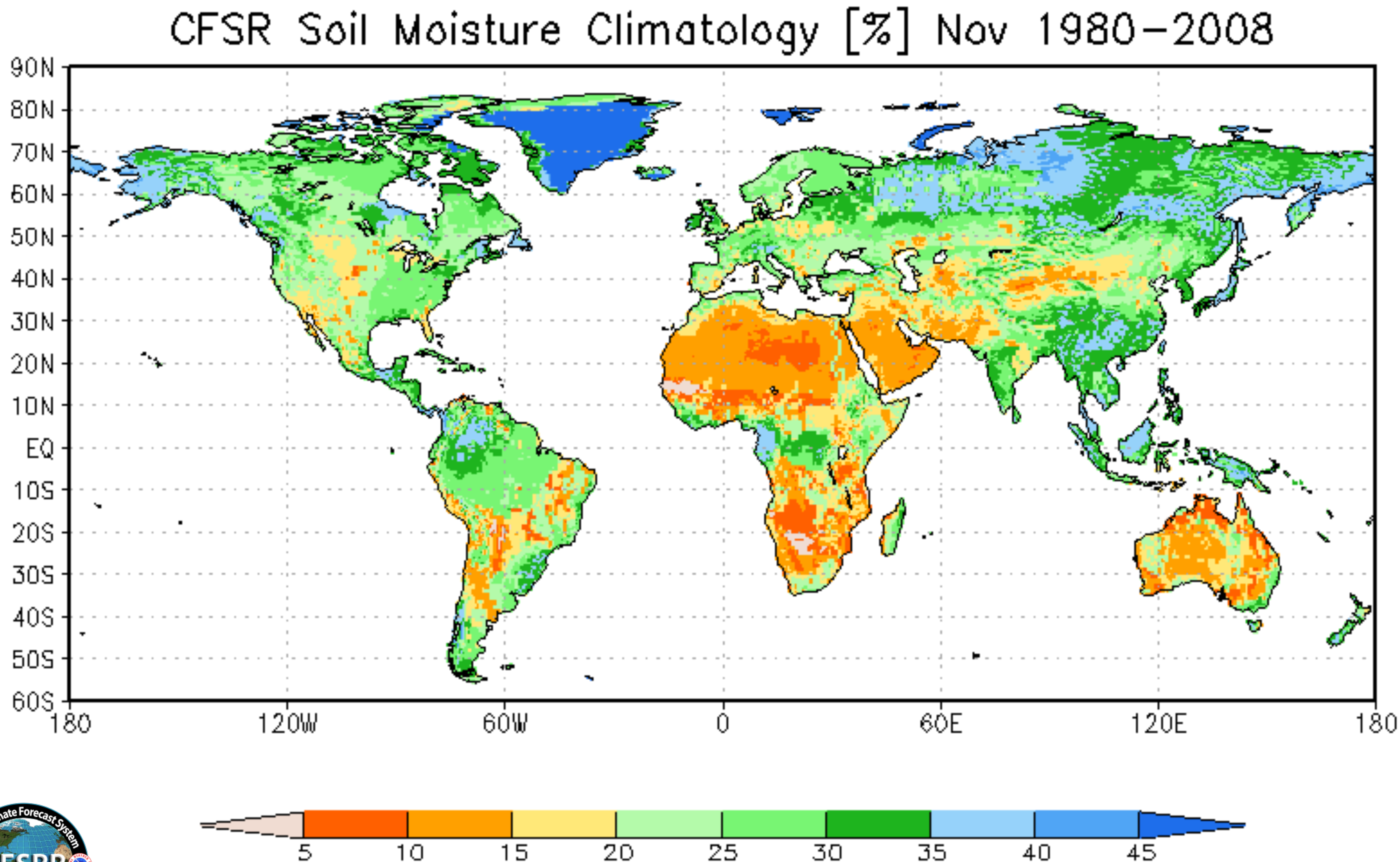

Courtesy: Jesse Meng

Global Soil Moisture Fields in the NCEP CFSR

The CFSR soil moisture climatology is consistent with GR2 and NARR on regional scale. The anomaly agrees with the Illinois observations, correlation coefficient = 0.61.

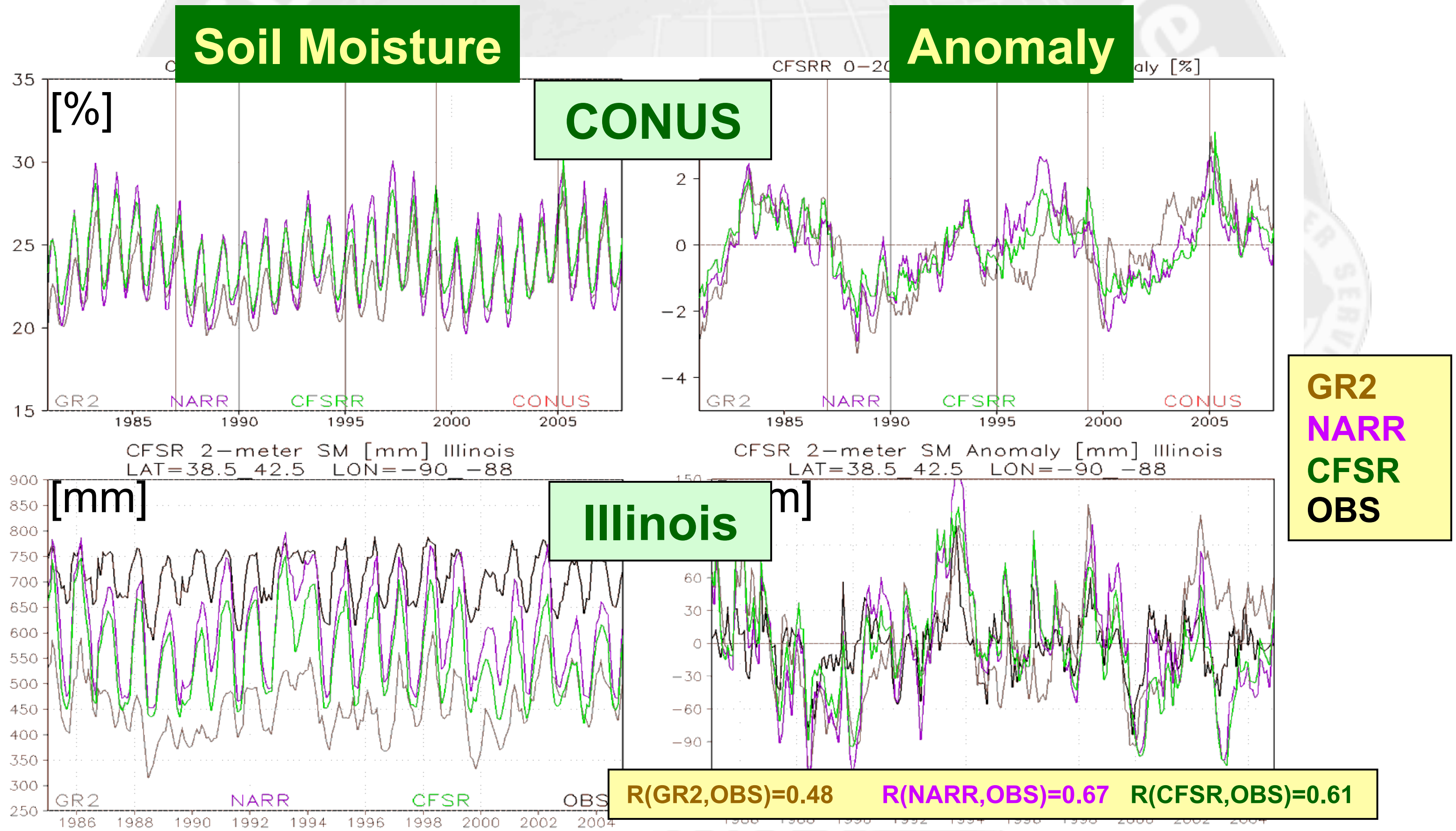

Courtesy: Jesse Meng

Surface water components in the NCEP CFSR and R2

Evaporation (20N-N. Pole) Soil Moisture (20N-N.Pole)

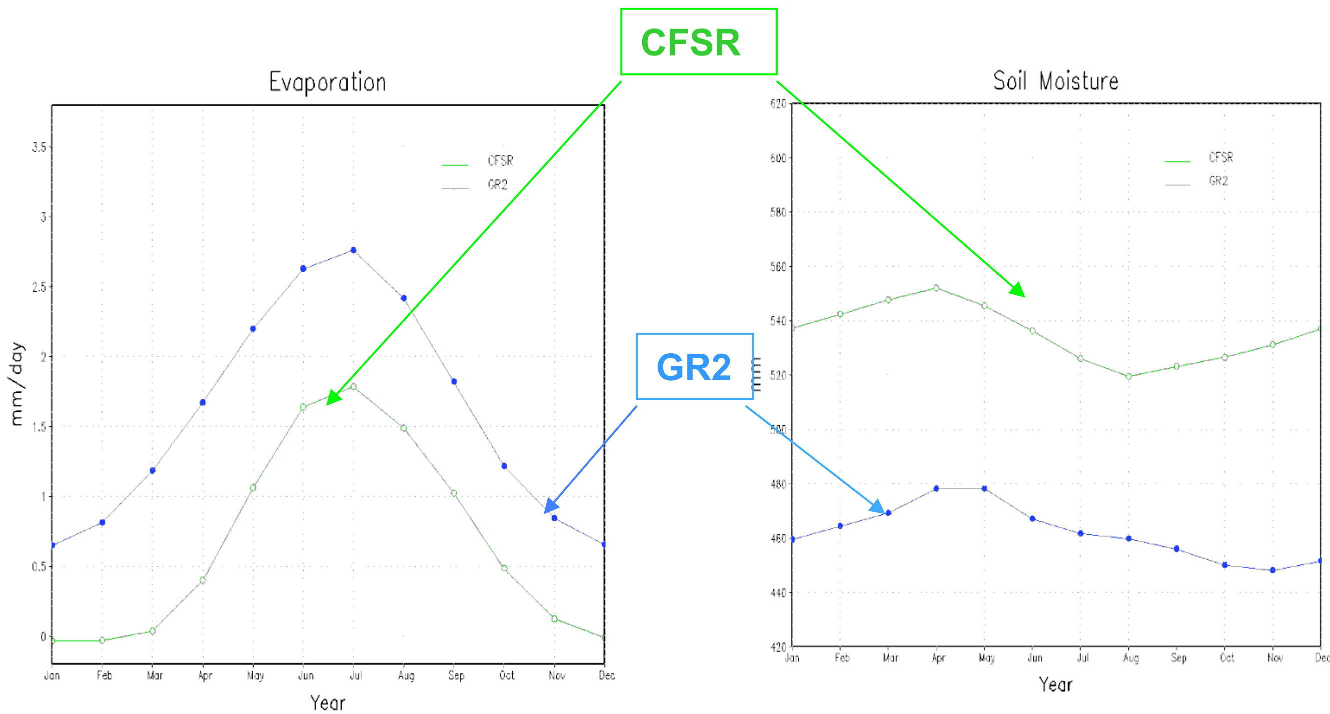

Annual Cycles of *Evaporation (left)* and *Soil Moisture (right)*

(Green: CFSR; Blue: GR2: averaged over 30 years)

CFSR has less evaporation and more soil moisture.

Courtesy: Rongqian Yang

Global average of monthly-mean Precipitation (a), Evaporation (b) and E-P (c).

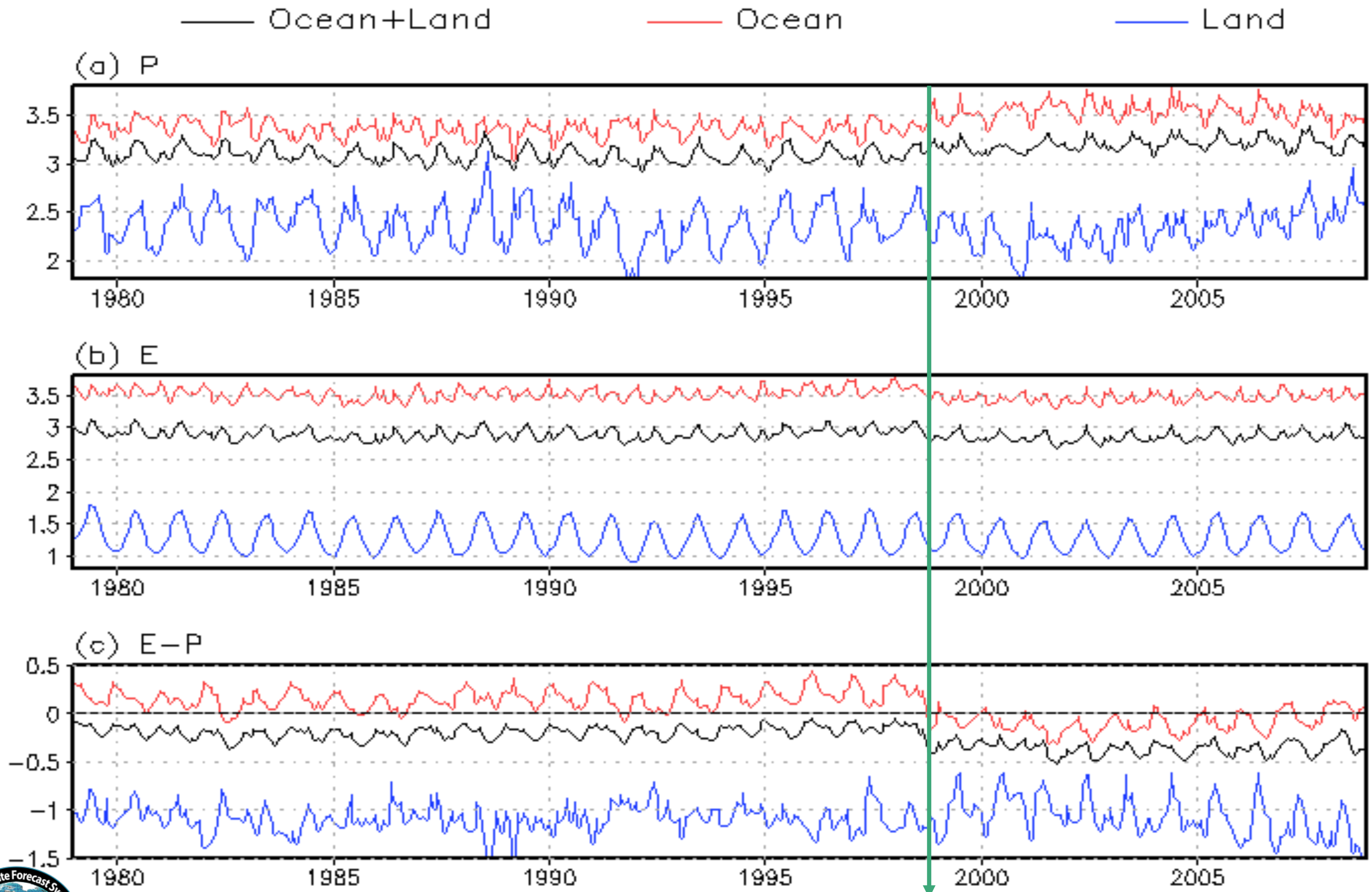

Courtesy: Wanqiu Wang

Monthly mean hourly surface pressure with the daily mean subtracted for the month of March 1998

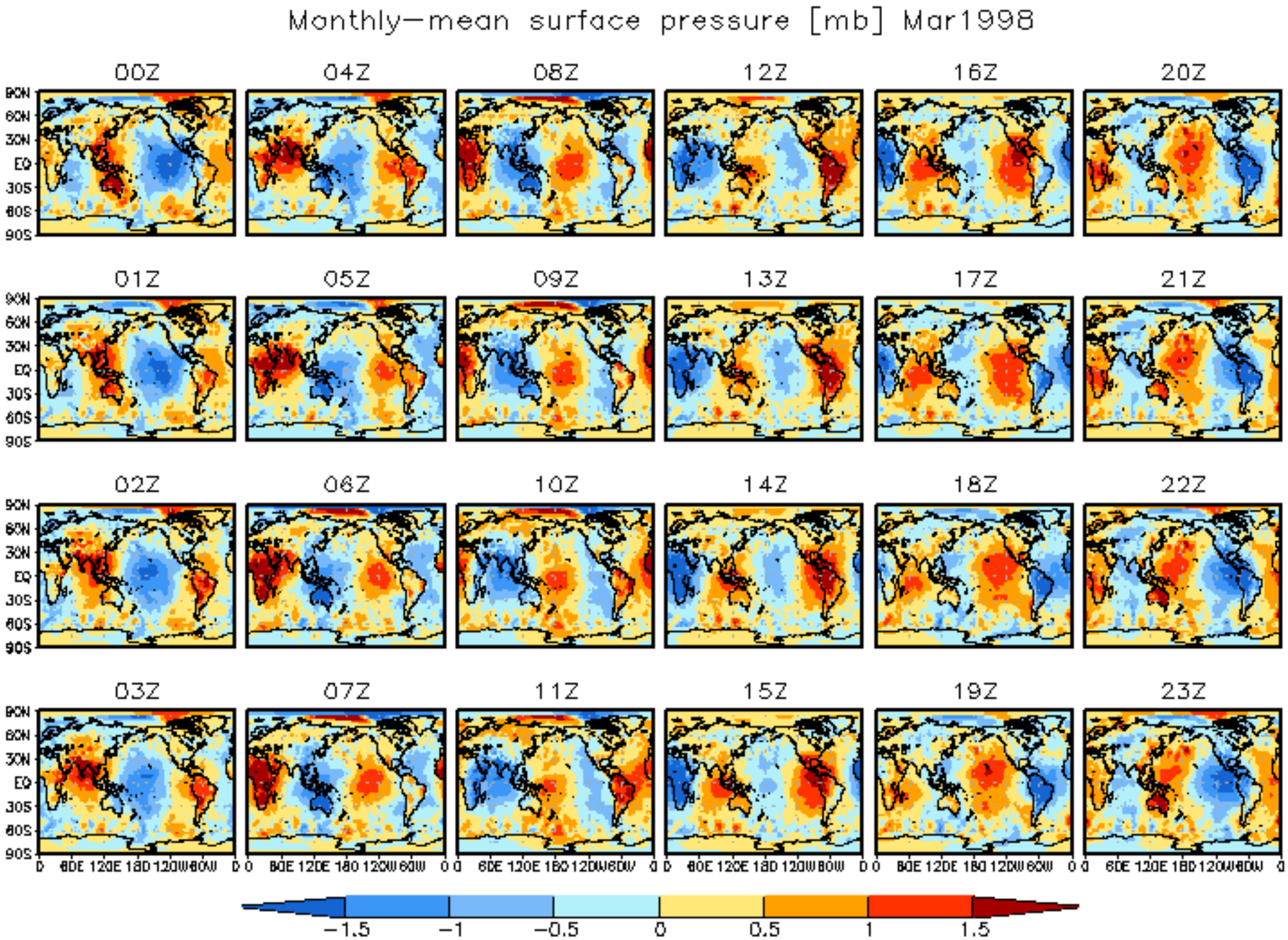

Courtesy: Huug van den Dool

The fit of 6 hour forecasts of instantaneous surface pressure against irregularly distributed observations (yearly averages)

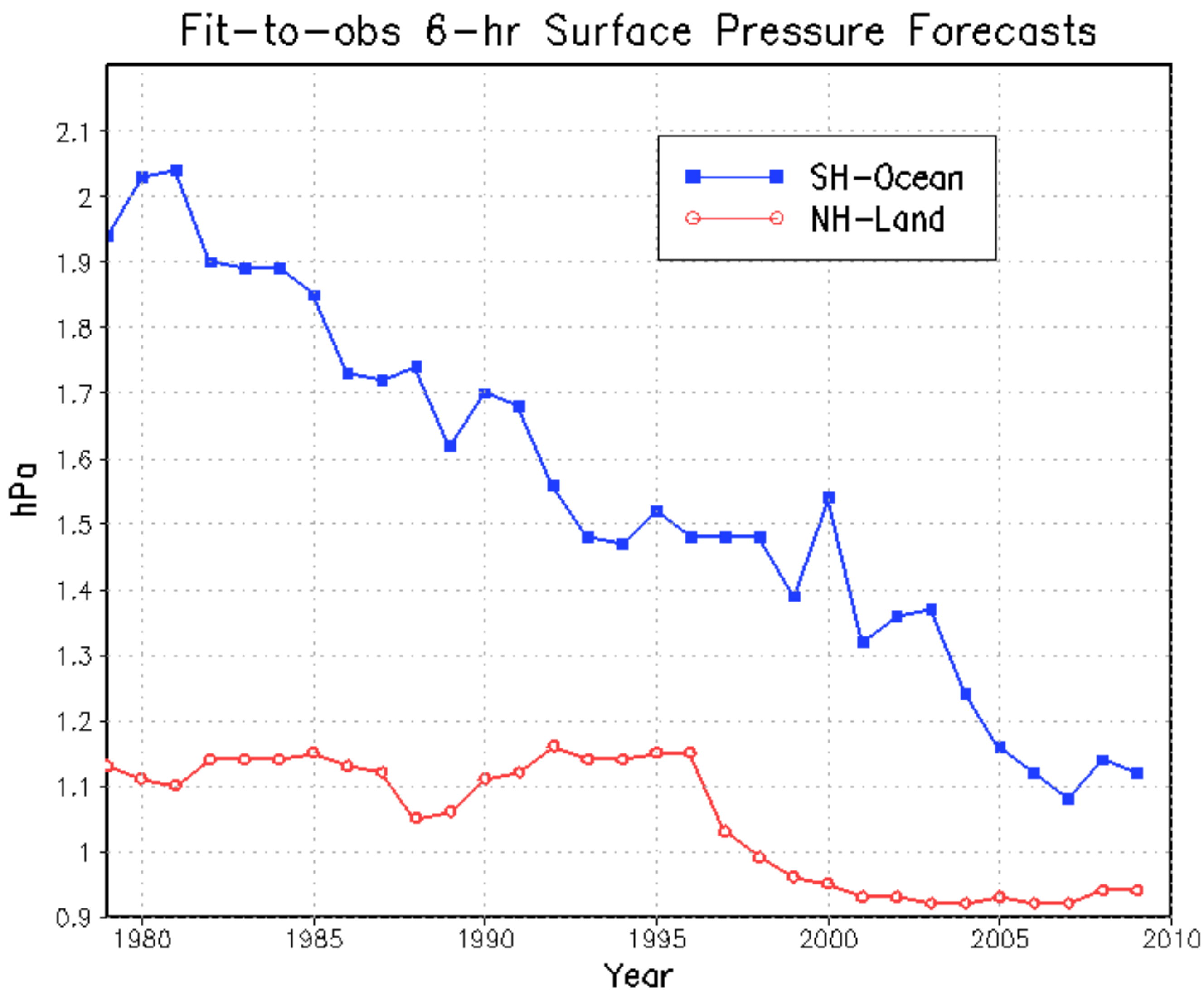

Courtesy: Huug van den Dool

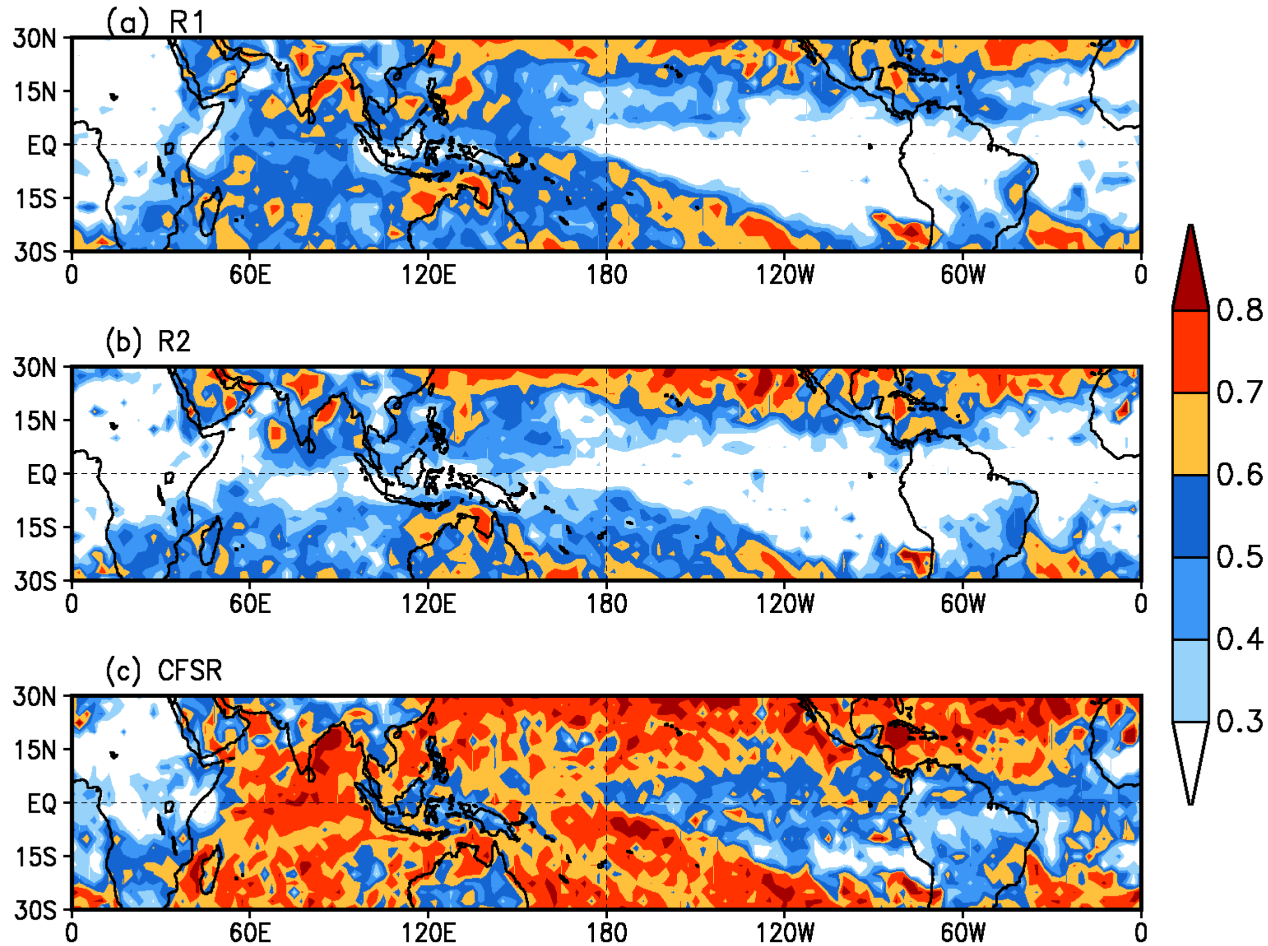

Fig. 3 Correlation of intraseasonal precipitation with CMORPH. (a) R1, (b) R2, and (c) CFSR. Contours are shaded starting at 0.3 with 0.1 interval.

Courtesy: Jiande Wang et al

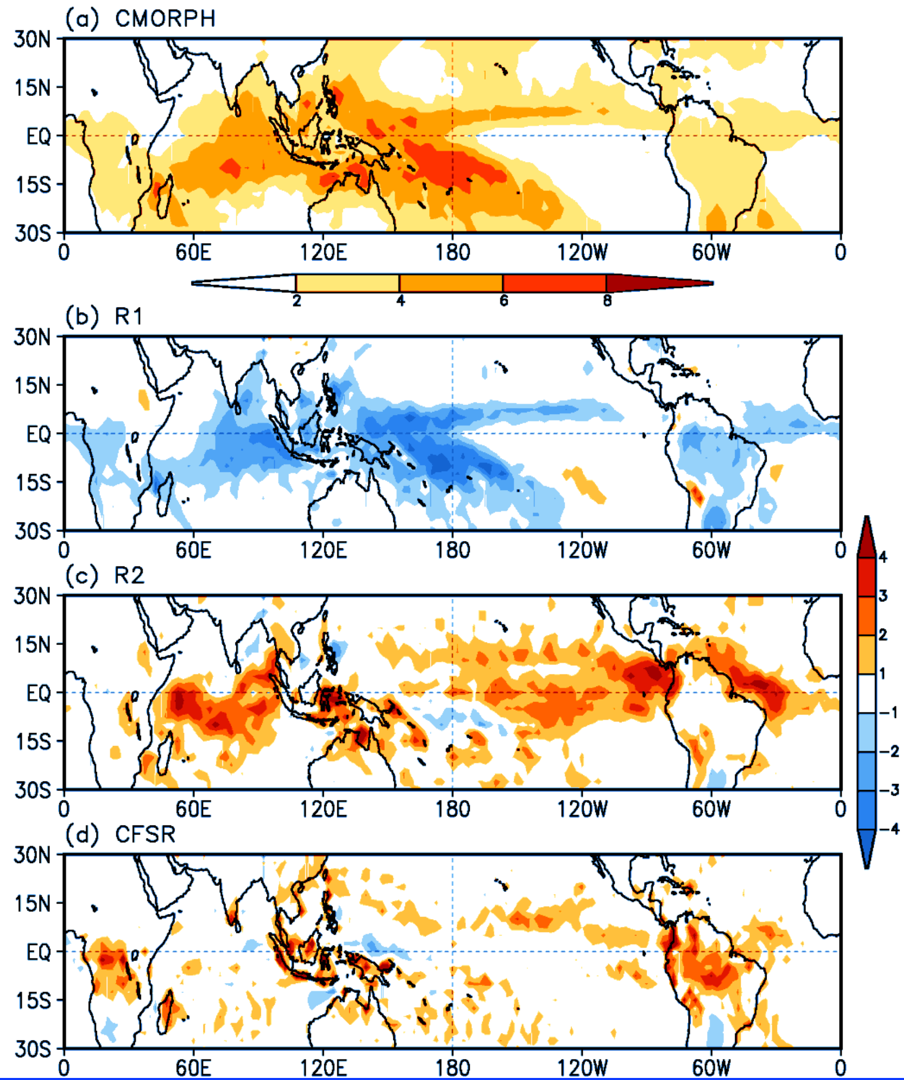

Fig. 4. (a) Standard deviation of intraseasonal rainfall anomalies from CMORPH. (b) differences in standard deviation of intraseasonal rainfall anomalies between R1 and CMORPH. (c) As in (b) except for R2. (d) As in (b) except for CFSR. Contours are shaded at an interval of 2 mm/day in (a) and 1 mm/day in (b), (c) and (d) with values between -1 and 1 plotted as white.

Courtesy: Jiande Wang et al

Reference: Joyce, R. J., J. E. Janowiak, P. A. Arkin, and P. Xie, 2004: CMORPH: A method that produces global precipitation estimates from passive microwave and infrared data at high spatial and temporal resolution.. J. Hydromet., 5, 487-503.

CMORPH (CPC MORPHing technique) produces global precipitation analyses at very high spatial and temporal resolution. This technique uses precipitation estimates that have been derived from low orbiter satellite microwave observations *exclusively*, and whose features are transported via spatial propagation information that is obtained entirely from geostationary satellite IR data. At present we incorporate precipitation estimates derived from the passive microwaves aboard the DMSP 13, 14 & 15 (SSM/I), the NOAA-15, 16, 17 & 18 (AMSU-B), and AMSR-E and TMI aboard NASA's Aqua and TRMM spacecraft, respectively. These estimates are generated by algorithms of Ferraro (1997) for SSM/I, Ferraro et al. (2000) for AMSU-B and Kummerow et al. (2001) for TMI. Note that this technique is not a precipitation estimation algorithm but a means by which estimates from existing microwave rainfall algorithms can be combined. Therefore, this method is extremely flexible such that any precipitation estimates from any microwave satellite source can be incorporated.

The amplitude of the diurnal cycle (1st harmonic) in precipitation (mm/day)

Gang and Slingo, 2001

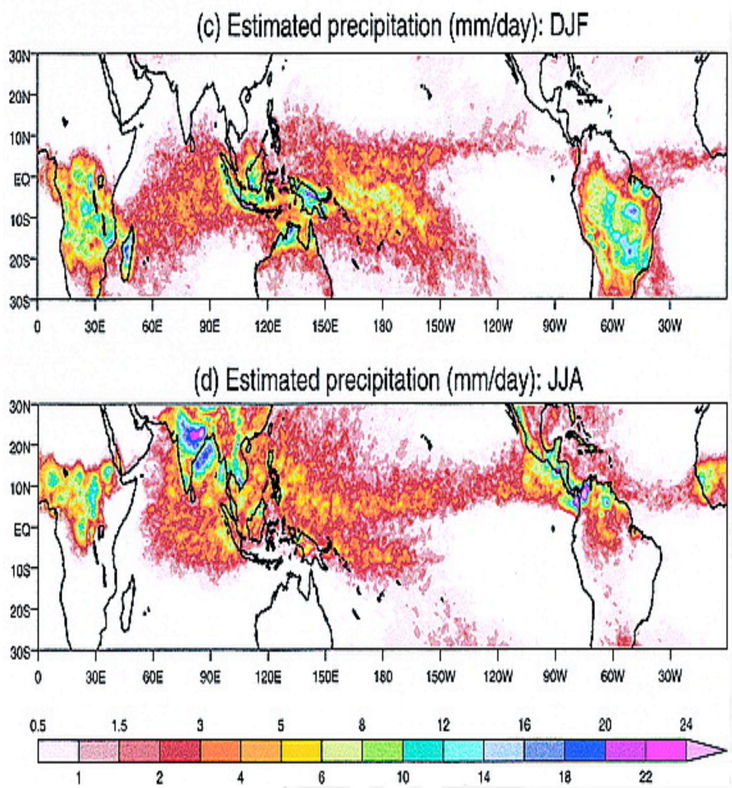

CFSR

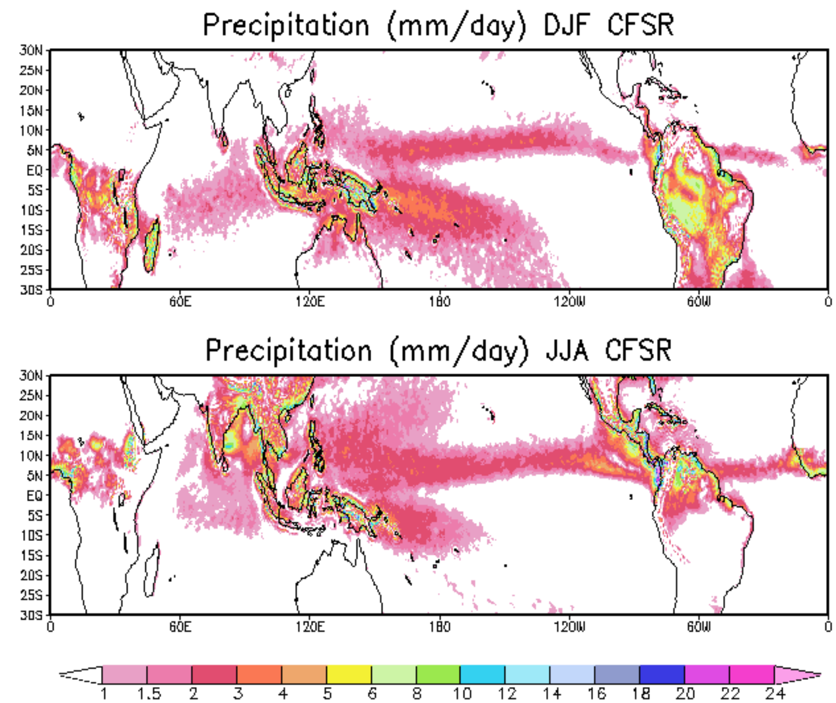

CFSR distribution is quite good, but amplitude is smaller than 'Slingo' (estimated from 3 hourly data)

The phase of the diurnal cycle (1st harmonic) in precipitation (hour – local time)

Gang and Slingo, 2001

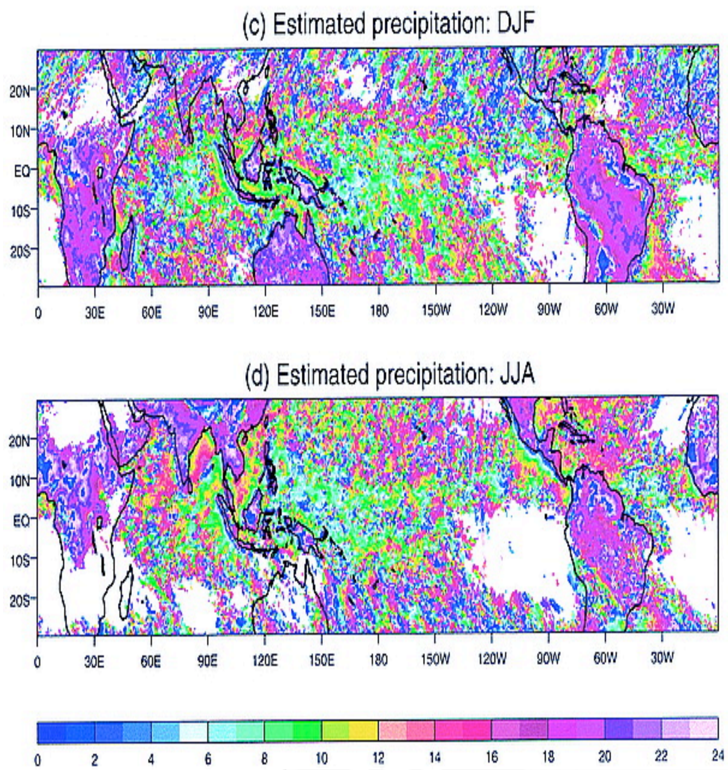

CFSR

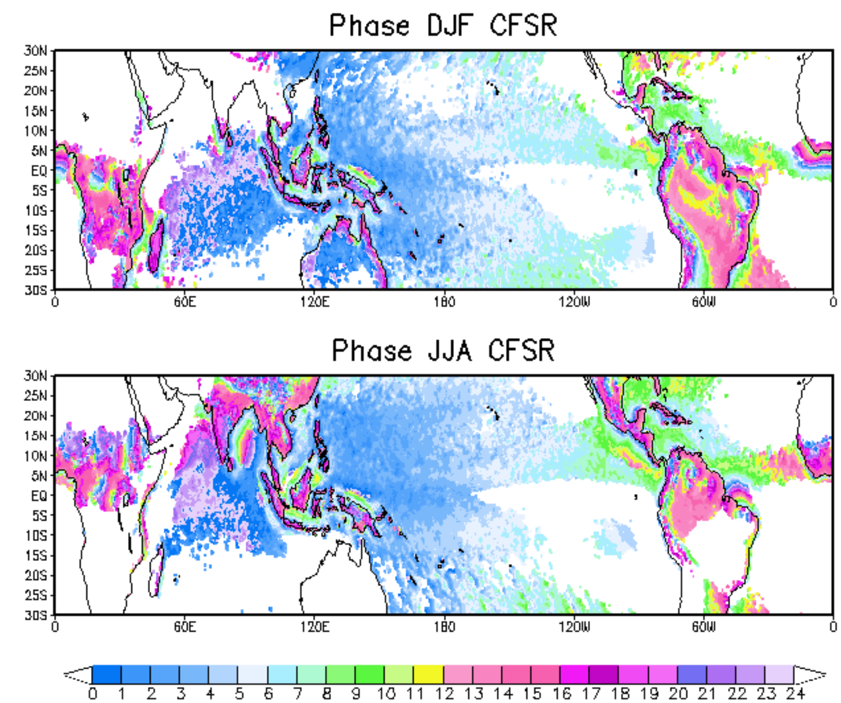

CFSR distribution of phase is quite good, just less detail than ‘Slingo’ (estimated from 3 hourly data)

THE STRATOSPHERE

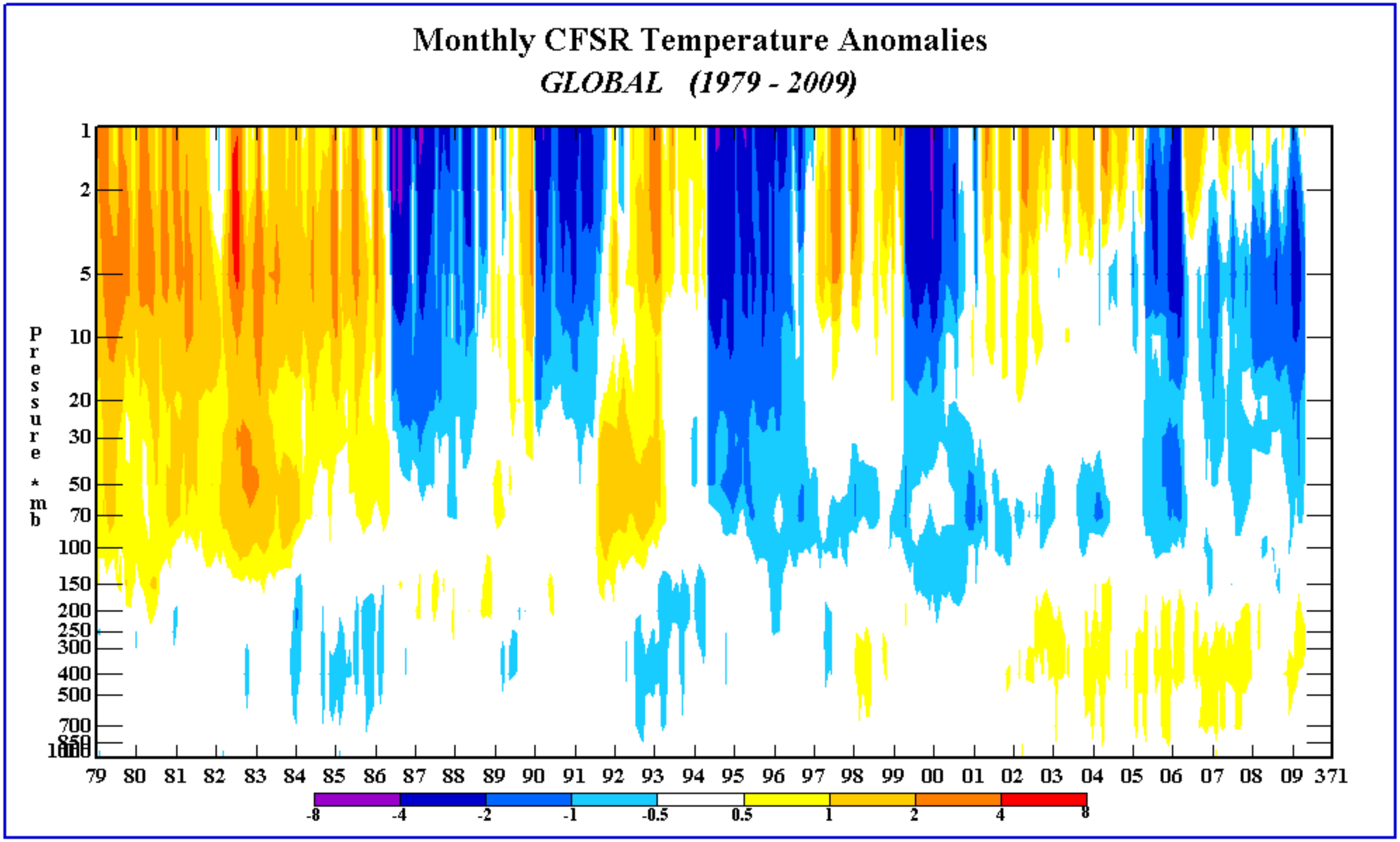

Courtesy: Craig Long

Monthly CFSR Zonal Wind (-5 to 5)

1979 - 2009

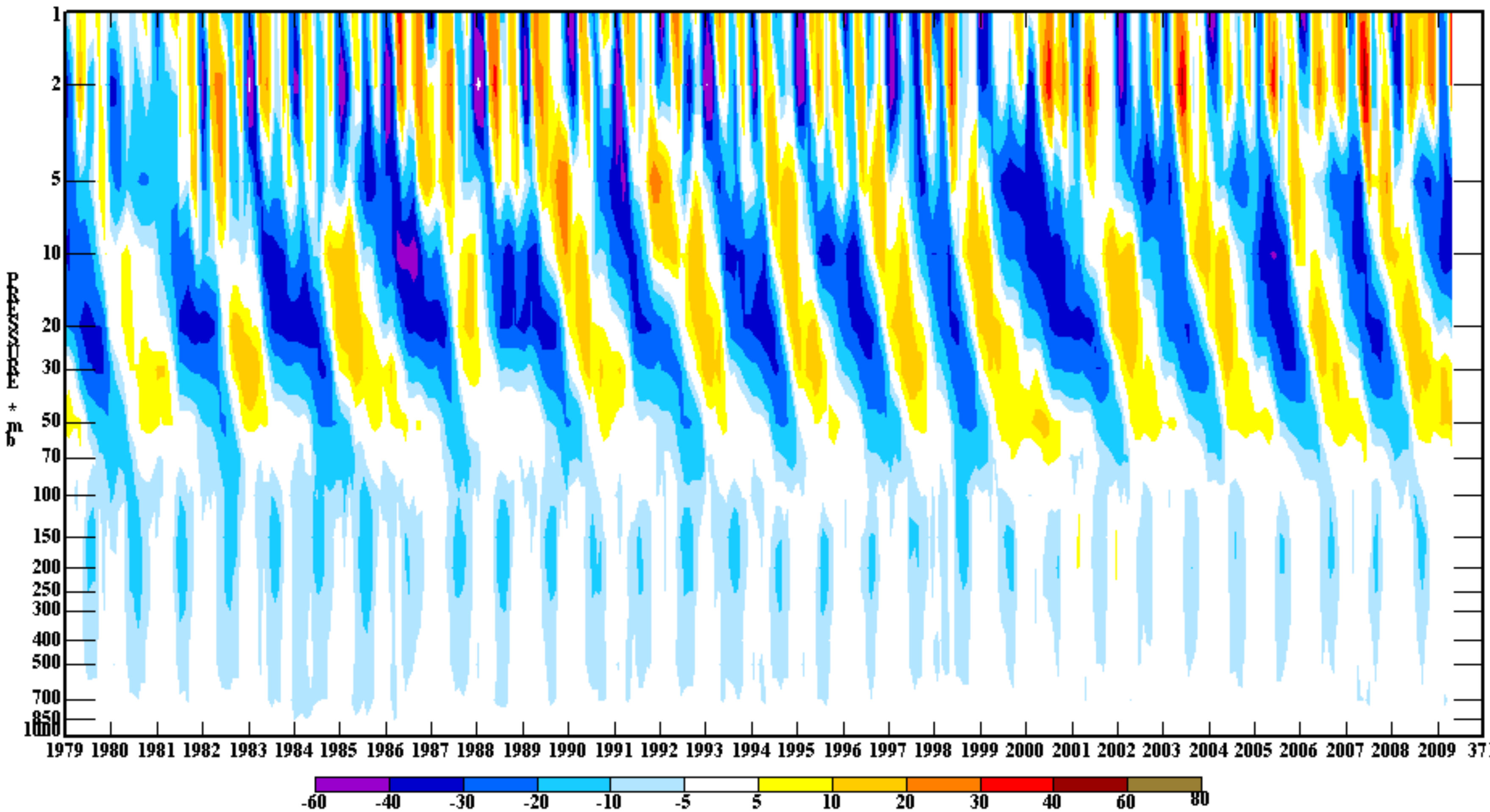

Courtesy: Craig Long

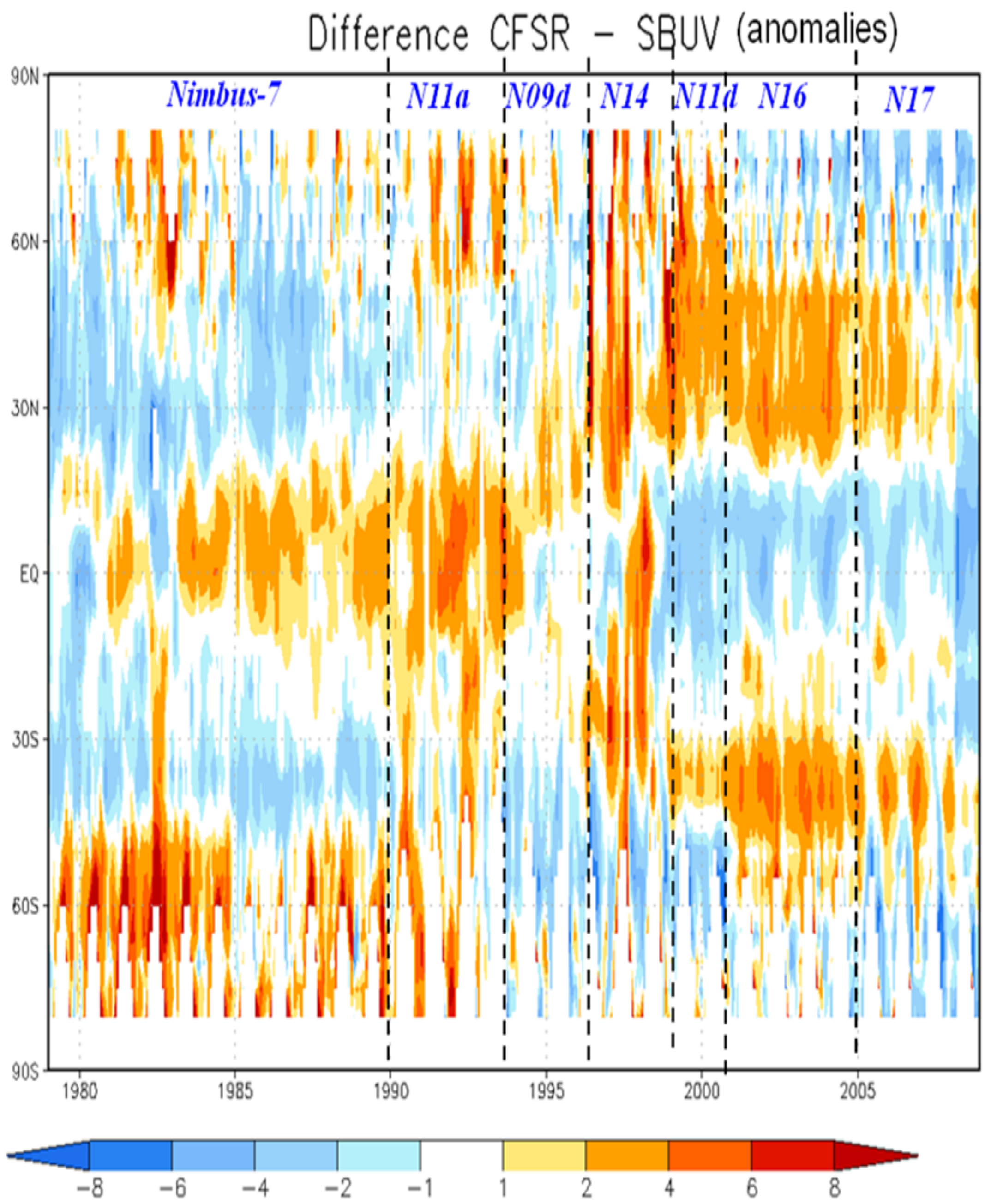

Courtesy: Craig Long

Future Plans

•Immediately conduct CFSRL: a ‘light’ (with a reduced horizontal resolution of T126) version of the reanalysis that was just completed. It will be done in a single stream to overcome the discontinuities found in the CFSR for the deep ocean, deep soil and the top of the atmosphere. It is possible that the CFSRL will be finished in 1 year, in time for CPC to use it when they change their climate normals to the last 30-year period from 1981-2010.

•A final activity to be conducted when the Reforecast project is complete, is to apply the reanalysis system, as used here, to the historical period 1948-1978.

•The CFSR is the successor of R2, and when extended back to 1948, will also be the successor of R1. It is possible this will be done in one-stream ‘light’ mode.

THE HUMAN FACE OF CFSR Production

Suru Saha
Xingren Wu
Jiande Wang
Patrick Tripp
Sudhir Nadiga

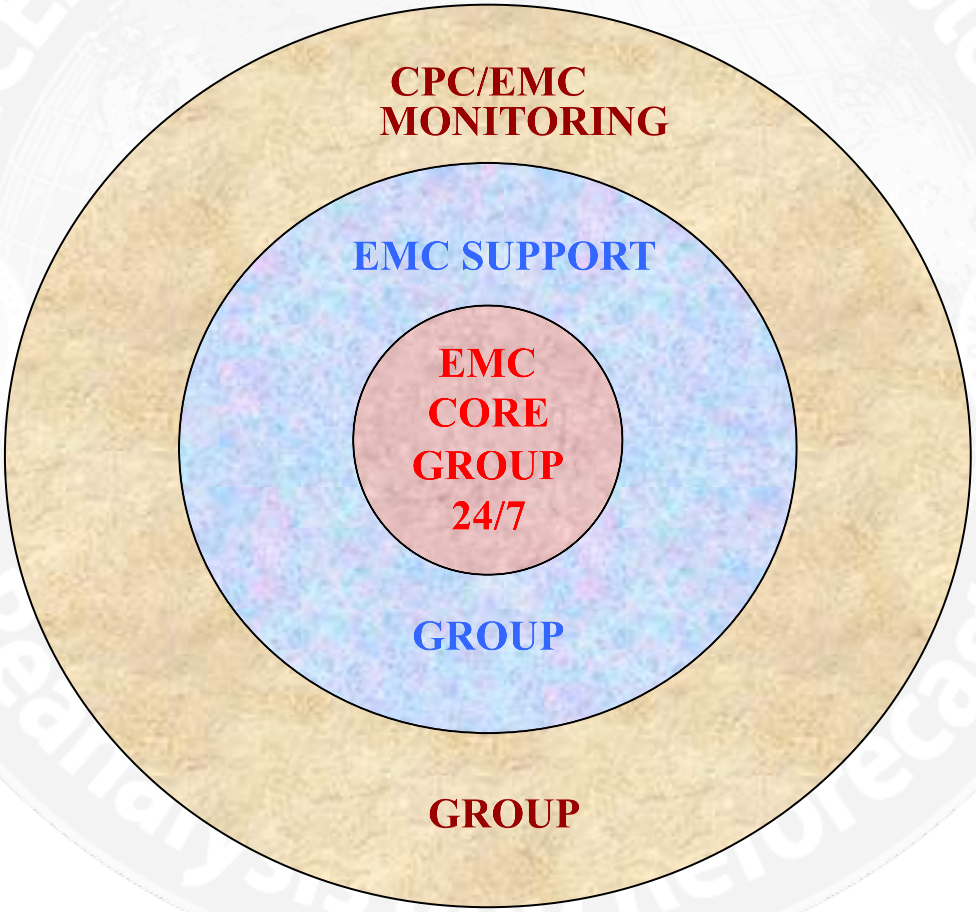

Hua-Lu Pan
Shrinivas Moorthi
Bob Kistler
Jack Woollen
Haixia Liu
Dave Behringer

Diane Stokes
Hui-ya Chuang
Mark Iredell
Jesse Meng
Ken Mitchell
Russ Treadon
Daryl Kleist
Glenn White
Yu-Tai Hou
Steve Lord
Helin Wei
Bob Grumbine
George Gayno
Jun Wang
Paul van Delst

CPC/EMC SCIENTISTS MONITORING CFSR

Arun Kumar

Troposphere	***Surface***	***Stratosphere***	***Ocean/SeaIce***
Muthuvel Chelliah	Wanqiu Wang	Craig Long	Yan Xue
Jae Schemm	Huug van den Dool	Shuntai Zhou	Boyin Huang
Wesley Ebisuzaki	Kingtse Mo	Roger Lin	Jiande Wang
Suru Saha	Yun Fan		Xingren Wu
Augustin Vintzileos	Glenn White		Sudhir Nadiga
	Hua-Lu Pan		
	Helin Wei		
	Ken Mitchell		

AND NOW……..

THE SECOND ‘R’ IN

NCEP Climate Forecast System

CFSRR

Reanalysis and Reforecast

Hindcast Configuration for next CFS

- 9-month hindcasts were initiated from every 5th day and run from all 4 cycles of that day, beginning from Jan 1 of each year, over a 29 year period from 1982-2010 This is required to calibrate the operational CPC longer-term seasonal predictions (ENSO, etc)
- There is also a single 1 season (123-day) hindcast run, initiated from every 0 UTC cycle between these five days, over the 12 year period from 1999-2010. This is required to calibrate the operational CPC first season predictions for hydrological forecasts (precip, evaporation, runoff, streamflow, etc)
- In addition, there are three 45-day (1-month) hindcast runs from every 6, 12 and 18 UTC cycles, over the 12-year period from 1999-2010. This is required for the operational CPC week3-week6 predictions of tropical circulations (MJO, PNA, etc)

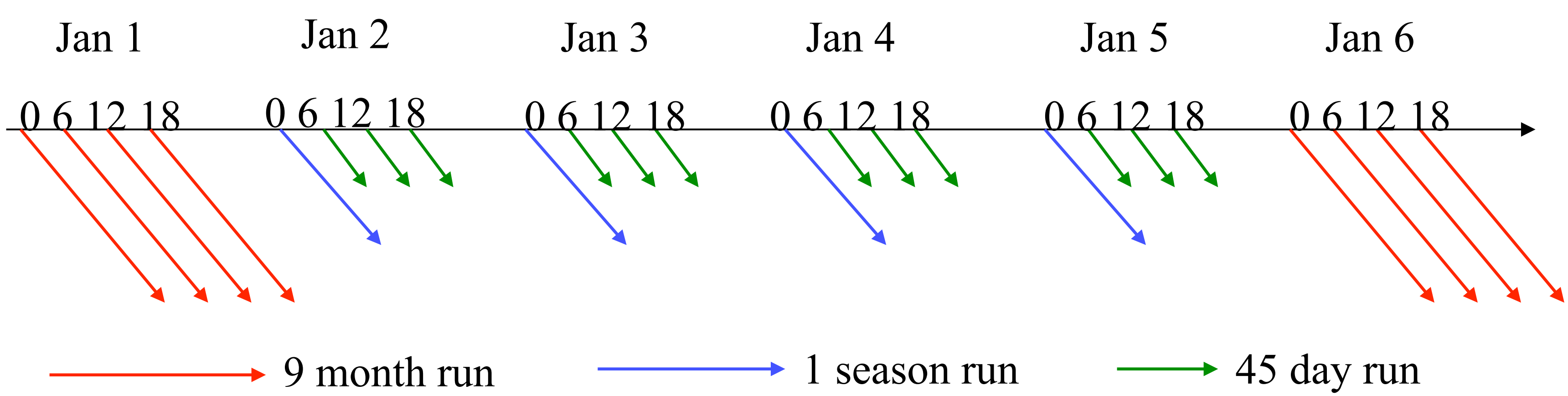

Operational Configuration for next CFS

- There will be 4 control runs per day from the 0, 6, 12 and 18 UTC cycles of the CFS real-time data assimilation system, out to 9 months.
- In addition to the control run of 9 months at the 0 UTC cycle, there will be 3 additional runs, out to one season. These 3 runs per cycle will be initialized as in current operations.
- In addition to the control run of 9 months at the 6, 12 and 18 UTC cycles, there will be 3 additional runs, out to 45 days. These 3 runs per cycle will be initialized as in current operations.
- There will be a total of 16 CFS runs every day, of which 4 runs will go out to 9 months, 3 runs will go out to 1 season and 9 runs will go out to 45 days.

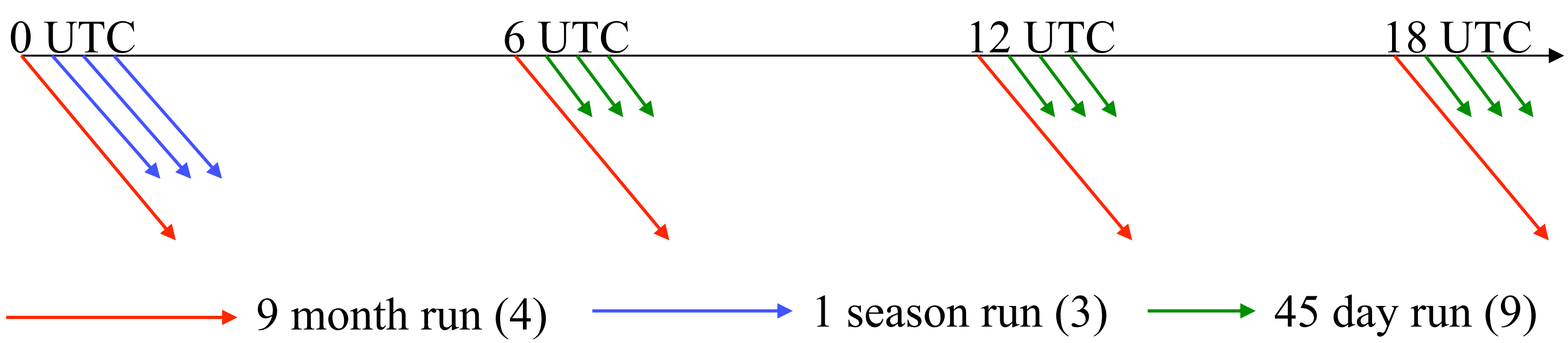

DATA DESCRIPTION

LEVEL 1 DATA :

5 TYPES OF FILES CREATED EVERY 6 HRS

File	*Grid*	*Description*
FLXF	T126(384x190 Gaussian)	Surface, radiative fluxes, etc.
PGBF	1 degree	3-D Pressure level data
OCNH	0.5 degree	3-D Ocean data
OCNF	1 degree	3-D Ocean data
IPVF	1 degree	3-D Isentropic level data

37 Pressure (hPa) Levels: pgb (atmosphere)

1000 975 950 925 900 875 850 825 800 775 750 700 650 600 550 500 450 400 350 300 250 225 200 175 150 125 100 70 50 30 20 10 7 5 3 2 1

40 Levels (depth in meters): ocn (ocean)

4478 3972 3483 3016 2579 2174 1807 1479 1193 949 747 584 459 366 303 262 238 225 215 205 195 185 175 165 155 145 135 125 115105 95 85 75 65 55 45 35 25 15 5

16 Isentropic Levels (K): ipv

270 280 290 300 310 320 330 350 400 450 550 650 850 1000 1250 1500

CONTENTS OF IPV FILES

• LAPRtht	16	** (profile) Lapse rate [K/m]
• MNTSFtht	16	** (profile) Montgomery stream function [m^2/s^2]
• PRESsfc	0	** (surface) Pressure [Pa]
• PVORTtht	16	** (profile) Pot. vorticity [km^2/kg/s]
• RHtht	16	** (profile) Relative humidity [%]
• TMPsfc	0	** (surface) Temp. [K]
• TMPtht	16	** (profile) Temp. [K]
• UGRDtht	16	** (profile) u wind [m/s]
• VGRDtht	16	** (profile) v wind [m/s]
• VVELtht	16	** (profile) Pressure vertical velocity [Pa/s]

CONTENTS OF PGB FILE (232 Variables)

- ABSVprs 37 ** (profile) Absolute vorticity [/s]
- CLWMRprs 32 ** (profile) Cloud water [kg/kg]
- GPAprs 2 ** (profile) Geopotential height anomaly [gpm]
- HGTprs 37 ** (profile) Geopotential height [gpm]
- O3MRprs 37 ** (profile) Ozone mixing ratio [kg/kg]
- RHprs 37 ** (profile) Relative humidity [%]
- SPFHprs 37 ** (profile) Specific humidity [kg/kg]
- STRMprs 37 ** (profile) Stream function [m^2/s]
- TMPprs 37 ** (profile) Temp. [K]
- UGRDprs 37 ** (profile) u wind [m/s]
- VGRDprs 37 ** (profile) v wind [m/s]
- VPOTprs 37 ** (profile) Velocity potential [m^2/s]
- VVELprs 37 ** (profile) Pressure vertical velocity [Pa/s]
- PRESmsl 0 ** mean-sea level Pressure [Pa]

AND MANY MORE……..

CONTENTS OF OCEAN FILE

POTdsl	40 levels (profile) Potential temp. [K]
SALTYdsl	40 levels (profile) Salinity [kg/kg]
UOGRDdsl	40 levels (profile) u of current [m/s]
VOGRDdsl	40 levels (profile) v of current [m/s]
DZDTdsl	40 levels (profile) Geometric vertical velocity [m/s]
DBSSt2p5c	2.5C isotherm Geometric Depth Below Sea Surface [m]
DBSSt5c	5C isotherm Geometric Depth Below Sea Surface [m]
DBSSt10c	10C isotherm Geometric Depth Below Sea Surface [m]
DBSSt15c	15C isotherm Geometric Depth Below Sea Surface [m]
DBSSt20c	20C isotherm Geometric Depth Below Sea Surface [m]
DBSSt25c	25C isotherm Geometric Depth Below Sea Surface [m]
DBSSt28c	28C isotherm Geometric Depth Below Sea Surface [m]
DBSSbmxl	Mixed layer Geometric Depth Below Sea Surface [m]
DBSSbitl	Isothermal layer Geometric Depth Below Sea Surface [m]
EMNPsfc	Evaporation - Precipitation [cm/day]
ICECsfc	Ice concentration (ice=1;no ice=0) [fraction]
ICETKsfc	Ice thickness [m]
OHC0_300m	0-300 m under water Ocean Heat Content [J/m^2]
SNODsfc	Snow depth [m]
SSHGsfc	Sea Surface Height Relative to Geoid [m]
TCHPl239	Tropical Cyclone Heat Potential [J/m^2]
THFLXsfc	Total downward heat flux at surface [W/m^2]
TMPsfc	Surface Temp. [K]
UFLXsfc	Zonal momentum flux [N/m^2]
VFLXsfc	Meridional momentum flux [N/m^2]
UICEsfc	u of ice drift [m/s]
VICEsfc	v of ice drift [m/s]

CONTENTS OF FLX FILE (103 Variables)

RADIATIVE FLUXES

• CDUVBsfc	surface Clear Sky UV-B Downward Solar Flux [W/m^2]
• DUVBsfc	surface UV-B Downward Solar Flux [W/m^2]
• CSDLFsfc	surface Clear sky downward long wave flux [W/m^2]
• CSDSFsfc	surface Clear sky downward solar flux [W/m^2]
• CSULFsfc	surface Clear sky upward long wave flux [W/m^2]
• CSULFtoa	top of atmos Clear sky upward long wave flux [W/m^2]
• CSUSFsfc	surface Clear sky upward solar flux [W/m^2]
• CSUSFtoa	top of atmos Clear sky upward solar flux [W/m^2]
• NBDSFsfc	surface Near IR beam downward solar flux [W/m^2]
• NDDSFsfc	surface Near IR diffuse downward solar flux [W/m^2]
• VBDSFsfc	surface Visible beam downward solar flux [W/m^2]
• VDDSFsfc	surface Visible diffuse downward solar flux [W/m^2]
• DLWRFsfc	surface Downward long wave flux [W/m^2]
• DSWRFsfc	surface Downward short wave flux [W/m^2]
• DSWRFtoa	top of atmos Downward short wave flux [W/m^2]
• LHTFLsfc	surface Latent heat flux [W/m^2]
• SHTFLsfc	surface Sensible heat flux [W/m^2]
• ULWRFsfc	surface Upward long wave flux [W/m^2]
• ULWRFtoa	top of atmos Upward long wave flux [W/m^2]
• USWRFsfc	surface Upward short wave flux [W/m^2]
• USWRFtoa	top of atmos Upward short wave flux [W/m^2]

CONTENTS OF FLX FILE (103 Variables)

LAND SURFACE VARIABLES

CNWATsfc	surface Plant canopy surface water [kg/m^2]
EVBSsfc	surface Direct evaporation from bare soil [W/m^2]
EVCWsfc	surface Canopy water evaporation [W/m^2]
SBSNOsfc	surface Sublimation (evaporation from snow) [W/m^2]
SFCRsfc	surface Surface roughness [m]
SFEXCsfc	surface Exchange coefficient [(kg/m^3)(m/s)]
SLTYPsfc	surface Surface slope type [Index]
SNODsfc	surface Snow depth [m]
SNOHFsfc	surface Snow phase-change heat flux [W/m^2]
SNOWCsfc	surface Snow cover [%]
GFLUXsfc	surface Ground heat flux [W/m^2]
SOTYPsfc	surface Soil type (Zobler) [0..9]
SRWEQsfc	surface Snowfall rate water equiv. [kg/m^2/s]
SSRUNsfc	surface Storm surface runoff [kg/m^2]
PEVPRsfc	surface Potential evaporation rate [W/m^2]
TRANSsfc	surface Transpiration [W/m^2]
VEGsfc	surface Vegetation [%]
VGTYPsfc	surface Vegetation type (as in SiB) [0..13]
WATRsfc	surface Water runoff [kg/m^2]
WEASDsfc	surface Accum. snow [kg/m^2]

CONTENTS OF FLX FILE (103 Variables)

LAND SURFACE VARIABLES (contd)

- TMP_10cm 0-10 cm underground Temp. [K]
- TMP10_40cm 10-40 cm underground Temp. [K]
- TMP40_100cm 40-100 cm underground Temp. [K]
- TMP100_200cm 100-200 cm underground Temp. [K]
- SOILL0_10cm 0-10 cm underground Liquid volumetric soil moisture (non-frozen)
- SOILL10_40cm10-40 cm underground Liquid volumetric soil moisture (non-frozen)
- SOILL40_100cm 40-100 cm underground Liquid volumetric soil moisture (non-frozen)
- SOILL100_200cm 100-200 cm underground Liquid volumetric soil moisture (non-frozen)
- SOILM0_200cm 0-200 cm underground Soil moisture content [kg/m^2]
- SOILW0_10cm 0-10 cm underground Volumetric soil moisture [fraction]
- SOILW10_40cm 10-40 cm underground Volumetric soil moisture [fraction]
- SOILW40_100cm 40-100 cm underground Volumetric soil moisture [fraction]
- SOILW100_200cm 100-200 cm underground Volumetric soil moisture [fraction]

CONTENT S OF FLX FILE (103 Variables)

RAIN AND CLOUDS

- CRAINsfc surface Categorical rain [yes=1;no=0]
- CWORKclm atmos column Cloud work function [J/kg]
- CPRATsfc surface Convective precip. rate [kg/m^2/s]
- PRATEsfc surface Precipitation rate [kg/m^2/s]
- PRESlcb low cloud base Pressure [Pa]
- PRESlct low cloud top Pressure [Pa]
- PRESmcb mid-cloud base Pressure [Pa]
- PRESmct mid-cloud top Pressure [Pa]
- PREShcb high cloud base Pressure [Pa]
- PREShct high cloud top Pressure [Pa]
- PREScvb convective cld base Pressure [Pa]
- PREScvt convective cld top Pressure [Pa]
- TCDCclm atmos column Total cloud cover [%]
- TCDCbcl boundary cld layer Total cloud cover [%]
- TCDClcl low cloud level Total cloud cover [%]
- TCDCmcl mid-cloud level Total cloud cover [%]
- TCDChcl high cloud level Total cloud cover [%]
- TCDCcvl convective cld layer Total cloud cover [%]
- TMPlct low cloud top Temp. [K]
- TMPmct mid-cloud top Temp. [K]
- TMPhct high cloud top Temp. [K]

CONTENTS OF FLX FILE (103 Variables)

TEMPERATURE, MOISTURE AND WINDS

- TMAX2m 2 m above ground Max. temp. [K]
- TMIN2m 2 m above ground Min. temp. [K]
- TMPsfc surface Temp. [K]
- TMP2m 2 m above ground Temp. [K]
- TMPhlev1 hybrid level 1 Temp. [K]

- PWATclm atmos column Precipitable water [kg/m^2]
- QMAX2m 2 m above ground Maximum specific humidity at 2m
- QMIN2m 2 m above ground Minimum specific humidity at 2m
- SPFH2m 2 m above ground Specific humidity [kg/kg]
- SPFHhlev1 hybrid level 1 Specific humidity [kg/kg]

- UGWDsfc surface Zonal gravity wave stress [N/m^2]
- VGWDsfc surface Meridional gravity wave stress [N/m^2]
- UFLXsfc surface Zonal momentum flux [N/m^2]
- VFLXsfc surface Meridional momentum flux [N/m^2]
- UGRD10m 10 m above ground u wind [m/s]
- VGRD10m 10 m above ground v wind [m/s]
- UGRDhlev1 hybrid level 1 u wind [m/s]
- VGRDhlev1 hybrid level 1 v wind [m/s]

CONTENTS OF FLX FILE (103 Variables)

AND THE REST……

ICECsfc	surface Ice concentration (ice=1;no ice=0) [fraction]
ICETKsfc	surface Ice thickness [m]
LANDsfc	surface Land cover (land=1;sea=0) [fraction]
ACONDsfc	surface Aerodynamic conductance [m/s]
ALBDOsfc	surface Albedo [%]
FRICVsfc	surface Friction velocity [m/s]
HGTsfc	surface Geopotential height [gpm]
HGThlev1	hybrid level 1 Geopotential height [gpm]
HPBLsfc	surface Planetary boundary layer height [m]
PRESsfc	surface Pressure [Pa]

LEVEL 2 DATA :

MONTHLY MEANS OF THE 5 TYPES OF FILES CREATED EVERY 6 HRS

(00Z,06Z,12Z, 18Z and daily averages for each month)

File	***Grid***	***Description***
FLXF	T126(384x190 Gaussian)	Surface, radiative fluxes, etc.
PGBF	1 degree	3-D Pressure level data
OCNH	0.5 degree	3-D Ocean data
OCNF	1 degree	3-D Ocean data
IPVF	1 degree	3-D Isentropic level data

LEVEL 3 DATA :

6 HOURLY TIMESERIES OF 88 SELECTED VARIABLES

File	*Grid*	*Number*
FLXF	T126(384x190 Gaussian)	32
PGBF	1 degree	32
OCNH	0.5 degree	21
IPVF	1 degree	3

6-Hourly Timeseries of 88 parameters : FLX file (32)

1. LHTFL (latent heat flux) : averaged
2. SHTFL (sensible heat flx) : averaged
3. UFLX (u-stress) : averaged
4. VFLX (v-stress) : averaged
5. PRATE (precipitation rate) : averaged
6. PRESSFC (Surface pressure) : instantaneous
7. PWAT (Precipitable Water) : instantaneous
8. TMP2M (2m air temperature) : instantaneous
9. TMPSFC (surface temperature) : instantaneous
10. TMPHY1 (temperature at hybrid level 1) : instantaneous
11. PEVPR (potential evaporation rate) : averaged
12. U10M (u at 10m) : instantaneous
13. V10M (v at 10m) : instantaneous
14. DLWSFC (Downward LW at the surface) : averaged
15. DSWSFC (Downward SW at the surface) : averaged
16. ULWSFC (Upward LW at the surface) : averaged
17. ULWTOA (Upward LW at the top) : averaged
18. USWSFC (Upward SW at the surface) : averaged
19. USWTOA (Upward SW at the top) : averaged
20. SOILM1 (Soil Moisture Level 1) : instantaneous
21. SOILM2 (Soil Moisture Level 2) : instantaneous
22. SOILM3 (Soil Moisture Level 3) : instantaneous
23. SOILM4 (Soil Moisture Level 4) : instantaneous
24. SOILT1 (Soil Temperature Level 1) : instantaneous
25. GFLUX (Ground Heat Flux) : averaged
26. SWE (Snow Water Equivalent) : instantaneous
27. RUNOFF (Ground Runoff) : accumulation
28. ICECON (Ice concentation)
29. ICETHK (Ice Thickness)
30. Q2M (2m Specific Humidity)
31. TMIN (Minimum 2m air temperature)
32. TMAX (Maximum 2m air temperature)

6-Hourly Timeseries of 88 parameters (contd) : PGB file (32)

1. Z200 (Geopotential at 200 hPa)
2. Z500 (Geopotential at 500 hPa)
3. Z700 (Geopotential at 700 hPa)
4. Z850 (Geopotential at 850 hPa)
5. Z1000 (Geopotential at 1000 hPa)
6. T2 (Temperature at 2 hPa)
7. T50 (Temperature at 50 hPa)
8. T200 (Temperature at 200 hPa)
9. T500 (Temperature at 500 hPa)
10. T700 (Temperature at 700 hPa)
11. T850 (Temperature at 850 hPa)
12. T1000 (Temperature at 1000 hPa)
13. WND200 (Zonal (u) and Meridional: (v) Wind at 200 hPa)
14. WND500 (Zonal (u) and Meridional: (v) Wind at 500 hPa)
15. WND700 (Zonal (u) and Meridional: (v) Wind at 700 hPa)
16. WND850 (Zonal (u) and Meridional: (v) Wind at 850 hPa)
17. WND1000 (Zonal (u) and Meridional: (v) Wind at 1000 hPa)
18. PSI200 (Streamfunction at 200 hPa)
19. PSI850 (Streamfunction at 850 hPa)
20. CHI200 (Velocity Potential at 200 hPa)
21. CHI850 (Velocity Potential at 200 hPa)
22. VVEL500 (Vertical Velocity at 500 hPa)
23. Q500 (Specific Humidity at 500 hPa)
24. Q700 (Specific Humidity at 700 hPa)
25. Q850 (Specific Humidity at 850 hPa)
26. Q925 (Specific Humidity at 925 hPa)
27. PRMSL (Mean Sea Level Pressure)

6-Hourly Timeseries of 88 parameters (contd) : IPV file (3)

1. IPV450 (Potential Vorticty at 450 K Isentropic Level)
2. IPV550 (Potential Vorticty at 550 K Isentropic Level)
3. IPV650 (Potential Vorticty at 650 K Isentropic Level)

6-Hourly Timeseries of 88 parameters (contd) : OCNH file (21)

1. OCNDT2.5C (Depth of 2.5C Isotherm)
2. OCNDT5C (Depth of 5C Isotherm)
3. OCNDT10C (Depth of 10C Isotherm)
4. OCNDT15C (Depth of 15C Isotherm)
5. OCNDT20C (Depth of 20C Isotherm)
6. OCNDT25C (Depth of 25C Isotherm)
7. OCNDT28C (Depth of 28C Isotherm)
8. OCNHEAT (Ocean Heat Content)
9. OCNSLH (Sea Level Height)
10. OCNSST (Ocean Potential Temperature at depth of 5m)
11. OCNU5 (Ocean Zonal Current at depth of 5m)
12. OCNV5 (Ocean Meridional Current at depth of 5m)
13. OCNSAL5 (Ocean Salinity at depth of 5m)
14. OCNU15 (Ocean Zonal Current at depth of 15m)
15. OCNV15 (Ocean Meridional Current at depth of 15m)
16. OCNT15 (Ocean Potential Temperature at depth of 15m)
17. OCNSAL15 (Ocean Salinity at depth of 15m)
18. OCNVV55 (Ocean vertical velocity at depth of 55 m)
19. OCNMLD (Ocean Mixed Layer Depth)
20. OCNSILD (Ocean Surface Isothermal Layer Depth)
21. OCNTCHP (Tropical Cyclone Heat Potential)

THANK YOU

CFSR Website : http://cfs.ncep.noaa.gov/cfsr

Email : cfs@noaa.gov